[redacted]

OAK RIDGE NATIONAL LABORATORY LIBRARY
3 4456 0022194 4

ORNL 870, Series A
PROGRESS REPORT 84

AEC RESEARCH AND DEVELOPMENT REPORT

DECLASSIFIED
CLASSIFICATION CHANGED TO:
BY AUTHORITY OF:
BY:
DOE 1979 REVIEW OF
DECLASSIFIED REPORTS
This Document is Properly Declassified.
Reviewed by P. S. Baker 7-3-79
Classification Officer

CHEMISTRY DIVISION

QUARTERLY PROGRESS REPORT FOR

PERIOD ENDING SEPTEMBER 30,1950

CENTRAL RESEARCH LIBRARY
DOCUMENT COLLECTION
LIBRARY LOAN COPY
DO NOT TRANSFER TO ANOTHER PERSON
If you wish someone else to see this document, send in name with document and the library will arrange a loan.

OAK RIDGE NATIONAL LABORATORY
U.S. ATOMIC ENERGY COMMISSION

OAK RIDGE NATIONAL LABORATORY
OPERATED BY
CARBIDE AND CARBON CHEMICALS DIVISION
UNION CARBIDE AND CARBON CORPORATION
UCC
POST OFFICE BOX P
OAK RIDGE, TENNESSEE

[redacted]

[redacted]

ORNL-870
Progress Report

This document consists of 159 pages.
Copy 8 of 110 copies. Series A.

Contract No. W-7405, eng. 26

CHEMISTRY DIVISION

E. H. Taylor, Director
G. E. Boyd, M. A. Bredig, Associate Directors

QUARTERLY PROGRESS REPORT

for Period Ending September 30, 1950

DATE ISSUED: MAR 1 1951

DECLASSIFIED
CLASSIFICATION CHANGED TO:
BY AUTHORITY OF:
BY:

OAK RIDGE NATIONAL LABORATORY
operated by
CARBIDE AND CARBON CHEMICALS DIVISION
Union Carbide and Carbon Corporation
Post Office Box P
Oak Ridge, Tennessee

[redacted]

OAK RIDGE NATIONAL LABORATORY LIBRARY
3 4456 0022194 4

[redacted]

INTERNAL DISTRIBUTION

1. G. T. Felbeck (C&CCD)
2-3. Chemistry Library
4. Physics Library
5. Biology Library
6. Health Physics Library
7. Metallurgy Library
8-9. Training School Library
10-13. Central Files
14. C. E. Center
15. C. E. Larson
16. W. B. Humes (K-25)
17. W. D. Lavers (Y-12)
18. A. M. Weinberg
19. J. A. Swartout
20. E. D. Shipley
21. E. J. Murphy
22. E. H. Taylor
23. A. H. Snell
24. A. Hollaender
25. F. C. VonderLage
26. K. Z. Morgan
27. F. L. Steahly
28. M. T. Kelley
29. W. H. Pennington
30. D. W. Cardwell
31. J. A. Wethington
32. G. E. Boyd
33. R. W. Stoughton
34. J. A. Lane
35. G. W. Parker
36. C. J. Borkowski
37. M. A. Bredig
38. G. H. Jenks
39. K. A. Kraus
40. H. A. Levy
41. R. S. Livingston
42. T. E. Willmarth
43. C. H. Secoy
44. C. J. Hochanadel
45. O. K. Neville
46. W. H. Baldwin
47. A. R. Brosi
48. R. N. Lyon
49. S. A. Reynolds
50. P. F. Thomason
51. E. H. Bohlmann
52. C. P. Keim
53. C. D. Susano
54. G. H. Clewett
55-56. Central Files (O.P.)

EXTERNAL DISTRIBUTION

57-64. Argonne National Laboratory
65-67. Atomic Energy Commission, Washington
68-71. Brookhaven National Laboratory
72-73. Knolls Atomic Power Laboratory
74-79. General Electric Company, Richland
80-83. Los Alamos
84. Mound Laboratory
85-87. NEPA Project
88-90. New York Operations
91. Patent Branch, Washington
92-106. Technical Information Branch, ORE
107-110. University of California Radiation Laboratory

[redacted]

[redacted]

TABLE OF CONTENTS

ABSTRACT 9

1. CHEMISTRY OF SOURCE, FISSIONABLE, AND STRUCTURAL ELEMENTS 15

Solution Chemistry 16

Hydrolytic behavior of thorium(IV) 16

Studies of anion complexing of aqueous thorium by the method of solvent-TTA extraction 16

Anion exchange studies of metal complexes 18

Ultracentrifugal study of uranyl fluoride solutions 22

Electromigration on filter paper 22

Phase Studies 23

The uranyl fluoride—water system 23

The compound uranyl orthosilicate trihydrate 25

Phase studies of plutonium sulfate—sulfuric acid—uranyl sulfate—water mixtures 28

Further study of the two-liquid phase region of the system UO_2SO_4-H_2SO_4-H_2O 29

The measurement of the solubility of fission-product salts at high temperatures and pressures 30

2. NUCLEAR CHEMISTRY 35

Radionuclides of Tin 36

The Characteristics of Nb^{96} and Tc^{96} 37

The Ca^{45} Beta Distribution Obtained in a Split-crystal Scintillation Spectrometer 39

A Two-day Xe^{133} Isomer 43

A Re-evaluation of the Half-life of Tc^{99} 45

Recovery of Fission Products and Neptunium from Chalk River Wastes 46

Initial operation 46

Coprecipitation of pertechnetate (TcO_4^-) and various anions by tetraphenyl arsonium chloride 47

Studies on Szilard-Chalmers Reactions with $KBrO_3$ 50

3. RADIO-ORGANIC CHEMISTRY 51

Synthesis of Low-molecular-weight Intermediates Containing C^{14} 52

Methanol-C^{14} 52

[redacted]

[redacted]

Synthesis of High-molecular-weight Compounds Containing C^{14} 53

Synthesis of chrysene-5,6-C_1^{14} 53

3,4-Benzofluorene-9-carboxylic acid 56

Reaction Mechanism Studies 57

The reaction of 9-formylfluorene with formaldehyde 57

The rearrangement of α,β-dioxobutyrate 58

The rearrangement of unsymmetrical benzils 62

The isotope effect in the decomposition of formic acid-C^{14} 64

Standardization of C^{14} Counting Methods 70

Polystyrene counting standards 70

4. CHEMISTRY OF SEPARATIONS PROCESSES 72

Volatility Studies 73

Breeder blanket studies 73

Solvent Extraction 76

The organic chemistry of solvents 76

Characterization of inorganic species in solvent extraction 88

Electrochemistry 99

Electrodeposition of silver from dilute solutions 99

Ion Exchange 104

Lithium Isotope Separation 104

5. CHEMICAL PHYSICS 109

Neutron-diffraction Studies 110

Development of double-crystal spectrometer 110

Neutron-diffraction investigations 111

Structure of KHF_2 111

Calorimetry of Radioactivity 112

Microwave Spectroscopy 113

Zero-point vibrational energy considerations in polyatomic molecules 113

Paramagnetic resonance phenomena 113

Methyl iodide studies 115

Experiments in Chemical Kinetics with Molecular Beams 118

6. RADIATION CHEMISTRY 119

Decomposition of Aqueous Solutions of Fissionable Materials 120

A Calorimetric Determination of the Yield for the Oxidation of Ferrous Sulfate by Cobalt Gamma Rays 121

[redacted]

[redacted]

Yields for Decomposition of Water by Co^{60} Gamma Radiation 125
Storage and Release of Energy in Ionic Solids Subjected to Ionizing Radiation 129
Effects of Ionizing Radiation upon Heterogeneous Catalysts 134

7. INSTRUMENTATION 135
A Gamma Scintillation Survey Meter 136
Pulse Analysis Using Photographic Density Measurements 138
Instrumentation for Neutron Diffraction 146
A Reliable Count-rate Meter 151
A High-stability Low-drain Portable High-voltage Supply 155

[redacted]

LIST OF TABLES

Table		Page
1.1	Formation Constants of Chlorothorium Complexes from TTA-Benzene Solvent Extraction Experiments at 25°C	16
1.2	Relative Percentage of Aqueous Thorium Species in Chloride Solutions at an Ionic Strength of 4.0 and at 25°C	17
1.3	Formation Constants of Bromothorium Complexes from TTA-Benzene Solvent Extraction Experiments at 25°C	17
1.4	Formation Constants of Thiocyanate Complexes from TTA—Carbon Tetrachloride Solvent Extraction Experiments at 25°C	18
1.5	Adsorption of Uranium(VI) by Dowex-1 from Nitric Acid Solutions	19
1.6	Adsorption of Uranium(VI) by Dowex-1 from Sulfuric Acid Solutions	21
1.7	Solid-phase Analyses, UO_2F_2-H_2O System	23
1.8	Exploratory Metal Corrosion Tests, UO_2F_2-H_2O System	24
1.9	Analytical Data for Uranyl Silicates	27
1.10	Two-liquid Phase Region of the System UO_2SO_4-H_2SO_4-H_2O	33
1.11	Upper and Lower Critical Temperatures	33
2.1	Recovery of By-products	47
2.2	Efficiency of Carrier Anions for TcO_4^- Precipitated with Tetraphenyl Arsonium Chloride	49
3.1	Percent Migration of Substituted Phenyl Groups in the Benzilic Acid Rearrangement	62
3.2	Sample Decomposition of $HC^{14}OOH$ at 23°	68
3.3	Comparison of Specific Activities as Carbon Monoxide and Carbon Dioxide	69
4.1	Approximate Solubility of Sulfones at 30°C	77

LIST OF TABLES (Cont'd)

4.2	Comparison of Extraction of 0.1 *M* Uranium from Nitrate, Sulfate, and Chloride by *n*-Propyl Sulfone at 30°C	78
4.3	Extraction of 0.1 *M* Uranium from Aqueous HNO_3 by Various Sulfones	79
4.4	Extraction of U from Ammonium Nitrate Solution with Sulfones	79
4.5	Distribution of U, Pu, and Fission Products in Extraction with Sulfones and Tributyl Phosphate	81
4.6	Distribution of Th(IV) and H^+ Between Sulfones and Aqueous Phase	82
4.7	Distribution of P^{32} in Batch Extractions	85
4.8	Distribution of U and HNO_3 Between Alkyl Phosphates in CCl_4 and Water	87
4.9	Zirconium Partition Between Aqueous and Benzene Phases	91
4.10	Formation Constants for the Monochloro Zirconium Complex	92
4.11	Lithium Isotope Separation on Ion-exchange Resin Column at 70°C	104
4.12	Capacity for Li^+ + NH_4^+ of IRC-50 Ion-exchange Resin	106
6.1	Yield of H_2 During Oxidation of Acid Ferrous Sulfate Solution	126
6.2	Yield of H_2O_2 in Radiation Decomposition of Water in Presence of Bromide	127
7.1	Performance Specifications for Regulated Battery-operated High-voltage Supply	158

[redacted]

LIST OF FIGURES

Fig. 1.1	Two Liquid Phase Region of the System UO_2SO_4-H_2SO_4-H_2O	31
Fig. 1.2	Upper and Lower Critical Temperatures as Functions of Acid Concentration	32
Fig. 2.1	Decay Scheme of Nb^{96} and Tc^{96}	37
Fig. 2.2	Nb^{96} Kurie Plot for an Allowed Transition	38
Fig. 2.3	Ca^{45} Kurie Plot Using Single Crystal	40
Fig. 2.4	Ca^{45} Kurie Plot Using Double Crystal	42
Fig. 3.1	Hammett Plot of Percent Migration vs. Substituent Constant	65
Fig. 3.2	Apparatus Used in Studying the Rate of Formic Acid-C^{14} Decomposition and the Isotope Effect	66
Fig. 4.1	Chloride Complexing of Zr at $\mu(HClO_4 + HCl) = 3$	95
Fig. 4.2	Logarithm of HNO_3 Concentration in 100% TBP at 25°C vs. Logarithm of Square Root of HNO_3 Activity Product in Aqueous Phase at Equilibrium	97
Fig. 4.3	Logarithm of Activity Coefficient vs. HNO_3 Concentration in 100% TBP at 25°C	97
Fig. 4.4	Equivalent Conductance at 25°C vs. Log HNO_3 Concentration in 100% TBP	97
Fig. 4.5	The Electrodeposition of Silver on Gold from Solutions Containing Various Silver Ion Concentrations	101
Fig. 4.6	Electrode Position and Stripping Curves for a 5.4×10^{-6} *M* Silver Solution Using a Gold Cathode	102
Fig. 4.7	Li^7 Enrichment	105
Fig. 6.1	Calorimeter for Measurement of Gamma Ray Energy Absorbed in Water	122
Fig. 6.2	Glow Curves for KBr (Fused) from Two Sources Before and After Ion Exchange Purification	130
Fig. 6.3	Typical Phosphorescence Spectra of Fused Purified KBr After 10 min Irradiation at 2000 r/min and -196°C	131
Fig. 6.4	Glow Curves for Baker's Analyzed Potassium Bromide Irradiated 10 min at 2000 r/min and -196°C	133
Fig. 7.1	Portable Gamma Scintillation Counter	137
Fig. 7.2	Deflection on Film vs. Input Voltage to Preamp	140
Fig. 7.3	Opacity of Film vs. Number of Pulses Applied	141
Fig. 7.4	Energy Spectra of Two Radioactive Samples	144

[redacted]

[redacted]

LIST OF FIGURES (Cont'd)

Fig. 7.5	Energy Spectrum of La^{138} Source with Background Subtracted	145
Fig. 7.6	Instrumentation for Neutron Diffraction	148
Fig. 7.7	Neutron Diffraction Pattern, Powdered Nickel	149
Fig. 7.8	Linear Count Rate Meter	152
Fig. 7.9	Regulated Battery Operated High Voltage Supply	156

[redacted]

[redacted]

ABSTRACT

CHEMISTRY OF SOURCE, FISSIONABLE, AND STRUCTURAL ELEMENTS

Solution Chemistry. Previous hydrolytic studies of thorium tetrachloride solutions in perchlorate media are being extended to chloride media. Further information about thorium complexes is being obtained from extraction experiments, and tentative equilibrium constants are reported for chlorothorium complexes up to an ionic strength of 6 and for the bromide the thiocyanate complexes at ionic strengths of 0.5 and 1.

Anion exchange studies have been extended to uranium(VI) in nitric and sulfuric acid solutions. Uranium is strongly adsorbed from the latter (distribution constant maximum about 10^4) and weakly from the former (distribution constant maximum about 20). In chloride solution (previously reported) the value is about 1300.

An ultracentrifuge study of aqueous UO_2F_2 solutions has been completed, and can be interpreted by assuming that the principal species in solution is undissociated UO_2F_2.

Phase Studies. The solid phases observed in the system UO_2F_2-H_2O up to about 350°C are being identified. One phase appears to be a product of reaction with the fused silica vessel and to have the composition $(UO_2)_2SiO_4 \cdot 3H_2O$. The other three phases appear to be $UO_2F_2 \cdot 2H_2O$, presumably in allotropic modifications if the tentative results are correct. Plans are underway for a phase study of the $Pu(SO_4)_2$-H_2SO_4-H_2O-UO_2SO_4 system.

Solubility measurements of fission-product sulfates are being made by two methods. A synthetic method, intended for fairly soluble compounds, is being checked against the known solubility-temperature data for $ZrSO_4$. An analytical method, intended for less soluble compounds, will use radioactive tracers to facilitate analysis.

[redacted]

NUCLEAR CHEMISTRY

Recent improvements in methods for measuring the energies of nuclear radiations continue to be applied to a number of nuclei. The work on tin, recently summarized, has been extended by some scintillation spectrometer studies of the radiations from 9.5-min Sn^{125} and 40-min Sn^{123}. The radiations of 22.9-hr Nb^{96} and 4.25-day Tc^{96} were examined, and the results agree with a decay scheme recently prepared elsewhere but include three new cross-over transitions.

A 51-hr isomer of Xe^{133} has been established, and found to be the product of about 2% of the beta disintegration of I^{133}.

A split-crystal scintillation spectrometer has been devised to eliminate spurious low-energy pulses resulting from scattering of betas before complete absorption in the crystal. With this arrangement, the beta spectrum of Ca^{45}, already known, can be reproduced satisfactorily, showing the applicability of this method to low-energy beta emitters in general.

Tentative results seem to confirm the half-life of about 2×10^5 years reported elsewhere for Tc^{99}.

Two full-scale fission-product-recovery runs have been made on the Chalk River wastes. Only minor difficulties have been encountered, and about 0.25 g of Tc^{99} and about 0.1 g of Nb^{237} have been recovered.

Extensive work on enrichment of radiobromine by a Szilard-Chalmers reaction on $KBrO_3$ has been nearly completed. Activities of Br^{82} as high as 820 rutherfords/mg, corresponding to an enrichment of 21,000-fold, have been obtained.

RADIO-ORGANIC CHEMISTRY

Preparations. One hundred and twenty millicuries of methanol-C^{14} has been prepared by catalytic reduction of carbon dioxide.

The preparation of chrysene-5,6-$C_1{}^{14}$ has been repeated, and a new technique, the "double-dilution method," has been applied to the analysis of the product.

Triphenylmethyl sodium has been used to carbonate 3,4-benzofluorene in 84% yield.

Reaction Studies. The action of excess aqueous basic formaldehyde solution upon 9-formylfluorene-10-C^{14} has been shown to give nonradioactive 9-fluorenemethanol and C^{14}-labeled formic acid. The mechanism previously suggested by Brown and Bluestein was supported.

Benzilic acid rearrangement of ethyl α,β-dioxobutyrate-β-C^{14} has been shown to involve migration of the carbethoxy group only. The product of rearrangement, methyltartronic acid, was decarboxylated to yield nonradioactive carbon dioxide and lactic acid, which was recovered as the zinc salt and shown to contain all the initial activity.

The benzilic acid rearrangements of *p*-methylbenzil and *m*-chlorobenzil have been shown to give respectively 38.2% and 81.1% migration of the substituted phenyl groups. These percentage migrations and the percentage migrations of *p*-chloro and *p*-methoxy groups previously measured for the analogous reactions have been correlated using Hammett's equation.

An isotope effect has been demonstrated in the sulfuric acid dehydration of C^{14}-labeled formic acid. Attempts to evaluate this isotope effect accurately at several temperatures are underway.

Standards. Polystyrene-C^{14} films, 0.01 in. thick, which were laid down on a pool of mercury have shown a 6% difference in counting rate between the two sides. This difference was apparently the result of diluting labeled polymer with commercial polymer of different molecular weight.

Radiation Effects. In order to gain experience in the techniques to be employed in studying the effects of various kinds of radiation on organic compounds, several samples of organic acids have been exposed to beta radiation

using the ORNL Van de Graaff machine and to gamma radiation using the 300-curie Co^{60} source. Preliminary data have shown the necessity of analyzing the noncondensible gases produced, and an apparatus for this has been designed and constructed. Cells for holding the compounds during irradiation have been constructed and tested.

Owing to the preliminary nature of this work, which is being performed by A. R. Jones in collaboration with the radiation chemistry group, no detailed experimental results are available for presentation in this report.

CHEMISTRY OF SEPARATIONS PROCESSES

Interaction between ThF_4 and phosphorus fluorides appears to reduce the particle size of part of the ThF_4 to 200 to 500 A. There is some evidence that this facilitates subsequent removal of Pa^{233} (in irradiated ThF_4) by fluorination.

Several compounds have been synthesized for use in studies of solvent extraction. These include a number of sulfones which show interesting extraction properties, some alkyl phosphates for comparison with tributyl phosphate (TBP), some hydrolytic products of TBP, and TBP labeled with P^{32} for tracer studies in extraction.

Characterization of the species present in solution in various systems relevant to solvent extraction has been continued. In aqueous zirconium solutions containing Cl^- and ClO_4^-, the chief zirconium species is $ZrCl^{3-}$ with much less of the higher complexes. In TBP, the HNO_3 extracted from H_2O exists almost entirely as $HNO_3 \cdot TBP$.

Separation of the lithium isotopes by ion exchange has been studied further by runs with Nalcite HCR resin at 70°C and with IRC-50 resin at 30°C. Preliminary isotopic analyses indicate that there is probably no advantage in operating a Nalcite HCR column at 70°C rather than at 30°C and that IRC-50 resin is probably no better than the Nalcite HCR.

CHEMICAL PHYSICS

The apparatus for neutron diffraction has been improved by the introduction of automatic recording and of a new monochromator crystal (copper) giving a fivefold increase in intensity over the sodium chloride crystal used previously. Results on the bifluoride ion (in KHF_2) are in good agreement with the symmetrical structure. Diffraction patterns of a number of other substances have been obtained and are awaiting analysis.

The comparison of ionization-chamber readings with calorimetric measurements has been extended to a comparison of relative ionizations produced by cobalt gamma rays in dry air, CO_2, argon, and helium.

The determination of nuclear and molecular properties by microwave spectroscopy has taken three directions, the expansion being a result of work of summer participants in the program. Work on iodine isotopes, the field of chief immediate interest, comprised further measurements on I^{127} and I^{129}, giving improved values for the moment of inertia of CH_3I and for the quadrupole coupling constants, as well as mapping the spectra for use in future studies with the other isotopes. A theoretical study was started of the effect of zero-point vibrations on moments of inertia measured by microwave spectroscopy. At present, the uncertainty in this effect limits the accuracy with which moments of inertia can be obtained. Finally, apparatus has been assembled for study of paramagnetic resonance absorption.

RADIATION CHEMISTRY

The study of the radiation decomposition and corrosion of aqueous uranyl sulfate in stainless steel is receiving increasing emphasis. It appears that the proposed HRE solution (40 g of U^{235} per liter) can be contained satisfactorily in stainless steel at 250°C and a flux of 10^{11} for at least two weeks, although the sources of occasional earlier failures must still be found.

The measurement of radiation dosage in chemical experiments has been put on a sounder basis by a calorimetric calibration of the acid ferrous sulfate actinometer. The yield for ferrous ion oxidation was found to be 15.7 Fe^{++} oxidized per 100 ev absorbed. This is lower than the values of other investigators but is believed to be more reliable.

With this value for the yield, the dose rate of the cobalt gamma-ray source in Building 706A is 4850 r/min instead of the previous 3880 based on a yield of 20.6.

The yield of the forward reaction (H_2 and H_2O_2 formed immediately after radiation dissociation) in the radiation decomposition of H_2O by cobalt gamma rays has been estimated as 0.35 and 0.43 molecules of H_2O_2 per 100 ev by two different methods. The mechanism requires further study to explain the difference. The yield of radicals (not initially combining to form H_2O_2 and H_2) was measured as 2.47 radicals (H + OH) per 100 ev. Summation of these gives 3.33 molecules of H_2O decomposed per 100 ev.

INSTRUMENTATION

Considerable attention has been given to instrumentation of the neutron-diffraction apparatus. In particular, a count-rate meter of exceptional reliability has been designed and built, and has made possible continuous recording of diffraction patterns requiring up to a day for scanning.

A scintillation survey meter for gamma radiation has been designed and built, with the aim of providing maximum sensitivity with adequate stability and portability.

1. CHEMISTRY OF SOURCE, FISSIONABLE, AND STRUCTURAL ELEMENTS

SOLUTION CHEMISTRY

HYDROLYTIC BEHAVIOR OF THORIUM(IV)

R. W. Holmberg and K. A. Kraus

Hydrolytic studies of thorium tetrachloride solutions have been extended from perchlorate to chloride media in an attempt to evaluate the chloride-complex constant of thorium(IV). The tentative value of the formation constant obtained from these data (K = approximately 0.2) is considerably smaller than that previously obtained by Day and Stoughton[1] (K = approximately 1.8) from TTA partition coefficient measurements. The reason for the discrepancy is being investigated.

STUDIES OF ANION COMPLEXING OF AQUEOUS THORIUM BY THE METHOD OF SOLVENT-TTA EXTRACTION[2]

W. C. Waggener and R. W. Stoughton

Chloride. Studies of chlorothorium complexes by thenoyl trifluoroacetone (TTA)—benzene extraction reported in the two preceding quarterly reports have been extended to cover the ionic strength range 0.5 to 6.0. Tentative results, including constants of formation (concentration constants, uncorrected for TTA-thorium complexing in the aqueous phase) are tabulated in Table 1.1.

TABLE 1.1

Formation Constants of Chlorothorium Complexes from TTA-Benzene Solvent Extraction Experiments at 25°C

μ	$[H^+]_{aq}$	$[TTA]_{benz}$	[Th]	CONSTANTS OF FORMATION (CONCENTRATIONS) FOR CHLOROTHORIUM SPECIES			
				k_{C1}	k_{2C1}	k_{3C1}	k_{4C1}
0.5	0.20 and 0.50	0.10 and 0.25	10^{-5}-10^{-6}	2.30			
0.7	0.20	0.10	10^{-5}-10^{-6}	1.80			
1.0	0.20	0.10	10^{-5}-10^{-6}	1.61			
2.0	0.20	0.10	10^{-5}-10^{-6}	1.21	0.1	0.2	
4.0	0.32	0.25	10^{-5}-10^{-6}	1.70	0.14	0.10	0.018
6.0	0.32	0.25	10^{-5}-10^{-6}	2.10	0.55	0.35	

(1) Day, R. A., Jr., and Stoughton, R. W., *Chemistry of Thorium in Aqueous Solutions. I. Some Organic and Inorganic Complexes*, ORNL-468 (Jan. 1950).

(2) For description of the method and experimental technique see Waggener, W. C., and Stoughton, R. W., "Studies of Chloride Complexing of Aqueous Thorium by TTA-Benzene Extraction Method," *Chemistry Division Quarterly Progress Report for Period Ending March 31, 1950*, ORNL-685, 24-30 (June 16, 1950).

The concentration constant, k_{Cl} (for $Th^{4+} + Cl^- \rightleftharpoons ThCl^{3+}$), decreases from 2.30 at $\mu = 0.5$ to a minimum of 1.21 at $\mu = 2.0$, then increases regularly to 2.10 at $\mu = 6.0$. The corresponding true activity constant, k_{Cl} (μ = zero), has been estimated to be roughly 24 by linear extrapolation of log k_{Cl} versus $f(\mu)$ (an extended form[3] of the Debye equation) employing our data in the range $\mu = 0.5$ to 2.0.

Data up to $\mu = 4.0$ were previously reported to fit satisfactorily the assumption of two chloro species, the mono- and trichlorothorium ions. However, with accumulation of additional data it has become apparent that the di- and tetrachlorothorium species are probably present in measurable concentrations. Table 1.2 shows the relative importance, percentagewise, of the thorium species in 1, 2, and 4 *M* chloride solution at an ionic strength of 4.0.

TABLE 1.2

Relative Percentage of Aqueous Thorium Species in Chloride Solutions at an Ionic Strength of 4.0 and at 25°C

SPECIES	PERCENT OF THORIUM AS INDICATED SPECIES		
	1 *M* Cl^-	2 *M* Cl^-	4 *M* Cl^-
Th^{4+}	33.8	16.5	4.8
$ThCl^{3+}$	57.5	56.2	32.3
$ThCl_2^{2+}$	4.7	9.3	10.6
$ThCl_3^{+}$	3.4	13.2	30.4
$ThCl_4$	0.6	4.8	29.9

Bromide. The formation constant (concentration constant) for aqueous monobromothorium ion has been determined as 2.09 from two series of experiments at $\mu = 0.5$ (see Table 1.3). This value is to be compared with 2.30 obtained for monochlorothorium at the same ionic strength.

TABLE 1.3

Formation Constants of Bromothorium Complexes from TTA-Benzene Solvent Extraction Experiments at 25°C

μ	$[H^+]_{aq}$	$[TTA]_{benz}$	[Th]	CONSTANT OF FORMATION (CONCENTRATION) FOR BROMOTHORIUM SPECIES (k_{Br})
0.5	0.1	0.050	10^{-5}-10^{-6}	2.08
0.5	0.5	0.25	10^{-5}-10^{-6}	2.10

(3) Kraus, K. A., and Nelson, F., *Hydrolytic Behavior of Metal Ions. I. The Acid Constants of Uranium(IV) and Plutonium(IV)*, ORNL-496, p. 22 (Jan. 3, 1950).

Thiocyanate. Thiocyanate ion has been found to complex aqueous thorium much more strongly than chloride or bromide. Studies have been made at an ionic strength of 0.5 and 1.0, and tentative results, including constants of formation of consecutive complexes (concentration constants, uncorrected for TTA-thorium complexing in the aqueous phase), are tabulated in Table 1.4.

TABLE 1.4

Formation Constants of Thiocyanate Complexes from TTA—Carbon Tetrachloride Solvent Extraction Experiments at 25°C

μ	$[H^+]_{aq}$	$[TTA]_{CCl_4}$	Th	CONSTANTS OF FORMATION (CONCENTRATION) FOR THIOCYANATOTHORIUM SPECIES		
				k_{NCS}	k_{2NCS}	k_{3NCS}
0.5	0.5	0.25	10^{-5}-10^{-6}	11.8	27.0	23.7
1.0	0.5	0.25	10^{-5}-10^{-6}	10.0	23.0	29.0

Future Work. It is planned to study the TTA complexes of thorium existing in the aqueous phase in order to correct for their effect in these anion complexing experiments.

ANION EXCHANGE STUDIES OF METAL COMPLEXES

Adsorption of Uranium(VI) from Nitric Acid Solutions (K. A. Kraus and Frederick Nelson). Since uranium(VI) can be readily extracted from concentrated nitrate solutions by organic solvents, it is probably present in appreciable concentrations as a neutral complex [*e.g.*, $UO_2(NO_3)_2 \cdot nH_2O$] in these solutions. At the same or higher nitrate concentrations negatively charged uranyl complexes [*e.g.*, $UO_2(NO_3)_3^-$] might exist in sufficient concentration to permit adsorption of uranium by anion exchangers. This assumption was verified in a series of experiments in which tracer solutions of uranium(VI) (using U^{233}) were equilibrated with weighed amounts of anion exchange resin (Dowex-1) for about 14 hr and the amount of adsorbed material was determined radiochemically from the decrease in uranium(VI) concentration of the solutions. The results of the experiments are shown in Table 1.5.

The distribution coefficient D_w [amount per gram of oven-dried (110°C) resin/amount per milliliter of solution] was found to increase with increasing nitric acid concentration up to about 8 *M* HNO_3, and then to decrease appreciably. Since the resin floats at these very high nitric acid concentrations and is difficult to separate from the solution, and since the resin may be attacked by the rather concentrated nitric acid, the significance of the maximum is in doubt.

The maximum adsorbability (D_w = approximately 20 in 8 *M* HNO_3) is surprisingly low if contrasted with adsorbabilities from chloride solutions where, approximately, D_w = 1300 in 8 *M* HCl.[4,5]

The reason for this difference in behavior is not clear, since low adsorbabilities at high ionic strength could be due to very low concentrations of a negatively charged complex of proper charge (-1) and high adsorbability, or to the formation of a negatively charged complex of low adsorbability, *e.g.*, of too high a negative charge (-2 or more negative).

TABLE 1.5

Adsorption of Uranium(VI) by Dowex-1 from Nitric Acid Solutions

(Room temperature; solution volume, 2.0 ml; 10^{-3} *M* U(VI) with tracer U^{233}; initial α activity per λ, 38.2 d/min)

HNO_3 (*M*)	WEIGHT OF AIR-DRIED RESIN (mg)	FINAL α ACTIVITY PER λ (d/min)	D_w *
0.58	82.2**	38.3	<<1
3.1	62.3**	35.2	4.0
	189.8***	30.7	2.9
4.7	61.8**	33.1	7.4
	179.1***	24.4	7.3
6.3	68.7**	30.2	11.3
	172.6***	20.8	10.7
7.9	75.2**	27.1	15.9
	165.2***	18.1	19.9
9.4	79.6**	32.3	6.8
	160.5***	23.2	8.9
12.6	86.8**	33.5	4.7
15.7	74.0**	33.8	5.1

* D_w = amount per gram of oven-dried resin/amount per milliliter of solution.

** Commercial screened 200-230 mesh resin, water-washed and air-dried; weight loss on drying at 105-110°C, 32%.

*** 200-230 mesh resin in nitrate form, washed and air-dried; weight loss on drying at 105-110°C, 9.7%.

(4) Kraus, K. A., and Moore, G. E., *Chemistry of Protactinium. V. Separation of Thorium, Protactinium, and Uranium with Anion Exchange Columns in HCl Solutions*, ORNL-330 (Apr. 27, 1949).

(5) Moore, G. E., and Kraus, K. A., "Anion Exchange Studies of Uranium(VI) in HCl-HF Mixtures, Separation of Pa(V) and U(VI)," *Chemistry Division Quarterly Progress Report for Period Ending June 30, 1950*, ORNL-795, p. 16 (Oct. 3, 1950).

Adsorption of Uranium(VI) from Sulfuric Acid Solutions (K. A. Kraus and Frederick Nelson). The adsorbability of uranium(VI) from sulfuric acid solutions is being studied over a wide concentration range. A series of preliminary equilibration experiments has been carried out. Only the supernatants were analyzed, and distribution coefficients were calculated from the change in uranium(VI) concentration on addition of resin and from the known weight-volume ratios. Uranium analyses were carried out radiochemically and polarographically, making the tentative assumption that the diffusion-current constants are independent of uranium(VI) concentration.

The results of the experiments are summarized in Table 1.6. While uranium(VI) is only weakly adsorbed from relatively concentrated sulfuric acid solutions, its adsorbability increases rapidly with decreasing molarity of H_2SO_4, D_w reaching a maximum value of about 3×10^4 in 0.001 M H_2SO_4. In the region 0.1 to 1 M H_2SO_4, D_w decreases approximately with the square of the sulfuric acid concentration. Since under these conditions the solution contains primarily the singly negatively charged bisulfate ion, this square dependence suggests that the adsorbable sulfate complex carries a double negative charge and hence may be $UO_2(SO_4)_2^{=}$. Below 0.1 M H_2SO_4, D_w increases less rapidly with decreasing sulfuric acid concentration. This may be due to the fact that for elution the doubly negatively charged sulfate ion becomes important, or it may be due to a decrease in concentration of the negatively charged uranyl complex. Further studies in sulfuric acid and sulfate solutions are underway to determine the relative importance of the two effects and possibly to determine the stability constants of the uranyl sulfate complexes.

Anion-exchange Studies of Transition Elements (G. E. Moore and K. A. Kraus). Anion-exchange studies in chloride solutions of the elements chromium through zinc have been carried out in HCl solutions up to about 12 M. The work is being written up and will appear as ORNL-906.

TABLE 1.6

Adsorption of Uranium(VI) by Dowex-1 from Sulfuric Acid Solutions
(Room Temperature)

Shaking experiments: U^{233} tracer, about 9×10^{-7} *M*; initial α activity per λ, 24.9 d/min; about 5 hr equilibration

H_2SO_4 (*M*)	SOLUTION VOLUME (ml)	WEIGHT OF AIR-DRIED RESIN* (mg)	FINAL α ACTIVITY PER λ (d/min)	D_w**
5×10^{-5}	5.0	19.8	2.2	3.4×10^3
1×10^{-3}	5.0	10.3	0.43	3.8×10^4
	10.0	15.5	1.26	1.7×10^4
5×10^{-3}	5.0	10.3	0.66	2.5×10^4
	10.0	15.5	0.65	3.3×10^4

Polarographic experiments: about 30 min equilibration

H_2SO_4 (*M*)	U(VI) $\times 10^4$ (*M*)	SOLUTION VOLUME (ml)	WEIGHT OF AIR-DRIED RESIN* (mg)	FINAL U(VI) $\times 10^4$ (*M*)	D_w**
0.01	5.0	5.0	13.9	0.27	8.7×10^3
0.025	2.5	5.0	9.4	0.35	4.5×10^3
0.05	5.0	5.0	11.2	0.98	2.5×10^3
0.10	2.5	10.0	10.2	1.37	1.1×10^3
	2.5	10.0	18.4	0.89	1.4×10^3
	10.0	5.0	9.6	5.27	6.5×10^2
	10.0	5.0	47.6	8.96	1.2×10^3
	10.0	5.0	174.8	9.58	1.7×10^3
0.5	10.0	5.0	162.3	4.63	4.9×10
1.0	2.5	3.0	186.2	6.08	1.4×10
4.5	10.0	5.0	172.0	9.59	1.7

* 200-230 mesh screened and washed sulfate resin, air-dried, weight loss on drying at 105-110°C, 27.6%.

**D_w = amount per gram of oven-dried resin/amount per milliliter of solution.

ULTRACENTRIFUGAL STUDY OF URANYL FLUORIDE SOLUTIONS

J. S. Johnson and K. A. Kraus

The ultracentrifugal studies of inorganic systems have been extended to aqueous solutions of uranyl fluoride in an attempt to evaluate the significance of the extremely low activity coefficients previously observed by Marshall, Gill, and Secoy.[6] Studies have been carried out with 0.25, 0.75, 1.56 *M* and saturated UO_2F_2 solutions and one 0.17 *M* UO_2F_2 solution containing 1 *M* $NaClO_4$ as supporting electrolyte. The centrifugal measurements together with the freezing point measurements of Marshall, Gill, and Secoy can be interpreted by assuming that undissociated UO_2F_2 is the principal species in these solutions. Although this interpretation is not necessarily unique, it is in agreement with conductivity studies,[7] *p*H measurements,[8] and estimates of the uranyl fluoride complex constants.[9] A detailed report on this work is in preparation.

ELECTROMIGRATION ON FILTER PAPER

G. W. Smith and K. A. Kraus

Work is continuing on the investigation of the applicability of filter paper electromigration to the study of the complexing of metal ions.[10,11] Attempts are being made to increase the precision of the method and to extend the useful ionic strength range.

(6) Marshall, W. L., Gill, J. S., and Secoy, C. H., "The Uranyl Fluoride—Water System," *Chemistry Division Quarterly Progress Report for Period Ending June 30, 1950*, ORNL-795, p. 28 (Oct. 3, 1950); and private communication.

(7) Dean, G. R., *Properties of Uranyl Fluoride*, CC-2092 (Sept. 11, 1944).

(8) Marshall, Gill, and Secoy, *op. cit.*

(9) Moore and Kraus, *op. cit.*; and unpublished results.

(10) Kraus, K. A., and Smith, G. W., "Filter Paper Electromigration for the Determination of Charges of Complex Ions," *Chemistry Division Quarterly Progress Report for Period Ending March 31, 1950, Part I, Chemical Research*, ORNL-685, p. 19 (June 16, 1950).

(11) Kraus, K. A., and Smith, G. W., "Electromigration on Filter Paper," *Am. Chem. Soc. J.* 72, 4329 (1950).

ORNL-870
9/50

PHASE STUDIES

THE URANYL FLUORIDE—WATER SYSTEM

W. L. Marshall and J. S. Gill

In the phase study of the uranyl fluoride—water system[12] further work has been done to determine the solid phases and the thermal stability of the fluoride.

Solid Phases X, Y, and Z. Solubility data indicate the existence of a solid phase X in contact with saturated solution from the ice eutectic to 150°C, phase Y between 150 and 240°C, and phase Z between 240 and 347°C. Solid X was determined by direct removal of the amorphous solid, attempted drying between filter papers, actual drying in the open, and ignition to U_3O_8 at 900°C. Above 100°C the solids were obtained by two methods: (1) A "slow" method consisted in rocking at constant temperature a saturated solution and solid in a 4-mm-I.D. sealed silica tube. The rocker was stopped and the contents were allowed to cool to give a translucent gel and the solid. The assumption was made that equilibrium attainment during the cooling process is sufficiently slow under conditions of such high solution viscosity as not to alter the solid composition materially. The tube was broken and the solid was analyzed. (2) A "quick" method consisted in holding the tube at constant temperature in a special heating unit, then suddenly pushing the tube into a dry ice—trichloroethylene mixture and subsequently analyzing the solid phase.

TABLE 1.7

Solid-phase Analyses, UO_2F_2 — H_2O System

SOLID-PHASE REGIONS	TEMPERATURE (°C)	METHOD	ANALYSIS (%)	
			AS UO_2F_2	AS $UO_2F_2 \cdot 2H_2O$
Solid X	Room	Drying	90.75	101.5
Solid Y	195	Slow	88.07*	98.5*
Solid Y	195	Quick	91.14	101.9
Solid Z	295	Slow	89.73	100.3
Solid Z	322	Quick	89.29	99.72

*Previous value, reference 12.

(12) Marshall, Gill, and Secoy, ORNL-795, *op. cit.*, p. 22.

-87C
9/50

The data are given in Table 1.7 and appear to indicate that solids X, Y, and Z are uranyl fluoride dihydrate. This might be the case if allotropy of the dihydrate occurred. However, because of the difficulty of obtaining samples and because of the relatively small fraction of the compound which is water, these values should be considered tentative.

Solid Phases W. At low concentration between 200 and 350°C a solid phase W was reported.[13] Further work indicates, rather, two solid phases. The work is discussed elsewhere in this report (p. 25) and shows these solids to be formed by attack on the quartz tube to produce silica and a uranium-silicon compound. The solids W should therefore not appear on the two-component phase diagram.

Corrosion Tests, Stability Experiments. Exploratory corrosion tests have been made on metals for possible use as containers in stability studies of uranyl fluoride solutions. The procedure was to place weighed wire samples in quartz tubes containing 20 wt. % UO_2F_2 solution and to observe any corrosion change occurring at different temperatures. These data are given in Table 1.8 and serve to indicate the approximate expected corrosion. Fluosilicic acid could be a possible causative agent in these tests.

TABLE 1.8

Exploratory Metal Corrosion Tests, UO_2F_2-H_2O System

WIRE SAMPLE	TEMPERATURE (°C)	TIME (hr)	INITIAL WEIGHT (g)	FINAL WEIGHT (g)	% CHANGE	OBSERVATIONS
347 stainless steel	150	16	0.1161			No apparent change; very slight UO_2^{++} reduction
347 stainless steel	200	8	0.1161	0.1201	~ +3	Metal turns black; extensive UO_2^{++} reduction to U_3O_8
Monel	250	60	0.0254			Extensive corrosion; wire broken
Silver	300	16	0.1771	0.1726	~ -2	White product on wire; some black precipitate in solution
Platinum	320	20	0.2325	0.2325	0	No change
Gold	310	20	0.3028	0.3029	0	No change

(13) Marshall, Gill, and Secoy, ORNL-795, *op. cit.*, p. 22.

-97c
9/50

As a result of the above work, gold liners with gold disk covers were fitted into small steel bombs, thus presenting a closed gold system to the solution. In current work, solutions are shaken in the gold container in the temperature and concentration regions where corrosion in quartz tubes was observed. So far, this work indicates no thermal decomposition but rather hydrolytic changes in the region in which the solids W appeared.

Summary. 1. Tentative analyses for solids X, Y, and Z in the UO_2F_2-H_2O system indicate the composition $UO_2F_2 \cdot 2H_2O$ for all three solids.

2. The solids W represent two corrosion products of silica and must be omitted entirely from the two-component phase diagram, UO_2F_2-H_2O.

3. Further thermal studies of the uranyl fluoride—water system indicate a thermally stable but hydrolytically unstable system in the range 200 to 300°C. Exploratory metal corrosion data are given.

THE COMPOUND URANYL ORTHOSILICATE TRIHYDRATE

W. L. Marshall and J. S. Gill

In the course of experimental investigation of the uranyl fluoride—water system[14] at elevated temperatures in silica tubes, a yellow insoluble product was obtained. This product was analyzed by chemical, spectrographic, and X-ray diffraction methods, and the results indicate uranyl orthosilicate trihydrate as the most probable structure. No data concerning uranyl-silicon compounds of this type have been found in the literature. A description is given of the synthesis and of the properties of the compound.

Experimental procedure. A silica liner containing 5.6% aqueous uranyl fluoride solution was held at 300°C for 16 hr in an American Instrument Company bomb. Solid products were observed in silica capillary tubes under these conditions.[15]

Two solids were obtained from the bomb, one white and one yellow. These solids were washed and were separated from each other by centrifugation, in which the yellow product settled much faster than the white compound.

The white solid was identified as silica by spectrography, by X-ray diffraction, and by reaction with hydrogen fluoride.

(14) Marshall, Gill, and Secoy, ORNL-795, *op. cit.*, p. 22.

(15) *Ibid.*

-870
9/50

The yellow product was identified as a uranyl silicate hydrate by analyses for water, silicon, and uranium. The water was determined from the weight difference of a sample after a preliminary ignition at 1000°C to U_3O_8, correcting it for the reduction change on ignition.

$$(UO_2)_2SiO_4 \cdot 3H_2O \longrightarrow 2/3\ U_3O_8 + SiO_2$$

$$\text{water correction factor} = \frac{3H_2O}{3H_2O + 2/3\ (O)}$$

Silicon was determined by difference in weight of the ignited sample upon removal of silica by hydrogen fluoride and subsequent ignition at 1000°C. Uranium was then determined from the final weight of U_3O_8.

A variation was to first decompose the compound with concentrated HNO_3 and H_2SO_4 (run 2). The gel type of silica appeared at this point. Another variation was to combine the silica determination of Scott[16] with a uranium analysis (run 3). Uranium was also determined by a potentiometric method carried out by Corbin *et al.* of the Analytical Chemistry Division (run 4).

Analysis for trace amounts of fluorine was carried out by conversion to SiF_4, distillation, and subsequent colorimetric determination of fluoride. This showed approximately 0.4% fluorine, indicating absence of fluorine from the compound. The analysis was performed by Horton of the Analytical Chemistry Division.

Data and Discussion. Because of the small amount of compound available, the analytical samples taken were about 0.100 g each. Owing to the large proportion of uranium, the accuracy is much better for it than for silicon or water, probably about ±0.3%. Therefore greater reliance should be placed on the uranium data.

The analytical data are compared with theoretical values for various uranyl silicates in Table 1.9. From the data it can be seen that $(UO_2)_2SiO_4 \cdot 3H_2O$ is the most probable compound with the possible exception of $(UO_2)_3Si_2O_7 \cdot 3H_2O$. However, this latter silicate does not fit the experimental data so well as the ortho compound since higher silicon (and, consequently, lower water) values would be expected as a result both of possible incomplete dehydration of the silica and of incomplete initial separation from the SiO_2.

(16) Scott, W. W., *Standard Methods of Chemical Analysis*, Ed. by N. H. Furman, 5th ed., vol. 1, p. 804, Van Nostrand, 1939.

-170
9/50

TABLE 1.9

Analytical Data for Uranyl Silicates

COMPOUND	PERCENT		
	URANIUM	SILICON	WATER
	Theoretical		
UO_2SiO_3	68.78	8.11	0
$UO_2SiO_3 \cdot H_2O$	65.38	7.71	4.95
$UO_2SiO_3 \cdot 2H_2O$	62.30	7.34	9.43
$(UO_2)_2SiO_4$	75.32	4.44	0
$(UO_2)_2SiO_4 \cdot H_2O$	73.23	4.32	2.77
$(UO_2)_2SiO_4 \cdot 2H_2O$	71.25	4.20	5.39
$(UO_2)_2SiO_4 \cdot 3H_2O$	69.38	4.09	7.88
$(UO_2)_3Si_2O_7$	73.03	5.73	0
$(UO_2)_3Si_2O_7 \cdot H_2O$	71.71	5.63	1.81
$(UO_2)_3Si_2O_7 \cdot 2H_2O$	70.43	5.53	3.55
$(UO_2)_3Si_2O_7 \cdot 3H_2O$	69.18	5.44	5.23
$(UO_2)_3Si_2O_7 \cdot 4H_2O$	68.02	5.33	6.86
	Experimental		
Sample 1	69.16	5.16	6.6
Sample 2	69.25	4.54	
Sample 3	69.83	4.6	7.37
Sample 4	69.27		
Sample 5			7.79
Sample 6			7.79
Average	69.38	4.77	7.39

-270
9/50

The formation of SiO_2 and $(UO_2)_2SiO_4 \cdot 3H_2O$ may be explained by the following reactions in the solutions at 300°C:

$$UO_2F_2 + H_2O \longrightarrow UO_3 + 2HF \quad (1)$$

$$4HF + SiO_2 \longrightarrow SiF_4 + 2H_2O \quad (2)$$

$$3SiF_4 + 4H_2O \longrightarrow Si(OH)_4 + 2H_2SiF_6 \quad (3)$$

$$2UO_3 + Si(OH)_4 + H_2O \longrightarrow (UO_2)_2SiO_4 \cdot 3H_2O \quad (4)$$

$$H_2SiF_6 + 2H_2O \longrightarrow SiO_2 + 6HF \quad (5)$$

The uranium-silicon compound appears insoluble or difficultly soluble in concentrated or dilute HNO_3, HCl, and H_2SO_4, but soluble with precipitation of silicic acid in concentrated $HClO_4$ or a mixture of concentrated HNO_3 and H_2SO_4. The compound is thermally stable up to about 400°C but liberates water between 400 and 450°C with possible additional decomposition to a light reddish solid which may be a mixture of UO_3 and SiO_2.

PHASE STUDIES OF PLUTONIUM SULFATE—SULFURIC ACID—URANYL SULFATE—WATER MIXTURES

W. L. Marshall and J. S. Gill

It is proposed to study the solubility of plutonium sulfate in aqueous solutions of sulfuric acid and uranyl sulfate from room temperature to 250°C. After an extensive literature survey, it appears feasible from a solution stability standpoint to study $Pu(IV)(SO_4)_2$ rather than Pu(III) or Pu(VI).

Proposed Procedure. The proposed method of study will be first to prepare and purify $Pu(IV)(SO_4)_2$, then to study its solubility in aqueous sulfuric acid of varying concentrations and temperatures up to 100°C. All work will be done in special hoods on milligram or smaller amounts of plutonium. The general procedure will be to investigate the system fully at lower temperatures before proceeding to higher temperatures.

A technique for safely sealing sample solutions in silica capillary tubes for experiments above 100°C has not been completely worked out. It is likely that solutions might be run in silica capillary tubes up to about 250°C. With

-870
9/50

respect to tube explosions, some two hundred tubes have been run above 300°C, and no tube failures have ever occurred below 320°C. Therefore it is believed that this technique can be used up to 250°C with reasonable safety, provided that safe methods of filling and sealing the tubes can be developed.

FURTHER STUDY OF THE TWO-LIQUID PHASE REGION OF THE SYSTEM UO_2SO_4-H_2SO_4-H_2O

R. E. Leed and C. H. Secoy

The effect of free sulfuric acid on the coexistence curve of the two-liquid phase region of the system uranyl sulfate—water at acid concentrations up to about 0.25 *M* was described previously.[17] The acid was found to decrease the scope of the region (increase miscibility) and to shift the minimum critical solution point to higher temperatures. The upper limit of the two-liquid phase region is the critical temperature of the water-rich phase at which the water-rich phase becomes identical with the vapor phase and the system gains a degree of freedom. The addition of sulfuric acid elevates the upper critical temperature not only because of the acid present but also because of the increased solubility of the uranyl sulfate in the super-critical fluid. The earlier data indicated that, at a sufficiently high acid concentration, the two-liquid phase region would vanish.

During the current quarter this study was pursued further with two objectives in mind. First, additional data were desired concerning the effect of acid and salt on the critical temperature of the water-rich phase, and, second, it was hoped that the vanishing of the two-liquid phase region could be demonstrated experimentally. Although data were obtained in the vicinity of the minimum critical temperature at three higher acid concentrations, neither of the stated objectives was realized. The limitation was the inability (or perhaps the impossibility) to prepare silica tubes with sufficient strength to withstand the high pressures developed. Out of 66 prepared tubes, 46 blew up before data could be obtained. From the remaining 20, fourteen usable points were obtained. The others were prepared for the specific purpose of determining upper critical temperatures, and, even though they did not blow up, they failed to yield reliable data since the liquid volume to vapor volume ratio was such that the meniscus migrated through the end of the tube instead of vanishing within the tube. When the liquid to vapor ratio was properly adjusted, the tubes failed.

(17) Secoy, C. H., "Phase Rule Studies, Effect of Free Sulfuric Acid on the Two-liquid Phase Coexistence Curve of the System Uranyl Sulfate—Water," *Chemistry Division Quarterly Progress Report for Period Ending December 31, 1949*, ORNL-607, p. 33 (Mar. 7, 1950).

-875
9/52

The new data are given in Table 1.10 and shown graphically in Fig. 1.1. The three lower curves in Fig. 1.1 were drawn from previously published data[18] and are reproduced here for the sake of comparison.

Table 1.11 gives the values for the minimum and maximum critical temperatures and in Fig. 1.2 these are plotted against the acid concentration. From these values it appears that both critical temperatures are linear functions of the acid concentration and that, by extrapolation of the straight lines to their intersection, the two-liquid phase region would vanish at an acid concentration of about 3.7 *M* and at a temperature of about 650°C. However, such an extrapolation is not justified. Furthermore, the nice straight lines of Fig. 1.2 are probably more fortuitous than correct since the values are read from Fig. 1.1 and are thus dependent on the manner in which the curves of Fig. 1.1 are drawn.

In view of the failure of the method to yield the desired information, it is improbable that the data can be obtained unless some ingenious method of detecting critical points in metal systems can be developed.

THE MEASUREMENT OF THE SOLUBILITY OF FISSION-PRODUCT SALTS AT HIGH TEMPERATURES AND PRESSURES

M. H. Lietzke and B. Zemel

The revival of interest in homogeneous reactors has created a need for information on the solubilities of fission-product and other salts at high temperatures. This program was begun in an effort to obtain such information. Thus far, the work has been concerned with the study and development of methods, two of which are receiving the most emphasis at the present time. The first of these, a synthetic method, is the quartz-tube method described by Benrath *et al.*[19,20] It depends on the visual observation of the appearance or disappearance of crystals in mixtures of known concentration. It is useful primarily with somewhat soluble salts, or in surveying unknown salts. An analytical method[21] is also being studied for use with solutions more dilute than can conveniently be handled with the quartz-tube method.

The quartz-tube method is presently being used to measure the solubilities of $ZnSO_4$ and $CdSO_4$ over a fairly wide range of temperatures. The $ZnSO_4$

(18) Marshall, Gill, and Secoy, ORNL-795, *op. cit.*, p. 22.

(19) Benrath, A., Gjedebo, F., Schiffers, B., and Wunderlich, H., "Solubilities of Salts and Salt Mixtures in Water at Temperatures above 100°C. I," *Z. anorg. allgem. Chem.* 231, 285 (1937).

(20) Benrath, A., "Solubilities of Salts and Salt Mixtures in Water at Temperatures above 100°C. III," *Z. anorg. allgem. Chem.* 247, 147 (1941).

(21) Booth, H. S., and Bidwell, R., "Solubilities of Salts in Water at High Temperatures," *Am. Chem. Soc. J.* 72, 2567 (1950).

NOT CLASSIFIED
DWG. 10085

-870
9/50

FIG. 1.1
TWO LIQUID PHASE REGION OF THE SYSTEM $UO_2SO_4 - H_2SO_4 - H_2O$

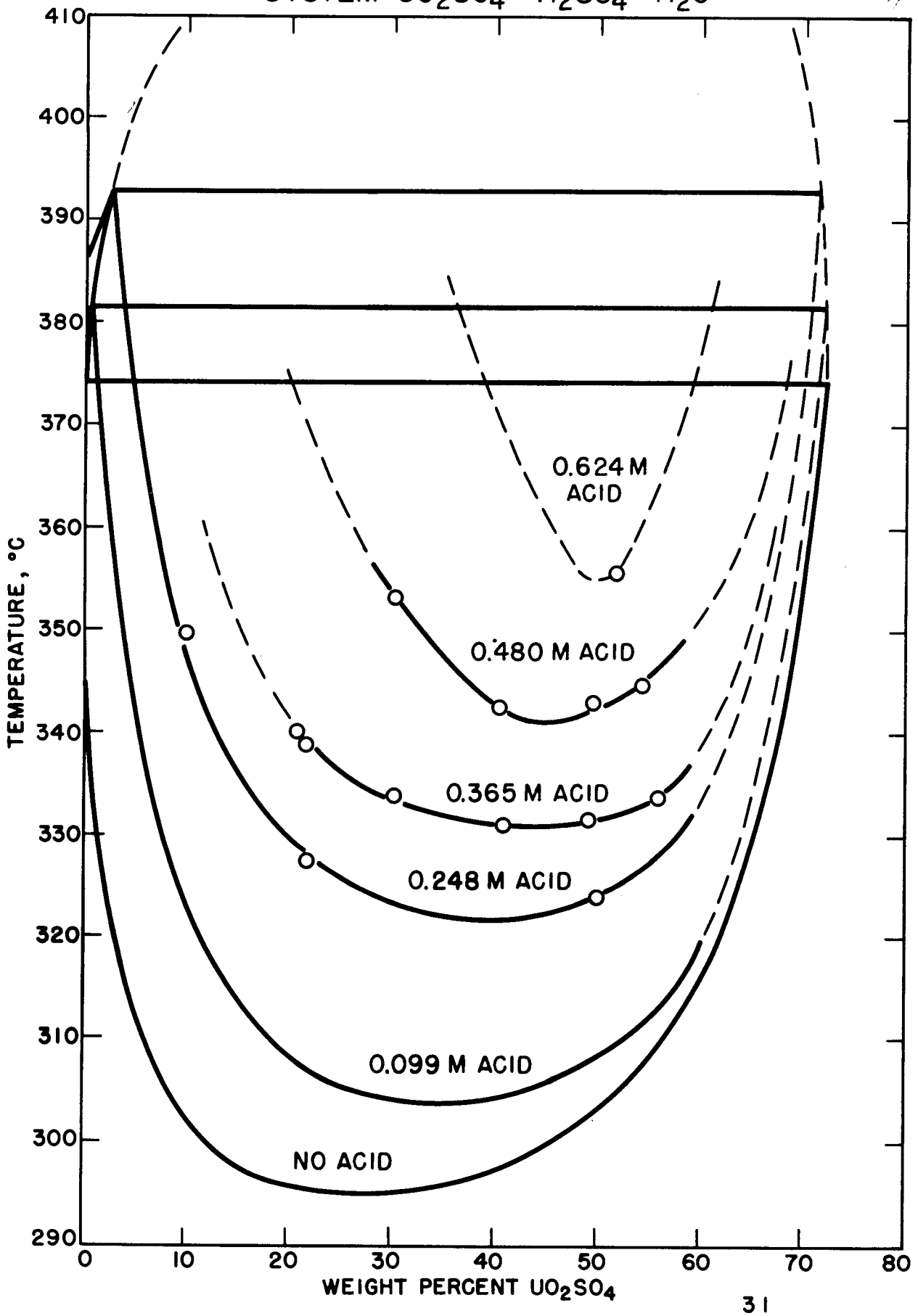

NOT CLASSIFIED
DWG. 9703

FIG. 1.2
UPPER AND LOWER CRITICAL TEMPERATURES
AS FUNCTIONS OF ACID CONCENTRATION

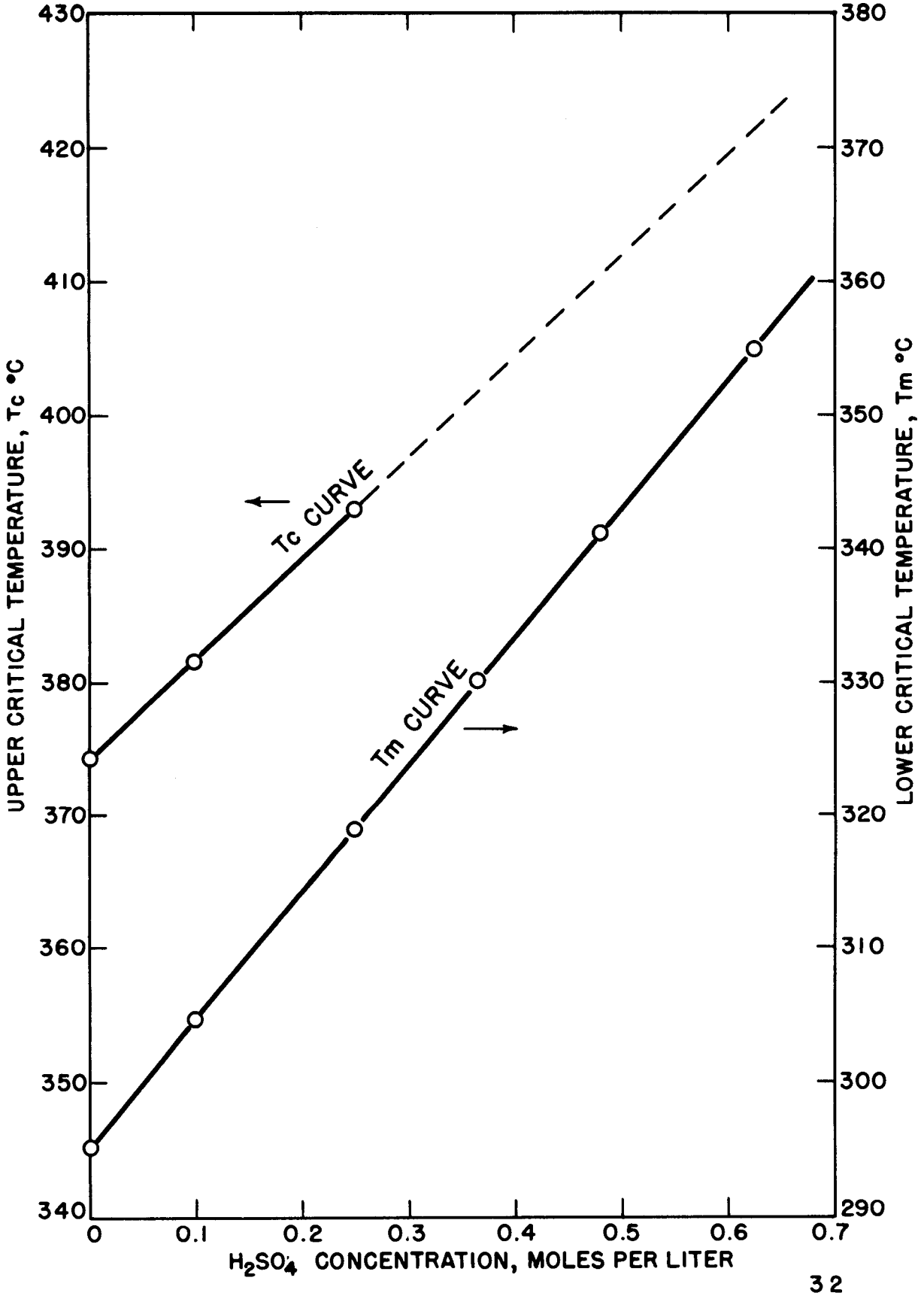

TABLE 1.10

Two-liquid Phase Region of the System UO_2SO_4-H_2SO_4-H_2O

H_2SO_4 (*M*)	UO_2SO_4 (%)	TEMPERATURE OF PHASE SEPARATION (°C)	PHASE SEPARATING
0.248	10.12	349.8	Salt
	21.66	327.5	Salt
	49.99	323.9	Water
0.365	20.90	340.2	Salt
	21.55	338.9	Salt
	30.29	333.9	Salt
	40.92	331.2	Salt
	49.16	331.7	Water
	55.93	333.7	Water
0.480	30.33	353.2	Salt
	40.48	342.7	Salt
	49.67	343.1	Water
	54.29	344.8	Water
0.624	51.84	355.8	Water

TABLE 1.11

Upper and Lower Critical Temperatures

H_2SO_4 (*M*)	LOWER CRITICAL TEMPERATURE, T_m (°C)	UPPER CRITICAL TEMPERATURE, T_c (°C)
0.000	295.2	374.4
0.099	304.7	381.6
0.248	319.0	393.0
0.365	330.2	
0.480	341.2	
0.624	355	

solubility curve has been determined from 135 to 255°C. In this range, the solubility of $ZnSO_4$ in water decreases from 40 to 5%. The data obtained agree extremely well with those of Benrath.[22] Further runs will be made to determine the shape of the solubility curve in solutions more dilute than 5%.

The $CdSO_4$ solubility curve also agrees well with that obtained by Benrath.[23] Values have been obtained over the range from 124 to 181°C. In this range the solubility of $CdSO_4$ in water decreases from about 30 to 7%. Further runs will be made to extend the curve to higher temperatures.

The measurements by the analytical method are being made in a stainless-steel bomb of 12 ml capacity. The bomb is connected through a filter to another tube large enough (3/8 in. I.D. by 2½ in. long) to hold the solution. The filter is of triple-weave stainless-steel cloth, and the tube is likewise of stainless steel. Radioactive tracers are used to simplify the analyses of the saturated solutions.

Preliminary experiments have shown that the sampling and counting are precise to within 1%, and the only difficulties have been with corrosion and with impurities in the tracers. Changes are being worked out to eliminate these problems.

(22) Benrath, 1941, *op. cit.*

(23) Benrath *et al.*, 1937, *op. cit.*

2. NUCLEAR CHEMISTRY

RADIONUCLIDES OF TIN

G. E. Boyd

Progress in the work on the radiochemistry of tin has been reported elsewhere.[1]

Further work has been directed toward clarifying certain details in the decay schemes of the 9.5-min Sn^{125} and 40-min Sn^{123} activities. In particular an examination of the gamma-ray spectrum for each of these radionuclides was made using a scintillation spectrometer on sources which were purified before neutron irradiation of the metal. The 1.9-Mev gamma ray in the 9.5-min Sn^{125} previously found using absorption techniques seemed to be absent, or else to occur in very low relative intensity. The possibility of the emission of a gamma ray of 1.37 Mev in low intensity was indicated, however. Additional measurements are planned to establish this point. No quantum radiations other than the 153-Kev ray appeared to be associated with the 40-min Sn^{123}. The previously reported 0.76-Mev gamma ray observed in absorption measurements must be attributed to an impurity.

(1) Nelson, C. M., Ketelle, B. H., and Boyd, G. E., *Studies on the Nuclear Chemistry of Tin*, ORNL-828 (Nov. 10, 1950).

THE CHARACTERISTISTICS OF Nb^{96} AND Tc^{96}

G. E. Boyd and B. H. Ketelle

Inasmuch as both the 22.9-hr Nb^{96} and the 4.25-day Tc^{96} decay to stable molybdenum, it was of interest to determine if the same levels in Mo^{96} were involved. Accordingly, the beta-ray and conversion-electron spectra of each of these nuclides were determined using a thin magnetic-lens spectrometer. The gamma ray spectrum of the 4.25-day Tc^{96} was measured with a thallium-activated sodium iodide crystal spectrometer. A re-examination of the gamma-ray spectrum of 22.9-hr Nb^{96} is planned. The tentative decay scheme shown in Fig. 2.1 serves to epitomize the available information on these isobars. The scheme for Tc^{96} is the same as that recently proposed by the Swiss[2] except for the additional crossover transitions observed by us at 1648, 1951, and 2419 Kev. Figure 2.2 shows the Kurie-Fermi plot for the 22.9-hr Nb^{96}, assuming an allowed transition.

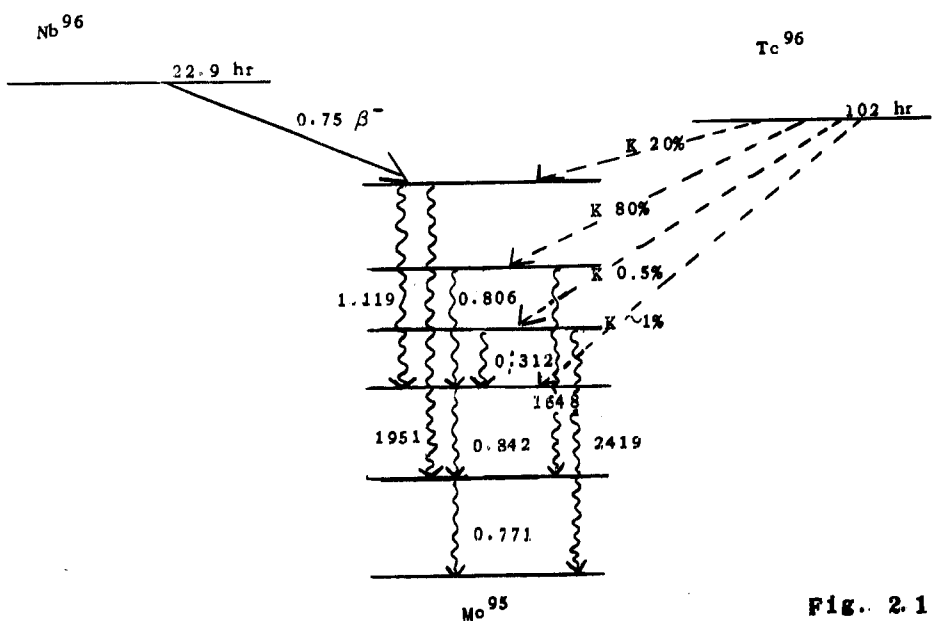

Fig. 2.1

(2) Medicus, H., Preiswerk, P., and Scherrer, P., "Radioactive Decay of the Isotopes of Technetium," *Helv. Phys. Acta* 23, 299 (1950); see also Boyd, G. E., and Ketelle, B. H., "Characterization of Cb96," *Chemistry Division Quarterly Progress Report for Period Ending June 30, 1950*, ORNL-795, p. 44 (Oct. 3, 1950).

NOT CLASSIFIED
DWG. 9571

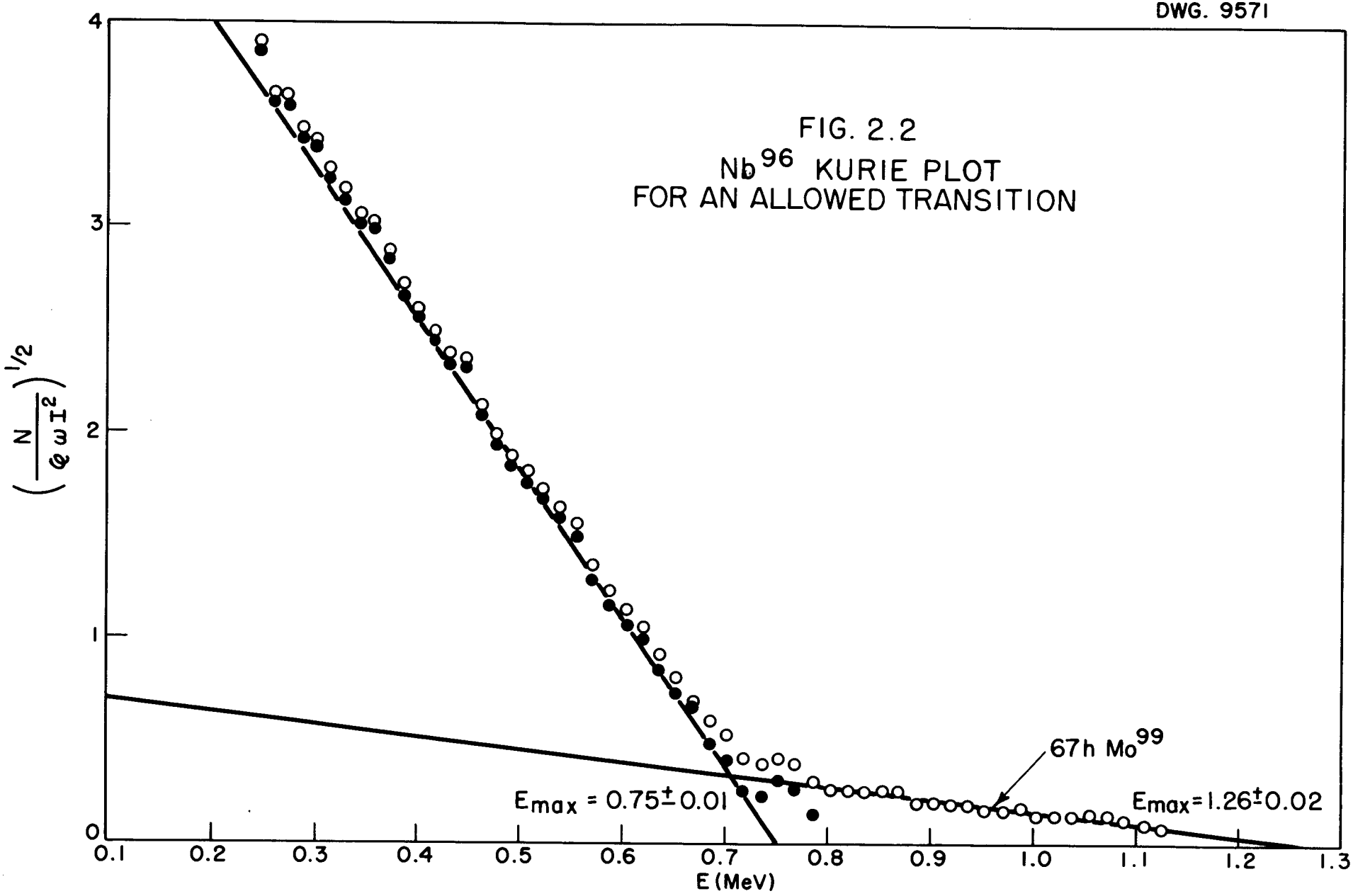

FIG. 2.2
Nb^{96} KURIE PLOT
FOR AN ALLOWED TRANSITION

THE Ca^{45} BETA DISTRIBUTION OBTAINED IN A SPLIT-CRYSTAL SCINTILLATION SPECTROMETER

B. H. Ketelle

Within the past year scintillation spectrometry has been improved to the point where it is possible to determine beta distribution end points with fair precision. Also, when the maximum energy of the distribution is great, the high-energy portion of the distribution appears to fit the shape of the theoretical curves. However, an excess of low-energy betas relative to those of higher energy is also observed. This is presumably due to high-energy betas giving up only a part of their energy within the scintillation medium before being scattered out. Therefore, not only is a small pulse observed but one which should have been large is not recorded. In spite of this difficulty Bell *et al.*[3,4] have been able to obtain useful information concerning the beta spectra of Be^{10} and K^{40}. However, as the maximum energy of the beta distribution under study is reduced, the difficulties of studying its shape increase. Figure 2.3 shows an extreme example in the Kurie plot of Ca^{45} which was obtained using the detection arrangement shown in the insert. The source was mounted on a Formvar film, 25 $\mu g/cm^2$ thick, placed against the crystal with a 0.2 mg/cm^2 aluminum-foil reflector surrounding the optical system. The electronic equipment is similar to that previously described.[5] In Fig. 2.3 the open circles represent the original data and the solid points are the results after correction for the resolution of the instrument, using the method of Owen and Primakoff.[6] Macklin *et al.*[7] have shown that the Ca^{45} disintegration gives an allowed beta distribution with an end point at 254 ± 3 Kev. The straight line in Fig. 2.3 is drawn from this end point through the high-energy experimental points. If the end point were not known, a satisfactory value could not be obtained from this set of data. Also, the discrepancy between the experimental points and the straight line demonstrates the problem of studying the shape of the distribution of such a low-energy beta.

(3) Bell, P. R., and Cassidy, J. M., "Beta Spectrum of Be^{10}," *Phys. Rev.* 77, 301 (1950).

(4) Bell, P. R., Weaver, B., and Cassidy, J. M., "The Beta Rays of K^{40}," *Phys. Rev.* 77, 399 (1950).

(5) Jordan, W. H., and Bell, P. R., "Scintillation Counters," *Nucleonics* 5, 30 (October, 1949).

(6) Owen, G. E., and Primakoff, H., "Relation Between Apparent Shapes of Monoergic Conversion Lines and of Continuous β Spectra in a Magnetic Spectrometer," *Phys. Rev.* 74, 1406 (1948).

(7) Macklin, P., Feldman, L., Lidofsky, L., and Wu, C. S., "The Beta Spectrum of Ca^{45}," *Phys. Rev.* 77, 137 (1950).

NOT CLASSIFIED
DWG. 9569

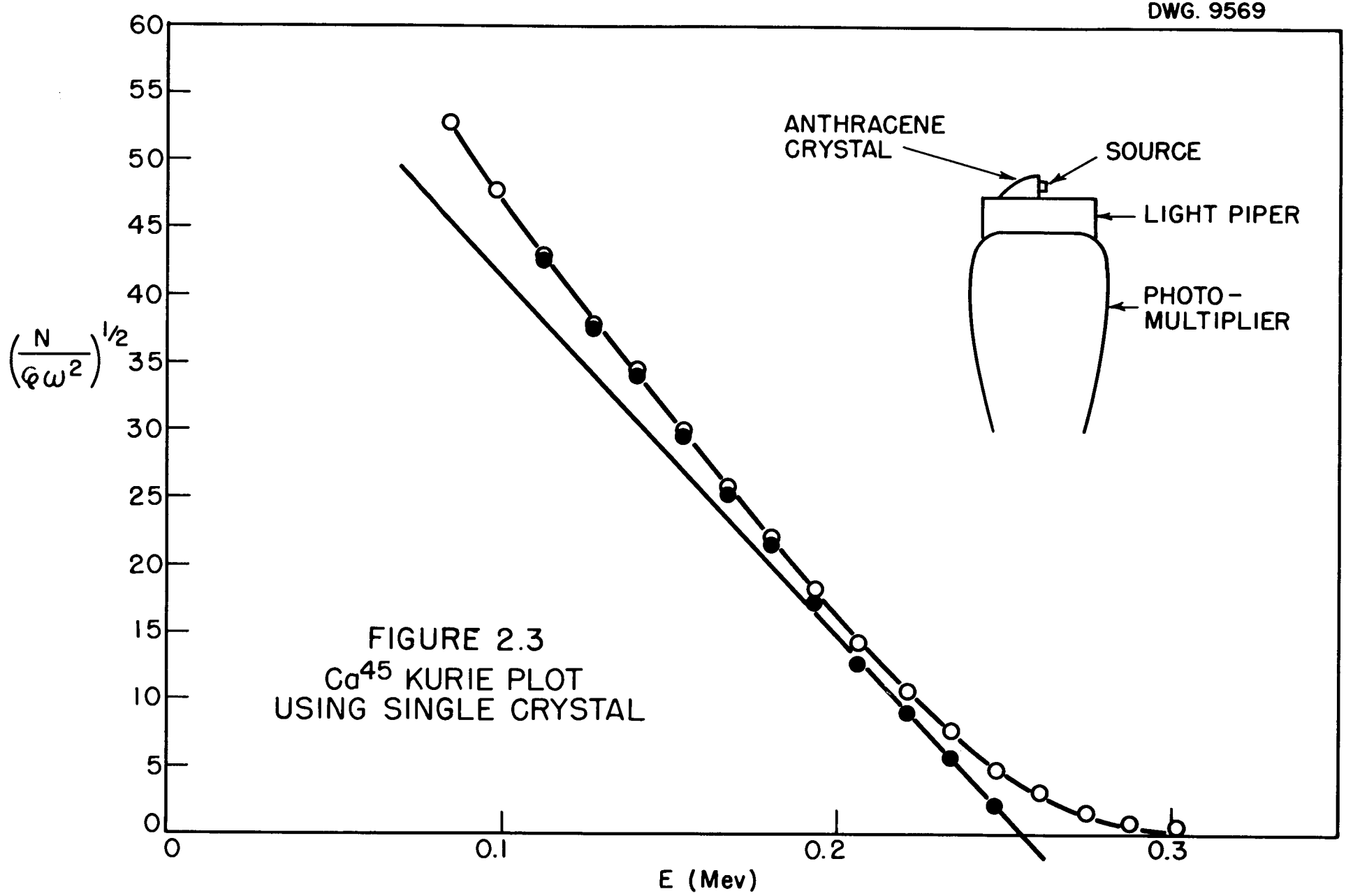

FIGURE 2.3
Ca^{45} KURIE PLOT
USING SINGLE CRYSTAL

Since the resolution correction is large only near the ends of the distribution, it would be desirable to utilize the data in the mid-region for determining the end-point energy. Furthermore, these data can be obtained with better counting statistics but only if the extraneous low-energy pulses can be eliminated. If the above explanation of their origin is correct, it should be possible to eliminate the difficulty by placing the source between two crystals in such a manner that the probability of observation of the scattered betas in the second crystal is great. Although this might be accomplished by using two crystals and two photomultipliers, the more simple arrangement shown in the insert of Fig. 2.4 was tried. The two anthracene crystals were matched to give equal pulse heights and resolution individually for the Cs^{137} conversion line. When this source was placed between the crystals the observed number of pulses doubled, but the pulse height of the peak was unchanged and the resolution remained equal to that of each crystal alone, *i.e.*, 6.5% half-width at half-height. The Kurie plot of Ca^{45} shown in Fig. 2.4 was obtained with the source mounted between 25 $\mu g/cm^2$ Formvar films placed between the two crystals which were in contact. The resolution correction has been made. Since the plot is linear from 50 Kev to the end point, we can now rely largely upon points obtained with good statistics to obtain the end point. The value obtained is 255 ± 4 Kev, in good agreement with the previously reported,[7] as is also the spectrum shape. Thus it appears that this split-crystal spectrometer can give reliable information about the shapes and maximum energies of low-energy beta emitters.

Credit for the success of this study is due in large part to helpful discussions with C. J. Borkowski, A. R. Brosi, and H. Zeldes, and to R. A. Dandl and E. Fairstein, who designed and calibrated the electronic circuits.

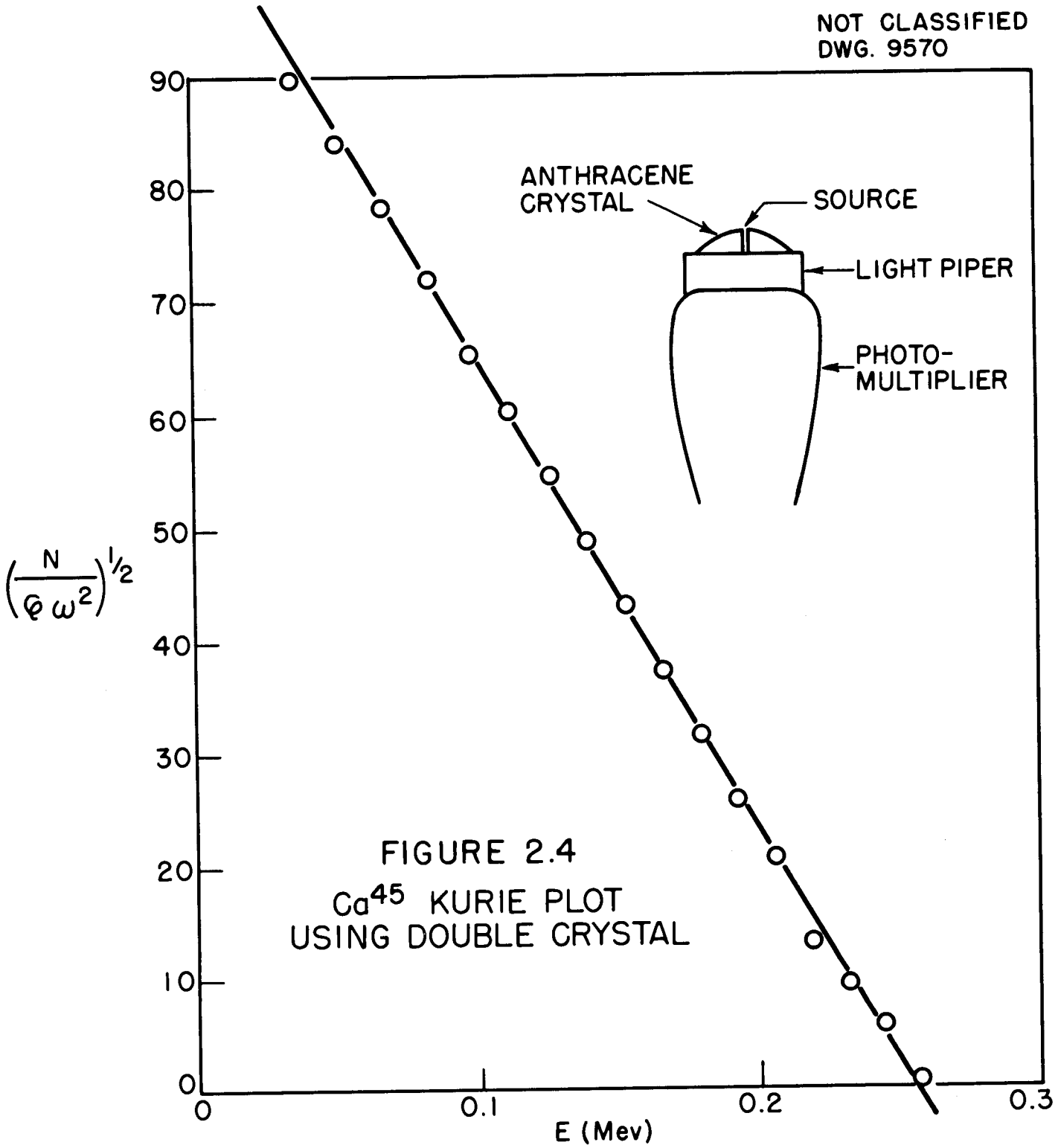

FIGURE 2.4
Ca^{45} KURIE PLOT
USING DOUBLE CRYSTAL

A TWO-DAY Xe^{133} ISOMER

B. H. Ketelle A. R. Brosi
H. Zeldes

A long-lived Xe^{133} isomer has been postulated in a decay scheme recently published by Bergström and Thulin.(8) Since the possible presence of a long-lived Xe activity among the products of uranium fission is important in several phases of project work, an attempt has been made to confirm the work of Bergström and Thulin. They collected the Xe^{133} produced in uranium fission in a thin aluminum foil using an electromagnetic isotope separator. This foil was then used as a source in a beta spectrometer. In addition to the known radiations of 5.3-day Xe^{133} they found conversion-electron lines corresponding to a gamma-ray energy of 232 Kev. Because they found the 232-Kev gamma ray to decay with the same half-life as the 5.3-day beta group, they proposed the theory that both transitions are from a single metastable level in Xe^{133}.

In repeating the work of Bergström and Thulin, the fission product xenons were produced by a bombardment and collection schedule which eliminated all known active xenons other than Xe^{133} except for a trace of 12-day Xe^{131}. The sample was highly purified from other elements, using an adsorption-column technique, and mounted as a source in the thin-lens spectrometer in the same way as that described for Kr^{85} in the last quarterly report.(9)

The conversion lines reported by Bergström and Thulin were found but did not decay with the same half-life as the beta spectrum. The half-life of the 235-Kev gamma ray was measured by following the decay of the unconverted gamma ray with a scintillation spectrometer and by following the decay of the conversion electrons in a thin-lens spectrometer. The half-life was found to be 51 hr in contrast to the 5.3-day half-life for the Xe^{133} beta radiation.

Tentative values for the branching ratio in I^{133} decay leading to the 51-hr Xe^{133} isomer and for the K conversion coefficient have been determined. It was found that 2.4% of the I^{133} disintegrations go through the 51-hr isomer

(8) Bergström, I., and Thulin, S., "On the Decay of Xe^{133m}," *Phys. Rev.* 79, 538 (1950).

(9) Zeldes, H., Ketelle, B. H., and Brosi, A. R., "Radiations of Long-lived Kr^{85} and A^{39}," ORNL-795, *op. cit.*, p. 48.

and that the K conversion coefficient of the 235-Kev gamma ray is 4.2. This conversion coefficient, together with the internal-conversion computations of Rose *et al.*,[10] indicates that a mixture of electric 2^5 pole and magnetic 2^4 pole radiation is emitted in this transition. This is consistent with the nuclear shell model of Mayer where the transition from the $H_{11/2}$ level to the $d_{3/2}$ level would have the observed conversion coefficient.

(10) Rose, M. E., *et al.*, unpublished work.

A RE-EVALUATION OF THE HALF-LIFE OF Tc^{99}

G. W. Parker

The direct measurement of the half-life of the long-lived isotope of element 43 (Tc^{99}), which is formed in high yield in U^{235} fission,[11] as well as by neutron irradiation of molybdenum has been reported, without much claim for precision, by several investigators.[12-14] A recent exception to this is some work by Sherman Fried[15] and coworkers[16] in which the absolute disintegration rates of accurately weighed compounds of technetium of known composition were determined. Before being apprised of the status of the work by Fried, a separate attempt to obtain an improved half-life value has been begun in conjunction with a program for the purification of gram quantities of the element.[17]

On the basis of the well-characterized compound formed by the perrhenate ion with tetraphenyl arsonium chloride,[18] the analogous pertechnetate compound has been prepared and used as a gravimetric form in a new measurement of the specific activity of Tc^{99}. As a result the half-life value has been revised downward to a tentative figure of 2.2×10^5 years, in almost perfect agreement with the value of 2.1×10^5 years given by Fried.

The inacceptability of the sulfide Tc_2S_7 in gravimetric work was confirmed also.

(11) The Plutonium Project, "Nuclei Formed in Fission: Decay Characteristics, Fission Yields, and Chain Relationships," *Am. Chem. Soc. J.* 68, 2411 (1946).

(12) Schuman, R. P., *Note on a New 43 Activity*, Chicago Report CC-3434 (Feb. 7, 1946).

(13) Motta, E. E., Boyd, G. E., and Larson, Q. V., "Production and Properties of a Long-lived Radioisotope of Element 43," *Phys. Rev.* 72, 1270 (1947).

(14) Parker, G. W., Reed, J., and Ruch, J. W., *Isolation of Milligram Amounts of Element 43 from Uranium Fission*, AECD-2043 (Jan. 9, 1948; decl. June 4, 1948).

(15) Fried, S., private communication, September, 1950.

(16) Jaffey, A. H., Fried, S., Hall, N. F., and Glendenin, L. E., "Half Life of the Long-lived Tc^{99}," *Bull. Am. Phys. Soc.*, 25, No. 5, 11 (1950).

(17) Parker, G. W., Lantz, P. M., Hebert, G. M., Martin, W. J., and Creek, G. E., "Recovery of Fission Products and Neptunium from ORNL Redox Pilot Plant CR Wastes," ORNL-795, *op. cit.*, pp. 51ff.

(18) Willard, H. H., and Smith, G. M., "Tetraphenylarsonium Chloride as an Analytical Reagent. Determination of Rhenium," *Ind. & Eng. Chem. Anal. Ed.* 11, 305 (1939).

RECOVERY OF FISSION PRODUCTS AND NEPTUNIUM FROM CHALK RIVER WASTES

INITIAL OPERATION

G. W. Parker G. M. Hebert
G. E. Creek P. M. Lantz
W. J. Martin

Summary. Since the previous quarterly progress report, full-scale runs (3000 curies of mixed fission products) have been handled in the three-cell installation described in ORNL-795.[19] It was found, in agreement with prior estimates, that radiation leakage through the cell walls was not above tolerance. Because of the considerably later starting time than had been hoped for, most of the chromium in the wastes now requires oxidation, thereby having the effect of diminishing by 25% the quantity (200 liters) previously intended to make up a run. The first two runs were made with only a minor difficulty resulting from a spill of part of the technetium product from run 2.

Analysis of Chalk River Fission Product Run 1. The technetium product, which was obtained in concentrated H_2SO_2 solution, was analyzed and was found to contain a gross beta activity of only about 40 millicuries, principally zirconium, niobium, and ruthenium. This represents a decontamination factor of about 10^5 in one step, illustrating the extreme selectivity of the tetraphenyl arsonium perchlorate as a carrier for technetium.

After decomposition of the organic portion of the solution by the Kjeldahl procedure using selenium as catalyst, the technetium was distilled into sulfuric acid and precipitated as the sulfide. The yield of about 250 mg of purified technetium is regarded as only fair, although no ultimate analysis has been made on the starting solution.

The neptunium product, together with the large amount of rare earth activities, was obtained in 15 liters of dilute nitric acid and was placed in storage after sampling for analysis. According to the initial size of

(19) Parker, G. W., *et al.* ORNL-795, *op. cit.*, pp. 51ff.

the runs, a total of 20 will be required to process all the Chalk River waste. Unfortunately a minor leak in the main line to the holding tanks has caused a delay in processing until it can be repaired and the contamination removed. A summary of the recovery of two of the by-products is given in Table 2.1.

TABLE 2.1
Recovery of By-products

RUN NO.	YIELD OF PURIFIED AND SEPARATED Tc^{99} (g)	YIELD OF UNSEPARATED Np^{237} (g)
1	0.25	0.05
2	Analysis incomplete	0.06

COPRECIPITATION OF PERTECHNETATE (TcO_4^-) AND VARIOUS ANIONS BY TETRAPHENYL ARSONIUM CHLORIDE

G. W. Parker and W. J. Martin

Introduction. In the process of selecting a carrier for technetium suitable for a precipitation process to be used in the recovery of Tc^{99} from the Chalk River Redox wastes, a method employing perrhenate as a carrier and tetraphenyl arsonium chloride (TPA chloride) as the precipitant was first proposed because of the unique similarity between the pertechnetate ion and the perrhenate ion. For several reasons, including the cost of rhenium and the difficulty of later separating it from the technetium, a substitute carrier which could be used liberally and separated easily has been sought.

Summary. Besides perrhenate, it has been found that any of a certain type of anion, especially those comprising the perhalogen acids perchlorate and periodate, will form an efficient carrier for pertechnetate. Of these, periodate is the most effective, although for decontamination perchlorate is more satisfactory. Besides these, fluoborate (BF_4^-) is at least as good as if not better than perrhenate, while permanganate is fair but forms an explosive mixture. The fact that anions of the type XY_4^- form the only good carriers seems to support the formula TcO_4^-. A few anions of the form $XY_4^=$, such as $CrO_4^=$ or $S_2O_8^=$, carry in a much weaker fashion with large excesses of the reagent.

Conditions for Comparing the Carrying Efficiency of Various Anions. Several conditions in the starting solution affect the choice of carrier. The presence of aluminum eliminates the use of fluoborate, since the latter, although a good carrier, is unstable in the presence of aluminum ion. The large volume of solution (85 gal per batch) and the small amount of precipitate feasible to handle (100 g) require a carrier working satisfactorily below 10^{-3} *M*. Large excess of tetraphenyl arsonium chloride must be avoided because it forms an insoluble precipitate with carbonate in a later step, and a suitable carrier must therefore precipitate nearly quantitatively with only a small excess of the reagent.

Procedure for Testing Various Anions. To 200 ml of the synthetic working solution, 0.1 ml (~10,000 c/m) of a Tc^{99} tracer solution was added, followed by 0.1 to 0.2 ml of the selected carrier in 1 *M* solution. This mixture was warmed in a 250-ml erlenmeyer flask to about 70°C before the calculated quantity (1.0 to 2 ml) of a 5% solution of the TPA chloride was introduced with stirring. At this temperature the TPA pertechnetate was usually completely soluble, but it precipitated slowly on cooling, forming large easy-filtering crystals.

For comparative counting, the precipitates were collected on 30-mm medium-porosity low-form filter crucibles which could be dried, weighed, and counted at known geometry under an end-window G-M counter. The weight of the precipitate as well as the count was used as a measure of yield. As a further check, a follow-up or scavenging precipitation was made by adding more carrier and more precipitant and counting and weighing as before.

A comparable standard was prepared for perchlorate, perrhenate, and periodate ions by precipitating aliquots of the tracer with these carriers under more favorable conditions, *i.e.*, in small volume salted with NaCl, for a quantitative yield. In this way, with duplicate samples and comparison of counting rates it was possible nearly to eliminate the effect of self-absorption, etc., in the different masses of the mounted sample. These, however, were kept within the limits of 60 to 100 mg. The results are given in Table 2.2.

TABLE 2.2

Efficiency of Carrier Anions for TcO_4^- Precipitated with Tetraphenyl Arsonium Chloride*

ANION	CONCENTRATION (*M*)	Tc CARRIED AS $(C_6H_5)_4As^+$ COMPOUND RELATIVE TO ReO_4^- (%)	REMARKS
ReO_4^-	0.0007	100	
IO_4^-	0.0007	106	Precipitate and anion relatively unstable; precipitates $Ce(IO_3)_4$, etc.
ClO_4^-	0.0007	95	
BF_4^-	0.0009	105	Unstable in presence of $Al(NO_3)_3$
MnO_4^-	0.0008	50	Dissolves in H_2SO_4 with explosive violence
IO_3^-, BrO_3^-, ClO_3^-, BO_3^-	0.01	None	
$SiF_6^=$, $ZrF_6^=$	0.01	None	
$SiO_2 \cdot 12WO_3^=$	0.001	Trace	
$CrO_4^=$, $S_2O_8^=$	0.001	None	Precipitates only with large excess of the reagent

*Approximately twice the equivalent volume of excess reagent was added in each test.

STUDIES ON SZILARD-CHALMERS REACTIONS WITH $KBrO_3$

G. E. Boyd and J. W. Cobble

The now extensive investigations on the recoil reactions in neutron-irradiated $KBrO_3$ are nearly completed. In the near future three laboratory reports will be issued presenting what are believed to be a number of interesting findings. The first of these (ORNL-815) will report on the production of high specific activity Br^{82} by a Szilard-Chalmers reaction with crystalline $KBrO_3$. Here, specific activities as high as 820 rutherfords/mg, corresponding to a 21,000-fold enrichment, were obtained. Quantitative measurements of the variation of the specific activity with irradiation time and neutron source intensity were found to agree with an elementary theory based upon the activation equation and the assumption that the rate of the nonactivating radiation decomposition of $KBrO_3$ was proportional to the mass irradiated and to the power. The prediction that the specific activity will be independent of the pile power and will decrease steadily with increasing irradiation time was confirmed, as was the predicted inverse dependence of the enrichment on power and time. The retention of radiobromine as bromate was found to increase with time and to be independent of power.

An account of the detailed investigation of the retention of 35.9-hr Br^{82} by neutron-irradiated $KBrO_3$ is given in a second report (ORNL-905), while a third report (ORNL-814) undertakes to present and discuss the various factors governing the nonactivating radiation decomposition of this salt.

3. RADIO-ORGANIC CHEMISTRY

SYNTHESIS OF LOW-MOLECULAR-WEIGHT INTERMEDIATES CONTAINING C^{14}

METHANOL-C^{14}

W. J. Skraba and E. Dowling

By a modification of a method developed by Tolbert,[1] carbon dioxide-C^{14} was catalytically reduced to methanol-C^{14} under 4000 psi pressure at 285° for 6 hr; 120 mc of pure methanol-C^{14} was prepared.

(1) Tolbert, B. M., "Synthesis of Carbon Radioactive Methyl Iodide and Methanol from Carbon Dioxide," *Am. Chem. Soc. J.* 69, 1529 (1947).

SYNTHESIS OF HIGH-MOLECULAR-WEIGHT COMPOUNDS CONTAINING C^{14}

SYNTHESIS OF CHRYSENE-5,6-C_1^{14}

C. J. Collins and R. H. Mayor*

Discussion. Chrysene has been prepared again with the emphasis upon obtaining accurate analytical data for the intermediate compounds. The reaction shown below, which was recorded in the last Quarterly Report,[2] has been repeated. The yield activity of the compounds is shown in microcuries per millimole.

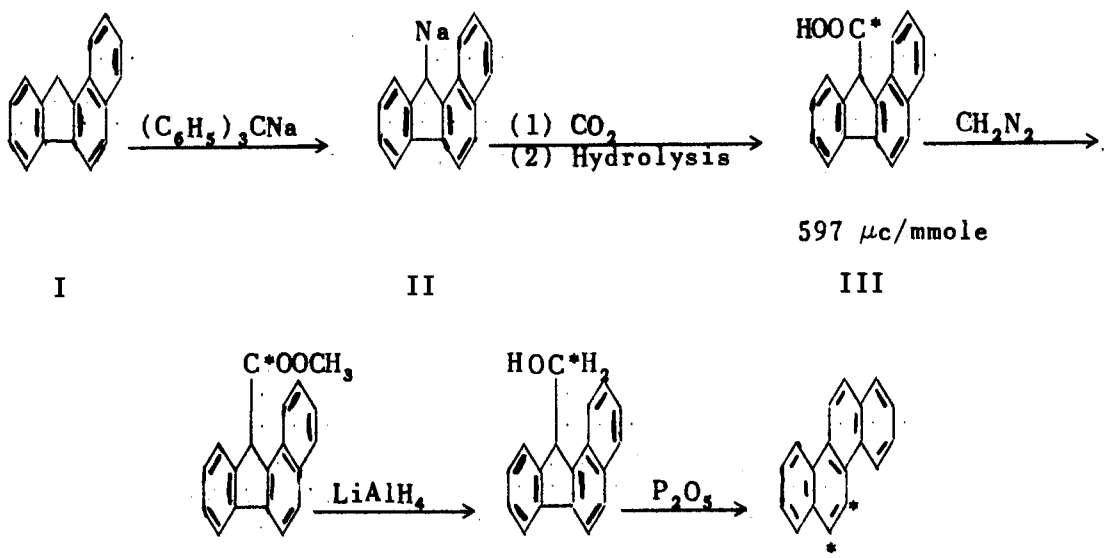

A new technique, the "double-dilution method," is described for the analysis of chrysene-5,6-C_1^{14} (VI).

Experimental.

(1) *1,2-Benzofluorene.* A normal-pressure hydrogenation using 1.75 g of 1,2-benzofluorenone, 1.66 g of 10% palladium-on-carbon catalyst, and 10 ml of

(2) Collins, C. J., Toffel, G., and Jones, A. R., "The Mechanism of the Wagner Rearrangement. II. The Synthesis of Chrysene-5,6-C_1^{14}," *Chemistry Division Quarterly Progress Report for Period Ending June 30, 1950*, ORNL-795 (Oct. 3, 1950).

* ORINS-ORNL research participant, Rhode Island State College.

95% ethanol was allowed to proceed with magnetic stirring for 24 hr. The catalyst was filtered and washed repeatedly with hot benzene, hot alcohol, and acetone. The filtrate and washings were evaporated to dryness, and the residue was recrystallized from benzene and from 95% alcohol, giving 1.05 g (64%) of the hydrocarbon, m.p. 182-183°.

(2) *1,2-Benzofluorene-9-carboxylic Acid-10-C^{14}.* Using the procedure of Collins,[3] 943 mg (4.37 mmoles) of benzofluorene was treated with 4 mmoles of triphenylmethyl sodium solution followed by excess $C^{14}O_2$ gas, 3.69 mmoles of which was absorbed. The activity of the $C^{14}O_2$ was 654 μc/mmole. The product was treated with water, extracted with ether to remove triphenylmethane and unreacted benzofluorene, acidified, and again extracted with ether to remove the 1,2-benzofluorene-9-carboxylic acid. The ether was evaporated, yielding 400 mg (42%) of the crude acid. A portion of the acid recrystallized several times from benzene assayed 597 μc/mmole.

(3) *Methyl 1,2-Benzofluorene-9-carboxylate-10-C^{14}.* Attempts to esterify the benzofluorene carboxylic acid using methanol and dry HCl and using 100% H_2SO_4 followed by methanol were unsatisfactory. The ester was prepared, however, by treating 146 mg of the acid in dry methanol with an excess of diazomethane in ether. The resulting solution was evaporated to dryness, and the residue was recrystallized from methanol, yielding 113 mg (73%) of white crystals, m.p. 135-135.5°, which assayed 596 μc/mmole.

(4) *1,2-Benzofluorene-9-carbinol-10-C^{14}.* Approximately 150 mg of crude ester was treated with excess $LiAlH_4$ in dry ether at 0°C. The resulting solution was stirred for 1 hr, treated with water to decompose excess hydride, and with hydrochloric acid to dissolve precipitated solids. The ether layer was decanted, and the aqueous layer was extracted with ether. The combined ether layers were washed with sodium bicarbonate solution and with water, and the ether was evaporated. The residual oil resisted all attempts at crystallization. Even after passage through a chromatograph consisting of a 12- by ¾-in. column of alumina, only traces of solid materials, coated with oils, could be obtained, and these could not be purified. They appeared to melt at about 55-60°. About 20 mg of the carbinol was heated with *p*-bromobenzoyl chloride in dry pyridine for 2 hr at 60-70°, poured into ice water, and filtered.

(3) Collins, C. J., *et. al., op. cit.*

The solid residue was dissolved in ether, washed with Na_2CO_3 solution and with water, and evaporated to dryness. The gummy residue was washed with alcohol, leaving a solid residue, which, after recrystallization from alcohol, melted at 167-167.5° after sintering at 162°; it assayed 592 μc/mmole.

(5) *Chrysene-5,6-C^{14}*. The remainder of the crude carbinol (containing a maximum of 80 mg of carbinol if the ester reduction was quantitative) was dissolved in 25 ml of dry xylene and heated under reflux with 3 g of P_2O_5 for 45 min. The mixture was cooled and treated with water, the organic layer was removed, and the aqueous layer was extracted several times with ether and with benzene. The combined organic layers were washed with water and evaporated to dryness. The yellow oily residue appeared to be very crude. Passage through a chromatograph followed by several recrystallizations from alcohol failed to give a sharply melting product. The product was finally isolated after dilution with inactive chrysene.

In order to determine the approximate activity of the original chrysene as well as the yield from the rearrangement reaction, two successive dilutions of the reaction product were made, and pure samples of the diluted chrysene were assayed after each dilution. Since a dilution can produce no change in total activity present, it is obvious that the product of specific activity and total weight must be constant for any dilution. Thus, after the first dilution,

$$A_0X = A_1(D_1+X) \qquad (1)$$

where A_0 and A_1 are the original and diluted activities, respectively, and X and D_1 are the weights of active and inactive chrysene, respectively. If the total weight of sample removed for assay after the first dilution is S, then after the second dilution

$$A_1(D_1+X-S) = A_2(D_2+D_1+X-S) \qquad (2)$$

where D_2 is the weight of inactive chrysene used for the second dilution and A_2 is the resulting activity.

From Eq. (2), then,

$$X = A_2D_2/(A_1-A_2) - (D_1-S)$$

and from Eq. (1)

$$A_0 = A_1 \ (D_1+X)/X$$

Data obtained in the isolation of chrysene are as follows: D_1 = 98.8 mg, D_2 = 950 mg, S = 6.7 mg, A_1 = 141.7 μc/mmole, and A_2 = 16.32 μc/mmole. From these data the yield, X, is 31.5 mg and the activity, A_0, 586 μc/mmole.

3,4-BENZOFLUORENE-9-CARBOXYLIC ACID

D. N. Hess

Discussion. As preparation for a study of the Wagner rearrangement of 3,4-benzofluorenemethanol, unlabeled ethyl cinnamate was converted by known procedures to 3,4-benzofluorene. This hydrocarbon was carbonated in 84% yield by the procedure used by Collins.[4]

Experimental. Triphenylmethyl sodium was added to 0.93 g (4.3 mmoles) of 3,4-benzofluorene, and the solution was equilibrated with 4.87 mmoles of carbon dioxide, of which 3.80 mmoles was absorbed. The reaction mixture was taken up in water, extracted with ether, and acidified to precipitate the product; 0.95 g of crude product was obtained, m.p. 217-222°.

(4) Collins, C. J., "The Synthesis of Phenanthrene-9-C^{14}," *Am. Chem. Soc. J.* 70, 2418 (1948).

REACTION MECHANISM STUDIES

THE REACTION OF 9-FORMYLFLUORENE WITH FORMALDEHYDE

J. G. Burr

Discussion. The action of excess aqueous basic formaldehyde solution upon 9-formylfluorene has been found by Brown and Bluestein[5] to give 9-fluorenemethanol. The usual action of this reagent on aldehydes with one alpha hydrogen gives β,β-disubstituted trimethylene glycols.[6] In the experiments described below it was shown that the action of excess aqueous basic formaldehyde solution upon 9-formylfluorene-10-C^{14} (I) gives 9-fluorenemethanol which is nonradioactive. Substantially all the initial radioactivity appeared as formate ion. Unreacted formaldehyde is nonradioactive, ruling out any exchange between formylfluorene and formaldehyde, or between formate and formaldehyde. Thus the mechanism suggested by Brown and Bluestein, shown below, is supported.

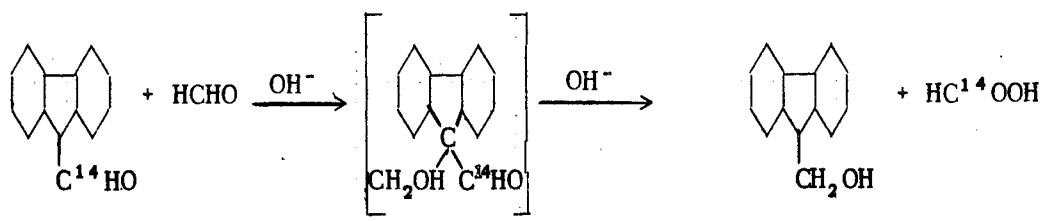

I II III

The instability to alkali of the tertiary aldehyde (II) is paralleled by the instability to alkali of other highly negatively substituted tertiary aldehydes such as chloral, triphenylacetaldehyde, and acetylenic aldehydes.[7]

It is probable that the factor which decides whether a tertiary aldehyde such as II will cleave or undergo a crossed Cannizzaro reaction to give a disubstituted trimethyleneglycol is the stability of the ionic intermediate

(5) Brown, W. G., and Bluestein, B. A., "Alkylation and Other Reactions of 9-Formylfluorene," *Am. Chem. Soc. J.* 65, 1082 (1943).

(6) Adams, R., *Organic Reactions*, Vol. II, p. 100, Wiley, New York, 1949.

(7) *Ibid.*, p. 99.

which would result from loss of the aldehyde group. Therefore the reactions of formaldehyde with other C^{14}-labeled tertiary aldehydes are now under study in this laboratory.

Experimental. Sodium formate-C^{14} was converted in quantitative yield to ethyl formate by the action of triethyl phosphate.[8] This ethyl formate-C^{14} was converted to 9-formylfluorene-10-C^{14} (I) by the procedure of Wislicenus and Waldmüller.[9] The product was assayed as the benzoate, m.p. 157-158°, radioactivity 10.15 μc/mmole. The formylfluorene (I) was converted in 97% yield to fluorenemethanol (III), which after two crystallizations melted at 99-100°, and showed only background radioactivity. The aqueous solution from this reaction was mixed with 1.057 g of nonradioactive sodium formate, and a portion of the solution was treated with S-benzylthiuronium chloride. The precipitated formate derivative, m.p. 148-149°, showed radioactivity of 0.00481 μc/mmole, corresponding to a total activity as formate of 21.5 μc as compared to 22.9 μc of initial activity as formylfluorene. Another portion of this aqueous solution was treated with aqueous dimedon solution. The precipitated dimedon-formaldehyde derivative, crystallized once, showed only background activity.

THE REARRANGEMENT OF α,β-DIOXOBUTYRATE

H. W. Davis* and O. K. Neville

Discussion. Ethyl α,β-dioxobutyrate rearranges and hydrolyzes in aqueous alkali to methyltartronic acid.[10] A benzilic acid type rearrangement would allow rapid, reversible addition of hydroxyl ion to one carbonyl group to form one or both of the ionic intermediates II and III. A more reasonable mechanism for the formation of the ion III would be ionization of a proton from the stable hydrate whose structure is probably IV. The acid product, V

---

* ORINS-ORNL Research Participant, University of South Carolina.

(8) Ropp, G. A., "Preparation of Ethyl Acetate-2-C^{14} and *n*-Butyl Acetate Using Alkyl Phosphates," *Am. Chem. Soc. J.* 72, 2299 (1950).

(9) Wislicenus, W., and Waldmüller, M., "9-Formylfluorene. I.," *Ber.*, 42, 785 (1909).

(10) Denis, W., "On the Behavior of Various Aldehydes, Ketones, and Alcohols Towards Oxidizing Agents," *Am. Chem. J.* 38, 561, esp. 587 (1907).

or VI, methyltartronic acid in either case, could then be formed by the migration of the methyl group in the first case or the carbethoxy group[11] in the

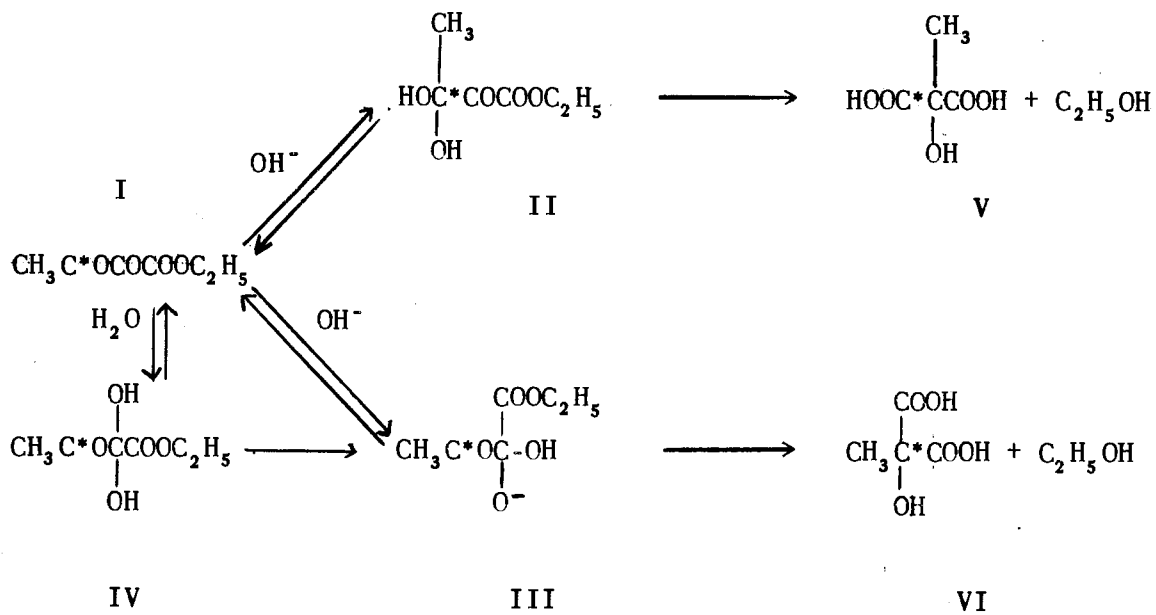

second case. The identity of the migrating group may be determined by the use of a labeled carbon atom (marked by an asterisk in the scheme above) in one of the carbonyl groups.

Roberts, Smith, and Lee[12] have recently shown that diphenyltriketone rearranges by the migration of a benzoyl group. Similar reasoning in the present case would predict a shift of the carbethoxy group following the formation of the intermediates IV and III.

In order to determine the identity of the migrating group, ethyl α,β-dioxobutyrate-β-C^{14} was prepared by oxidation of ethyl aceto-1-C^{14}-acetate and converted to methyltartronic acid. Decarboxylation of this product gave carbon dioxide which was nonradioactive and lactic acid (recovered as zinc lactate) containing all the initial C^{14} activity.

The radioactivities of the organic compounds, given in the reaction scheme below as microcuries per millimole, were determined by wet combustion of each

(11) Whether the carbethoxy group is hydrolyzed before or after rearrangement has not been determined.

(12) Roberts, J. D., Smith, D. R., and Lee, C. C., "Decarbonylation of Diphenyltriketone," *Am. Chem. Soc. J.*, in press.

compound to carbon dioxide and determination of the ion current with a vibrating-reed electrometer. Thus it was established that the migrating entity is the carbethoxy group.[11]

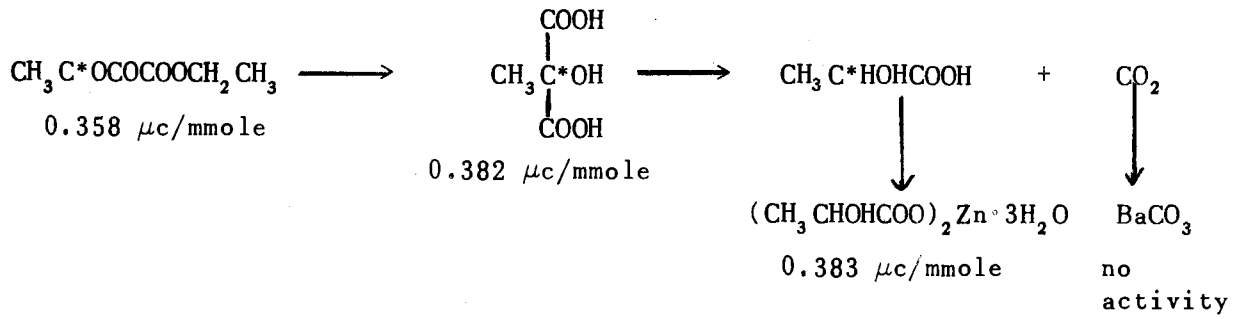

The preparation of α,β-dioxobutyrate-β-C^{14} from ethyl aceto-1-C^{14}-acetate[13] involved conversion to the isonitroso compound with nitrous acid and treatment of this with nitrogen trioxide. This procedure gave a cleaner product and better yield than did treatment of ethyl acetoacetate with selenium dioxide[14] or with nitrogen trioxide directly.

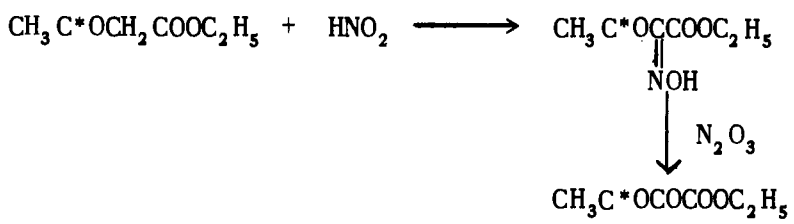

Experimental.

(1) *Ethyl α,β-Dioxobutyrate-β-C^{14}.* A 40-g portion of ethyl aceto-1-C^{14} acetate was mixed with 26.7 g of sodium nitrate in a 500-ml flask and cooled to 0°C. A cooled solution of 16.9 g of concentrated sulfuric acid in 100 ml of water was added over a 2-hr period. After the mixture was stirred for an

(13) The preparation of ethyl acetoacetate-β-C^{14} was described previously: Grovenstein, E., Jr., and Neville, O. K., "Ethyl Acetoacetate-3-C^{14}," *Chemistry Division Quarterly Report for Period Ending September 30, 1949*, ORNL-499, p.68 (Dec. 6, 1949).

(14) Müller, R., "Zur Kenntniss der spezifischen Oxydationswirkung des Selendioxyds," *Ber.*, 66, 1668 (1933).

additional 2-hr period, it was diluted with 90 ml of water and extracted with ether. The dried ether solution of the isonitroso compound was treated, at 0°, with nitrogen trioxide gas for a 2-hr period, until no more gas was absorbed. After the solution was allowed to stand for two days, it was stripped of ether and distilled at 23 mm. The fraction boiling at 77-85°, weighing 16.5 g, was collected and dissolved in 20 g of water. The aqueous solution, treated with solid calcium carbonate to remove acid by-products, was extracted thoroughly with fifteen 10-ml portions of ether. The ether solution was dried, evaporated, and distilled through a 3-ft Vigreaux column at 9.5 mm. The yield was 8 g, 20% of the theoretical amount, and assayed 0.0415 μc of C^{14} per 16.78-mg sample.

(2) *Methyltartronic Acid-α-C^{14}*. To 40 ml of aqueous solution containing 5 g of sodium hydroxide was added 5 g of ethyl α,β-dioxobutyrate-β-C^{14}. The solution, after standing two days at room temperature, was acidified with concentrated HCl and carefully neutralized with ammonia. Twelve grams of $BaCl_2$ in 35 ml of water was added, and the solution was chilled in ice water. The precipitated barium salt of the methyltartronic acid, filtered and carefully dried, weighed 9.1 g or 87.5% of the theoretical amount. To 5 g of the barium salt was added 90% of the theoretical amount of 0.935 *M* sulfuric acid. The solution, after removal of the $BaSO_4$ by filtration, was evaporated to dryness. The residue was recrystallized from benzene to yield 1.40 g of methyltartronic acid-α-C^{14} melting at 142° and assaying 0.0533 μc of C^{14} per 18.73-mg sample.

(3) *Zinc Lactate-α-C^{14} and Carbon Dioxide*. A 0.01030-g portion of methyltartronic acid was heated under reflux for 4 hr in 1 ml of water in a vessel designed so that the evolved carbon dioxide was trapped in barium hydroxide solution. The carefully washed and dried barium carbonate, weighing 50 mg, showed no radioactivity above background.

In another experiment with 0.2127 g of acid, the decarboxylation was carried out for a 24-hr period to ensure complete reaction. To the solution was added a slight excess of zinc carbonate. Zinc lactate, precipitated by the addition of ethanol, was separated, dissolved in 1.3 ml of hot 0.1 *N* $ZnCl_2$ solution, and allowed to stand at 0° overnight. Filtration and air-drying yielded 0.1148 g of the trihydrate of zinc lactate assaying 0.0318 μc of C^{14} per 12.32-mg sample.

THE REARRANGEMENT OF UNSYMMETRICAL BENZILS

M. T. Clark* and O. K. Neville

Two unsymmetrically substituted benzils, each labeled with C^{14} in the carbonyl group adjacent to phenyl, have been prepared and subjected to rearrangement in alkaline solution. The resulting substituted benzilic acids were degraded to carbon dioxide and the corresponding benzophenone. Radioanalysis of these two compounds demonstrated the relative extents of migration of the phenyl and substituted phenyl groups in the reaction.

Table 3.1 shows the percent migrations of the substituted group of the compounds *p*-methylbenzil and *m*-chlorobenzil, together with those of *p*-chlorobenzil and *p*-methoxybenzil reported by Roberts, Smith, and Lee[15] and by Neville.[16]

TABLE 3.1

Percent Migration of Substituted Phenyl Groups in the Benzilic Acid Rearrangement

X(in compound $XC_6H_5COCOC_6H_5$)	PERCENT MIGRATION OF C_6H_5X
m-chloro	81.1
p-chloro*	61.2
p-methyl	38.2
p-methoxy**	31.5

* Neville, ORNL-607, p. 85.

** Roberts, Smith, and Lee, *op. cit.*

A consideration of these results in terms of the mechanism previously proposed[17] indicates that the preferred point of attack by hydroxyl ion (*i.e.*, the relative stabilities of the postulated resulting ionic intermediates formed in the first step) is most affected by ring substituents and is, therefore, most important in determining the course of the rearrangement.

Since the proportional migrations of the two groups may be expressed as the relative rates of rearrangement of the benzil by separate reaction paths, it is interesting to compare the results in terms of the Hammett[18] equation.

(15) *Op. Cit.*

(16) Neville, O. K., "Table I," *Chemistry Division Quarterly Report for Period Ending December 31, 1949*, ORNL-607, p 82 (Mar. 7, 1950).

(17) Neville, O. K., "C^{14} Tracer Studies in the Rearrangements of α-Diketones. III. The Rearrangement of Unsymmetrical Benzils," *Brookhaven Conference Report, January 19-20, 1950*, BNL-44 (C-10), p. 52 (Mar. 1950).

(18) Hammett, L. P., *Physical Organic Chemistry*, pp. 186-199, McGraw-Hill, New York, 1940.

* ORINS-ORNL research participant, Emory University.

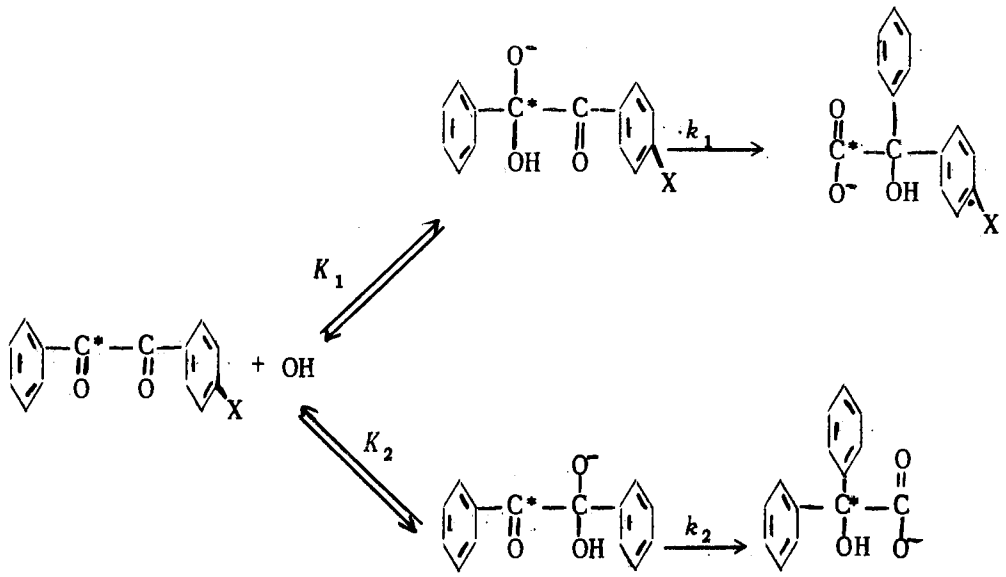

where

$k_1K_1 = k_0a$, the rate of rearrangement of the phenyl group

$k_2K_2 = ka$, the rate of rearrangement of the substituted phenyl group

Hammett has shown that a wide variety of chemical reactions can be related simply and quantitatively when two series of rate or equilibrium constants are compared which differ with respect to the reacting group but carry similar aromatic substituents. The equation is expressed as

$$\log k - \log k_0 = \rho (\log K - \log K_0)$$

where

k = rate of substituted reactant

k_0 = rate of unsubstituted reactant

K = acid dissociation constant of corresponding substituted benzoic acid

K_0 = acid dissociation constant of benzoic acid

ρ = reaction constant, which is constant for all substitutents and depends only on the reaction series

In the present case, k_0 represents the rate of formation of acid by rearrangement of the phenyl group and k_1 indicates the rate of conversion by migration of the substituted aryl group.

In Fig. 3.1 is shown a plot of the logarithm of percent migration of the substituted phenyl group vs. log K/K_0 for four benzils. That the curve is nearly a straight line indicates the applicability of the Hammett equation. With this relationship it would be possible to predict the relative migration with respect to phenyl of any unsymmetrical benzil for which the substituent constant (log K/K_0) is known.

The benzils were prepared as indicated by the reaction scheme

$$C_6H_5C^*ONH_2 + XC_6H_5CH_2MgBr \longrightarrow C_6H_5C^*OCH_2C_6H_5X$$

$$C_6H_5C^*OCH_2C_6H_5X + SeO_2 \longrightarrow C_6H_5C^*OCOC_6H_5X$$

The rearrangements were carried out at room temperature in an aqueous alcoholic sodium hydroxide solution. The benzilic acids were degraded by oxidation with chromic acid. The experimental procedures have been described in detail previously.[19]

THE ISOTOPE EFFECT IN THE DECOMPOSITION OF FORMIC ACID-C^{14}

G. A. Ropp and A. J. Weinberger

Formic-C^{14} acid-water azeotrope was decomposed at 23° to carbon monoxide-C^{14} and water by excess 95% sulfuric acid in a manometric system (Fig. 3.2) which permits the collection of successive 300-ml increments of evolved gas for direct specific activity determination in an ion chamber using a vibrating-reed electrometer. An isotope effect of the same order of magnitude as that reported by Stevens and Attree[20] in the hydrolysis of ethyl benzoate-α-C^{14}

(19) Neville, ORNL-607, *op. cit.*

(20) Stevens, W., and Attree, R., "The Effect on Reaction Rates Caused by the Substitution of C^{14} for C^{12}," *Can. J. Res.*, 27B, 807 (1949).

NOT CLASSIFIED DWG. #9589

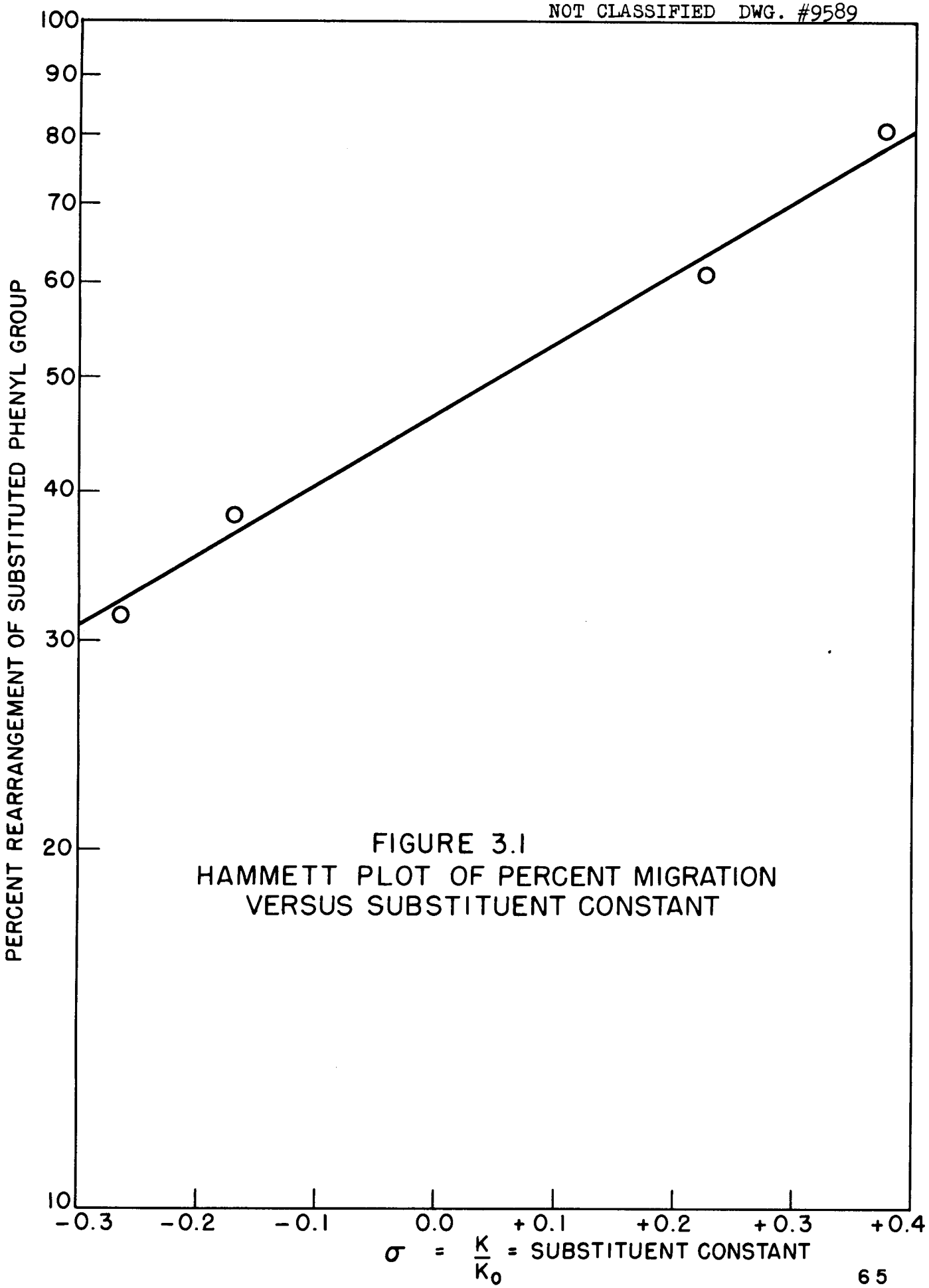

FIGURE 3.1
HAMMETT PLOT OF PERCENT MIGRATION
VERSUS SUBSTITUENT CONSTANT

NOT CLASSIFIED
DWG. 9572

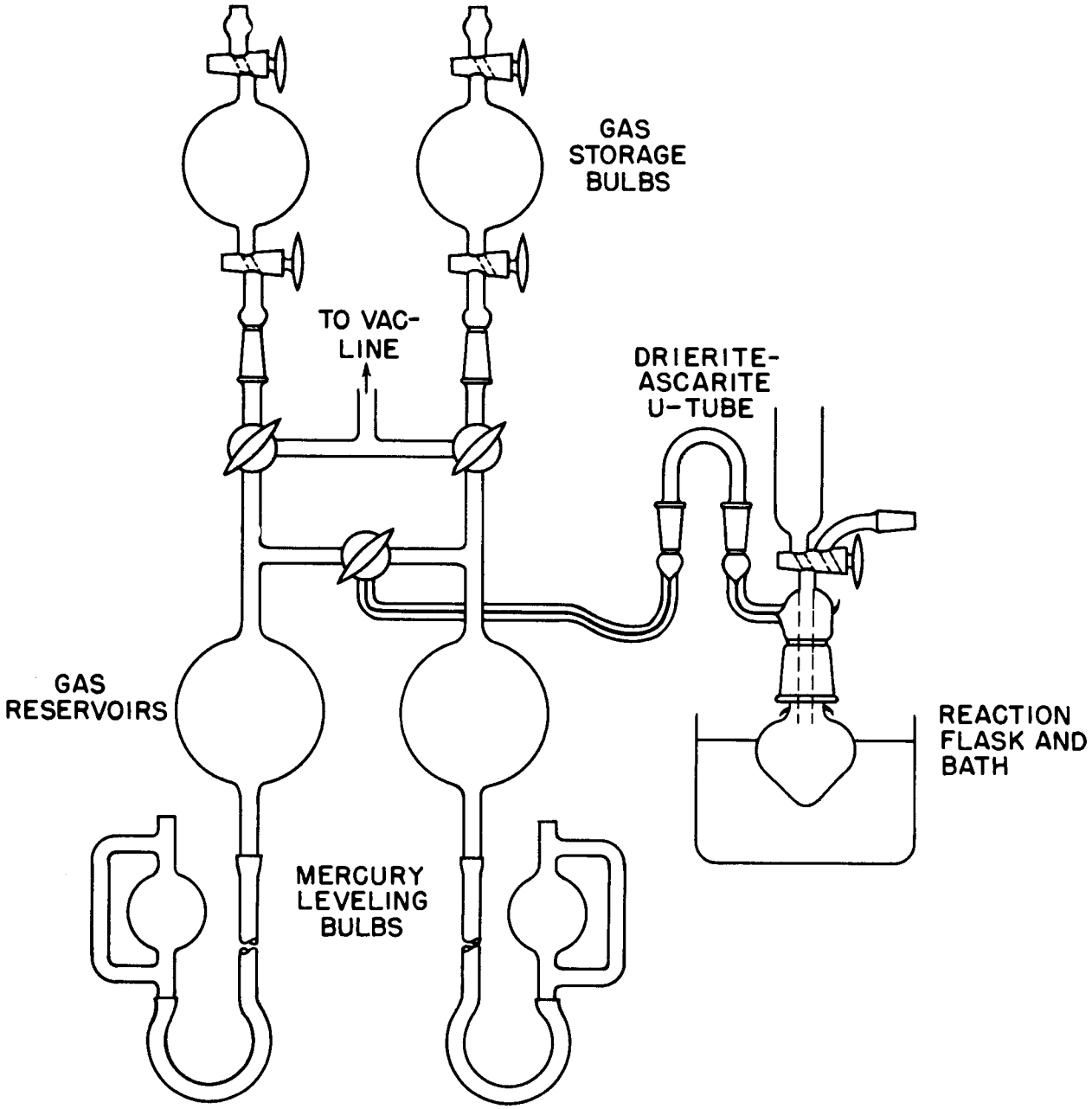

FIG. 3.2
APPARATUS USED IN STUDYING THE RATE OF FORMIC ACID-C^{14} DECOMPOSITION AND THE ISOTOPE EFFECT

was demonstrated. The decomposition of formic acid was also shown to be first order with respect to formic acid under the conditions used; hence a plot of the logarithm of the specific activity of the gas increment vs. the time at which the gas volume was collected should be linear, and it should be possible to evaluate the isotope effect from the slope according to the following derivation:

Let

k_{12} = the first-order rate constant for the decomposition of $HC^{12}OOH$

k_{14} = the corresponding value for $HC^{14}OOH$

$[C^{12}]$ = the concentration of $HC^{12}OOH$ remaining at any time t

$[C_0{}^{12}]$ = the initial concentration of $HC^{12}OOH$

$[C^{14}]$ and $[C_0{}^{14}]$ = the corresponding values for $HC^{14}OOH$

K, K', K'' = constants

S = specific activity of carbon monoxide (activity per unit volume) being produced at time t

$$S \propto \frac{\text{Rate of production of } C^{14}O \text{ at time } t}{\text{Sum of production rates of } C^{14}O \text{ and } C^{12}O \text{ at time } t}$$

$$\therefore S = K \frac{k_{14}[C^{14}]}{k_{14}[C^{14}] + k_{12}[C^{12}]} \approx K \frac{k_{14}[C^{14}]}{k_{12}[C^{12}]}$$

$$S = K \frac{k_{14}[C_0{}^{14}]e^{-k_{14}t}}{k_{12}[C_0{}^{12}]e^{-k_{12}t}}$$

$$S = K' \frac{e^{-k_{14}t}}{e^{-k_{12}t}} = K' e^{+(k_{12}-k_{14})t}$$

$$\log S = \log K' + (k_{12}-k_{14})t$$

$$\log S = K'' + (k_{12}-k_{14})t$$

This is a straight line whose slope is $(k_{12}-k_{14})$ and whose intercept is K''. Although fair correlation of the data with this equation has been obtained, the specific activities plotted do not represent point samples of evolved gas; for this reason a system is being constructed to permit continuous flow of the evolved gas through a 10-ml ion chamber connected to a glass amplifier with a continuous activity indicator.

When reproducible values for $(k_{12}-k_{14})/k_{12}$ are obtained, it is hoped that the variations of this quantity with temperature can be evaluated and correlated with theoretical values of the temperature coefficient.

The data on sample decomposition of $HC^{14}OOH$ at 23° are given in Table 3.2.

TABLE 3.2

Sample Decomposition of $HC^{14}OOH$ at 23°

TIME (min)	ACTIVITY (μc per 250 ml of CO at 25° and 740 mm)	FORMIC ACID REACTED (%)
6½	1.40	11.6
13¼	1.41	23.3
21	1.45	34.9
30½	1.47	46.5
43½	1.51	58.0
63¼	1.56	70.6

In order to prove that the variation of the carbon monoxide specific activity with time is due to an isotope effect and not to the evolution of some inactive gas at a changing rate, the first and last samples of carbon monoxide evolved were burned to carbon dioxide. The carbon dioxide was precipitated as barium carbonate and reconverted to carbon dioxide, and the specific activity of this was measured in the same ion chamber as that used

for the carbon monoxide. In Table 3.3 the specific activities determined as carbon monoxide are compared with those determined as carbon dioxide.

TABLE 3.3

Comparison of Specific Activities as Carbon Monoxide and Carbon Dioxide

SAMPLE NO.	μc PER 250 ml OF CO AT 25°, 740 mm	μc PER GRAM OF $BaCO_3$	μc PER 250 ml OF CO_2 AT 25°, 740 mm	$\frac{\text{SP. ACTIVITY AS } CO_2}{\text{SP. ACTIVITY AS CO}}$
1	1.38	0.840	1.65	1.20
10	1.93	1.17	2.30	1.19

The ratio 1.2 is approximately the ratio of the ion-pair yields obtainable in the 250-ml stainless-steel ion chamber when filled with carbon dioxide or carbon monoxide of the same specific activity.

STANDARDIZATION OF C^{14} COUNTING METHODS

POLYSTYRENE COUNTING STANDARDS

H. E. Heller

The polystyrene-C^{14} previously prepared[21] was converted to sheets, 0.010 to 0.012 in. thick, by solution in methylene chloride and deposition on a pool of mercury contained in a large box.[21] The solvent was evaporated under controlled conditions, and the film was removed from the box and divided into sections 1¼ in. square. The cutting of the sheet to the desired size was best accomplished by scoring the films with a razor blade and snapping the sheet in the same way a glass tube is cut. About two hundred samples were prepared.

Experiments to determine the counting characteristics of the film revealed an approximate 6 percent difference in counting rate between the two sides of each sample counted. (The samples were all above "saturation thickness.") Verification of this difference was obtained by wet combustion and ion-chamber measurement of samples removed from each side of the film.

This difference was not found in films prepared from polystyrene before dilution with commercial polymer,[21] and it seemed likely that it was due to a difference between the molecular weight of the polymer prepared here and that of the Dow commercial material. Samples of each polymer were therefore dissolved in benzene and titrated with methanol to equal turbidities. The results indicated a much lower molecular weight in the commercial material.

The fractionation that was believed to occur in the film preparation step could be explained in either of two ways: (1) Solvent evaporating from the surface layer of the solution left that layer richer in polystyrene than the main body of solution, and diffusion of the higher molecular weight material (containing the radioactivity) away from this region at a lower rate than the inactive material of lower polymer length resulted in an enrichment at the upper layer during evaporation of the solvent; (2) The lower solubility of

(21) Heller, H. E., and Weinberger, A. J., "Polystyrene Counting Standards," *Chemistry Division Quarterly Progress Report for Period Ending March 31, 1950*, ORNL-685, p. 88 (June 16, 1950).

high-molecular-weight material caused it to come out of solution first, and, since the solvent was more dense than the polymer, the long-chain material floated to the top as the solvent was removed.

That the first explanation was more likely was proved by laying down a film from benzene solution. Since benzene is less dense than the polymer, enrichment of the radioactivity would be expected in the bottom layer, but this was found not to be the case. Instead, a duplication of the results in methylene chloride, enrichment in the upper layer, was found.

Demonstration that there was no radioactivity gradient in a static solution of polystyrenes of different molecular weights was obtained by counting samples of the top and bottom of a long cylinder of solution after allowing it to stand one week. Both methylene chloride and benzene solutions were tested.

4. CHEMISTRY OF SEPARATIONS PROCESSES

VOLATILITY STUDIES

BREEDER BLANKET STUDIES

P. A. Agron and E. G. Bohlmann

Introduction. Studies on systems which provide the possibility of continuous removal of Pa^{233} or U^{233} as formed have been continued.

Thorium—Phosphorus Fluoride Systems. In continuation of the previously reported work,[1] additional survey experiments were carried out wherein $ThF_4(s)$ samples were exposed to various pressures of PF_3 and PF_5. In one instance the ThF_4 was exposed successively to $PF_3(l)$ and $PF_5(l)$ at temperatures slightly above their respective boiling points. For the remaining trials, gas pressures from 23 to 278 psi absolute were utilized over periods of several days. Gas uptakes were noted in each case. In most of the experiments heating cycles were applied to the solid contained in the lower portion of a vertical nickel tube. The solid products were examined by chemical analysis (for Th, F, and P), powder X-ray diffraction, and electron microscopy.

The gas was removed at the end of a run by freezing it out at -196°C followed by a short outgassing of the system at room temperature. The data, as in previous work,[2] indicate that the quantity of gas taken up during the experiments, presumably by the $ThF_4(s)$, was much greater than that finally found on the solid by chemical analysis for phosphorus. Blank runs at elevated pressures showed negligible consumption of the gas by the closed metal system. To date such a chemical or physical uptake of these gases appears to be confirmed only by the electron microscope pictures of the solid products.[3] These pictures indicate break-up of a portion of the treated material into particles 200 to 500 A in diameter. Identification of these small particles is being pursued.

As another approach to the problem, the movement of radioactive material from irradiated ThF_4 samples subjected to certain phosphorus fluoride treatments is being investigated. One sample that had 3 hr of exposure in the pile

(1) Agron, P. A., and Bohlmann, E. G., "Volatility Studies," *Chemistry Division Quarterly Progress Report for Period Ending March 31, 1950*, ORNL-685, p. 93 (June 16, 1950).

(2) *Ibid.*

(3) McNeer, F. D., *Electron Micrographs of Thorium Fluoride Treated with Phosphorus Fluorides*, ORNL CF-50-6-200, CF-50-7-162, CF-50-8-107.

was treated in a vertical quartz tube as follows:

GAS	PRESSURE (in. Hg Absolute)	TEMPERATURE (°C)	TIME (hr)
PF_3	20	300-350	1
F_2	11	315-365	½
PF_5	20	320-370	1½
POF_3	8	325-390	½
F_2	11	300-410	¾

This series of treatments failed to produce movement of the protactinium tracer to a cold finger located several inches above the heated solid. A second sample, supplied by F. T. Miles of Brookhaven National Laboratory, was exposed for 16 hr in the pile. This material was subjected to 140 psia of $PF_3(g)$ and then put through four heating and cooling cycles (to 350°C). Attempts at evaluating the effectiveness of these phosphorus fluoride treatments in accelerating the removal of Pa or U by subsequent fluorination in a metal apparatus are in progress at Brookhaven.[4] One preliminary result reported by Dr. Miles showed that 5 to 10% of the Pa^{233} came out much faster than usual at 600°C.

Future experiments will utilize ThF_4 particles of a narrow range of particle sizes, with high surface areas. More effort will also be concentrated on obtaining and working with larger quantities of $PF_5(g)$ and $POF_3(g)$.

Thorium Fluophosphates. As indicated previously[5] other thorium salts which are usable in a breeder blanket have also been investigated. While surveying the possibilities offered by the thorium monofluophosphate $[Th(PO_3F)_2]$ and the difluophosphate $[Th(PO_2F_2)_4]$ salts, it was found that thorium orthophosphate dissolved readily in 85% H_3PO_4 upon heating. At 160°C the uptake of solid indicates that more than 0.5g of thorium per milliliter of acid is held in solution. On cooling, a gel is formed, which goes into solution again on reheating. Consideration of this system for a homogeneous breeder indicates

(4) Bohlmann, E. G., *Treated Samples*, ORNL CF-50-8-101.

(5) Argon and Bohlmann, *op. cit.*

several advantages and disadvantages over that of the H_2O-UO_2SO_4 homogeneous reactor. The former system would probably give much lower operating pressures at 250°C (H_3PO_4 boils above 213°C). However, the radiation damage to the acid is unknown and would have to be investigated, and the feasibility of using this system would depend on overcoming the greater corrosion problems and the probably more difficult task of chemical cleanup of the fission products.

Both ThF_4 and UF_4 dissolve in 85% H_3PO_4 on warming, with the formation of the mono- or difluophosphate compounds. Relatively few chemical and physical data are available on the fluophosphates. However, investigation of the chemistry of this type of salt may uncover a possible means for the separation of fission products in a $Th_3(PO_4)_4$-D_3PO_4 homogeneous breeder.

SOLVENT EXTRACTION

THE ORGANIC CHEMISTRY OF SOLVENTS

C. E. Higgins J. M. Ruth
W. H. Baldwin

Sulfones. Since the earlier report[1] that symmetrical alkyl sulfones can extract uranium from aqueous nitrate solutions, several sulfones have been prepared by oxidation of the sulfides and have been equilibrated with aqueous solutions. The sulfones extracted uranium from nitrate solutions with much higher distribution ratios than from chloride or sulfate systems.

n-Propyl sulfone gives a distribution ratio of 1.0 for uranium at a lower nitric acid concentration (3.2 *M*) than the other sulfones tested. The solubility of the sulfones that have been examined so far varies directly with the concentration of nitric acid in the aqueous phase. Modifications of the structure (increased number of carbons in the alkyl group) that decreased the solubility in nitric acid resulted in less uranium extraction.

In the extraction tests with irradiated uranium, *n*-propyl and isobutyl sulfones showed selectivity in the extraction of Pu(IV) from U(VI) and fission products. Thorium(IV) was extracted with a lower distribution ratio than was uranium.

Preparation and Purification of Sulfones. The sulfones—isobutyl, isoamyl, and methyl *n*-butyl—were prepared by the oxidation of the corresponding sulfides with hydrogen peroxide.[2] In a typical preparation, 100 g of isobutyl sulfide was dissolved in 250 ml of glacial acetic acid and 250 ml of acetic anhydride. To the mixture cooled in an ice-salt bath 3 moles of hydrogen peroxide (30%) per mole of sulfide was added dropwise, keeping the temperature below 3°C. After the addition was complete the mixture was allowed to warm to room temperature, 1 g of MnO_2 was added to catalyze the decomposition of peroxides, and the acetic acid was removed with an aspirator. The residue was dissolved in benzene, washed with water (four times with one-fifth volume each time), and dried over $CaCl_2$, the benzene was distilled, and the sulfone was collected at reduced pressure.

(1) Higgins, C. E., Ruth, J. M., Wacker, R. E., and Baldwin, W. H., "The Organic Chemistry of Solvents," *Chemistry Division Quarterly Progress Report for Period Ending March 31, 1950, Part I. Chemical Research*, ORNL 685, p. 99 (June 16, 1950).

(2) Pomerantz, A., and Connor, R., "Alkylation of α-Sulfonylamides," *Am. Chem. Soc. J.* 61, 3139 (1939).

n-Propyl sulfone from the Eastman Kodak Company was dissolved in benzene and purified as above. *n*-Butyl sulfone was crystallized from aqueous alcohol and dried in an evacuated desiccator.

Solubility of Sulfones. To obtain the approximate solubilities of the sulfones in acids at the salting strength to be used, the sulfones were added dropwise with agitation to 5.0-ml volumes of 1, 3, and 5 *M* acid until one more drop left two phases in the liquid. The samples were tumbled overnight to ensure saturation. The solubility values are shown in Table 4.1. Solid *n*-butyl sulfone (5.0 g) was added to 5.0 ml of 5.1 *M* HNO_3 and agitated at 30°C. The sulfone melted to a liquid of volume 5.8 ml which was 1.3 *M* in HNO_3, while the aqueous phase diminished to 4.4 ml and was 4 *M* in HNO_3.

TABLE 4.1

Approximate Solubility of Sulfones at 30°C

AQUEOUS PHASE	SOLUBILITY (g/100 ml of aqueous phase)			
	n-PROPYL SULFONE	ISOBUTYL SULFONE	ISOAMYL SULFONE	METHYL *n*-BUTYL SULFONE
H_2O				20
3 *M* HNO_3	40	30	0.4	>100
5.1 *M* HNO_3	>100	38	0.6	>100
1 *M* HCl	12			
3 *M* HCl	16			
5 *M* HCl	69			

Distribution Tests.

1. General Method. Equal volumes of organic and aqueous phases were tumbled end-over-end in a thermostated water bath for at least 30 min at 22 rpm. Containers for the liquids were glass-stoppered graduated centrifuge cones, either 10 or 100 ml capacity. It has been found desirable to use fluorocarbon grease on the stopcocks to minimize leakage during the equilibration. After removal from the tumbling machine the tubes were centrifuged and the volumes noted. The phases were separated with the use of pipets that had been drawn out into capillaries at one end.

2. Time of Equilibration. Equal volumes of *n*-propyl sulfone and 0.1 *M* uranium nitrate hexahydrate solutions containing 1 *M* and 3 *M* HNO_3 were equilibrated at 30°C for 15 min, 1 hr, and 6 hr. The observed distribution coefficients at the end of these times were 0.24, 0.22, 0.22 and 0.98, 1.00, 0.98 for 1 *M* and 3 *M* HNO_3, respectively.

3. Salting with Nitric, Sulfuric, and Hydrochloric Acids. Neither hydrochloric nor sulfuric acid salted U into *n*-propyl sulfone as completely as did nitric acid (Table 4.2).

TABLE 4.2

Comparison of Extraction of 0.1 *M* Uranium from Nitrate, Sulfate, and Chloride by *n*-Propyl Sulfone at 30°C

AQUEOUS PHASE	DISTRIBUTION RATIO OF CATION, ORGANIC/AQUEOUS	
	H^+	U(VI)
1.1 *M* HNO_3	0.3	0.23
3.2 *M* HNO_3	0.6	0.99
0.55 *M* H_2SO_4		6.7×10^{-4}
1.6 *M* H_2SO_4		4.6×10^{-4}
2.65 *M* H_2SO_4		6.0×10^{-4}
1.1 *M* HCl	0.03	0.011
3.1 *M* HCl	0.05	0.41
5.1 *M* HCl	3.0	0.38

4. Extraction from Aqueous Nitric Acid with sulfones. Four sulfones (*n*-propyl, isobutyl, isoamyl, and *n*-butyl) have been compared for their extraction of uranium from nitric acid solutions (Table 4.3). *n*-Propyl sulfone gives a uranium distribution ratio of 1.0 at a lower concentration of HNO_3 (3.2 *M*) than any of the other sulfones tested.

TABLE 4.3

Extraction of 0.1 *M* Uranium from Aqueous HNO_3 by Various Sulfones

(equilibrated 1 hr at 30°C)

SULFONE	OBSERVATION	HNO_3 IN AQUEOUS FEED				
		1.1 *M*	1.5 *M*	3.15 *M*	3.65 *M*	5.7 *M*
n-Propyl	D.R. H^+	0.3		0.6		
	D.R. U(VI)	0.23		0.99		
	Vol. change*	Neg.		Neg.		
Isobutyl	D.R. H^+		0.1		0.2	0.3
	D.R. U(VI)		0.073		0.47	0.99
	Vol. change*		Neg.		+4%	+8%
Isoamyl	D.R. H^+		0.1		0.2	0.3
	D.R. U(VI)		0.048		0.25	0.75
	Vol. change*		Neg.		+3%	+9%
n-Butyl	D.R. H^+					0.3
	D.R. U(VI)					1.20
	Vol. change*					+12%

*Change in volume of the organic phase.

5. Extraction of Uranium from Ammonium Nitrate Solutions. Ammonium nitrate salts uranium into many organic solvents, including sulfones (Table 4.4).

TABLE 4.4

Extraction of U from Ammonium Nitrate Solution with Sulfones

Aqueous feed 6.9 *M* NH_4NO_3, 0.1 *M* HNO_3
equilibrated 1 hr at 30°C unless noted

ORGANIC FEED	DISTRIBUTION RATIO OF U, ORGANIC/AQUEOUS	ORGANIC FEED	DISTRIBUTION RATIO OF U, ORGANIC/AQUEOUS
n-Propyl sulfone	10.8 13.1 10.6 (50°C)	*n*-Butyl sulfone—CCl_4 (1:1 by wt.)	0.26
Isobutyl sulfone	2.06	*n*-Butyl sulfone—hexone (1:1 by wt.)	2.67
Isoamyl sulfone	1.02	Hexone	1.31
n-Butyl sulfone	3.48 (50°C)	*n*-Butyl sulfone—*n*-butanol (1:1 by wt.)	5.32
n-Butyl sulfone—benzene (1:1 by wt.)	0.09	*n*-Butanol	1.20

Of the sulfones tested *n*-propyl had the highest distribution ratio for uranium (10 to 13 at 30 to 50°C). The other sulfones have distribution ratios less than *n*-propyl but greater than 1. An interesting effect on the extraction with *n*-butyl sulfone resulted from dilution with various solvents. In benzene and carbon tetrachloride the extraction was low (distribution ratios 0.09 and 0.26, respectively). Extraction with a mixture of hexone and *n*-butyl sulfone was better by a factor of 2 than with hexone alone, and the mixture of *n*-butyl sulfone and butanol was better than butanol alone by a factor greater than 4.

6. Extraction of U, Pu(IV), and Fission Products. Samples of dissolved irradiated uranium slugs were obtained from W. B. Lanham of the Chemical Technology Division and adjusted to convert all plutonium to the tetravalent state. Comparison of extractions by sulfones with those by TBP (tributyl phosphate) are shown in Table 4.5. *n*-Propyl and isobutyl sulfones show a selectivity for the extraction of plutonium. The distribution ratio is 6 to 10 times higher for plutonium than for uranium.

7. Extraction of Th(IV). The preference of sulfones for Pu(IV) rather than U(VI) (Table 4.5) led to the testing of the extraction of Th(IV) with sulfones from 3 *M* HNO_3 solution. The distribution ratio was less for Th(IV) than for either U(VI) or Pu(IV) (Table 4.6).

Esters of Phosphoric Acid. Continued interest in tri-*n*-butyl phosphate (TBP) as a solvent for the extraction and purification of source and fissionable materials has prompted work with it and related compounds. The effect of substituents other than *n*-butyl in the molecule has been one of the first variables to be studied. A homologous series of esters has been obtained and purified for the direct comparison of uranium extraction from aqueous solutions containing nitric acid.

Although TBP has a relatively high stability toward decomposition by nitric acid there is evidence for reactions at high concentrations of nitric acid and particularly at temperatures above room temperature. Therefore it seemed advisable to obtain compounds that were expected to appear as hydrolytic products. Two of those, the mono-*n*-butyl (MBP) and the di-*n*-butyl phosphoric (DBP) acids have been or are being synthesized in large quantity and high purity. General reactions are being sought which will permit the synthesis of labeled compounds (P^{32}). The use of labeled compounds materially assists the analysis and separation of the known materials and will be useful in detecting unknown compounds that may result from manipulations of some of the known compounds.

TABLE 4.5

Distribution of U, Pu, and Fission Products in Extraction with Sulfones and Tributyl Phosphate

Conditions: Aqueous feed - 0.15 *M* uranium nitrate hexahydrate, 3 *M* HNO_3, Pu 5×10^4 to 5×10^5 alpha c/min/ml, 4×10^6 to 4×10^7 beta c/min/ml; 5 ml of each phase equilibrated 1 hr at 30°C

SOLVENT	D.R. O/A U	D.R. O/A Pu[a]	D.F. BETA[b]	D.F. GAMMA[c]	FEED[d]
0.75 *M* TBP in CCl_4	20.8	5.7	136	56	x-5
0.75 *M* TBP in CCl_4	20.0	5.0	202	92	x-8
n-Propyl sulfone	0.9	14.7	12	10	x-5
n-Propyl sulfone	0.83	7.3	13	10	x-8
3 *M* *n*-propyl sulfone in isopropyl ether	0.60	1.43	68	54	x-12
Isobutyl sulfone	0.48	3.4	72	74	x-5
Isobutyl sulfone	0.44	2.6	87	62	x-8
Isoamyl sulfone	0.29	0.4	160	157	x-5
Isoamyl sulfone	0.27	0.3	217	155	x-8
3 *M* *n*-butyl sulfone in isopropyl ether	0.44	0.94	98	76	x-12
3 *M* ethyl *n*-butyl sulfone in isopropyl ether	0.06	0.02	3,000	>100	x-12
Isopropyl ether	0.03	0.001	22,000	>100	x-12

(a) Counted at 52% geometry. D.R. is the ratio of concentration in organic phase to that in aqueous phase.

(b) Counted at 11% geometry. D.F. is ratio of c/min in feed to that in extract.

(c) Measured in high-pressure argon ionization chamber.

(d) Supplied by W. B. Lanham, Chemical Technology Division.

TABLE 4.6

Distribution of Th(IV) and H^+ Between Sulfones and Aqueous Phase

Conditions Aqueous Feed 3 *M* HNO_3, Th(IV) as indicated

OBSERVATION	0.15 *M* Th(IV) IN AQUEOUS FEED		0.0015 *M* Th(IV) IN AQUEOUS FEED	
	n-PROPYL SULFONE	ISOBUTYL SULFONE	*n*-PROPYL SULFONE	ISOBUTYL SULFONE
D.R. Th(IV)	0.41	0.064	0.44	0.058
D.R. H^+	0.6	0.29	0.6	0.25
Vol. change of organic phase	+5%	+3%	+3%	+2%

Synthesis.

1. Trialkyl Orthophosphates. One of the first effects to be studied is the effect of the size and configuration of the alkyl groups in the ester on the extraction properties. For example, the ethyl ester has an appreciably higher solubility in water than does the butyl ester. Two esters in this series, ethyl and *n*-butyl, were obtained from commerical sources and distilled before use. The other esters (*n*-propyl, isopropyl, *sec*-butyl, isobutyl, and *n*-amyl) were synthesized by the reaction of the corresponding alcohol with phosphorus oxychloride in the presence of pyridine.(1) With this method tertiary butyl alcohol yielded no product.

Radioactive phosphorus (P^{32}), being available as H_3PO_4 (from the Isotope Production branch), was introduced into the TBP molecule by making Ag_3PO_4(2) and carrying out a metathesis with *n*-butyl bromide to give tri-*n*-butyl phosphate in 59% yield.

2. Di-*n*-butyl Phosphoric Acid (DBP). The removal of one butyl group from TBP leaves dibutyl phosphoric acid, a monobasic acid. This compound has been prepared in our laboratory by the alkaline hydrolysis of tetrabutyl pyrophosphate, by alkaline hydrolysis of dibutyl chlorophosphate, and by catalytic reduction of dibutyl benzyl phosphate.

The common reagent for these three reactions is di-*n*-butyl chlorophosphate. The di-*n*-butyl chlorophosphate was prepared in two stages: First *n*-butyl alcohol was reacted with phosphorus trichloride to give di-*n*-butyl hydrogen phosphite; the second stage is the chlorination to di-*n*-butyl chlorophosphate.(3)

The controlled hydrolysis of di-*n*-butyl chlorophosphate to give tetra-*n*-butyl pyrophosphate has been described.(4) The hydrolysis of this compound with dilute alkali to give di-*n*-butyl phosphoric acid is new.

(1) Dutton, G. R., and Noller, C. R., in *Organic Syntheses, Collective Volume II*, Ed. A. H. Blatt, 109, Wiley, New York, 1943.

(2) Johnson, C. R., and Nunn, L. G., Jr., "Silver Phosphate in Quantitive Analysis," *J. Chem. Ed.* 17, 529 (1940).

(3) McCombie, H., Saunders, B. C., and Stacey, G. J., "Esters Containing Phosphorus. Part I," *J. Chem. Soc.* 1945, 380.

(4) Toy, A. D. F., "The Preparation of Tetraethyl Pyrophosphate and Other Tetraalkyl Pyrophosphates," *Am. Chem. Soc. J.* 70, 3882 (1948).

The selective catalytic reduction of phenyl or benzyl esters of phosphoric acids is a general reaction which has received wide application. Di-*n*-butyl chlorophosphate was reacted with benzyl alcohol in pyridine to produce di-*n*-butyl benzyl phosphate which was hydrogenated to di-*n*-butyl phosphoric acid (Pd on charcoal catalyst).

All three of the preparations were obtained in good yield and purity greater than 95%. An important finding was the fact that di-*n*-butyl phosphoric acid could be distilled at 10 μ Hg pressure. A yellow color developed in most of these samples on standing in the laboratory. It is recommended that di-*n*-butyl phosphoric acid not be kept for long periods of time but be made freshly as needed by the hydrolysis of tetra-*n*-butyl pyrophosphate.

Evaluation Tests.

1. Ester Interchange Between TBP and DBP. The interchange of alcohols with esters is a well-known reaction which has received technical application in the conversion of glyceryl trilaurate into methyl laurate by refluxing the glyceride with methyl alcohol in the presence of sulfuric acid as a catalyst.(5) Since DBP, MBP, and H_3PO_4 are strong acids, it appeared desirable to test the ester interchange reaction in mixtures of TBP with the phosphoric acids mentioned. The first test of this reaction involved the heating together of 5 g of tri-*n*-butyl phosphate (P^{32}) and 5 g of di-*n*-butyl phosphoric acid in a boiling water bath for 5 hr. At the end of this time the reaction mixture was diluted with CCl_4 to 50 ml, extracted four times with an equal volume of distilled water each time, then extracted four times with an equal volume of 0.5 *M* NH_4OH each time, and finally with four equal-volume portions of distilled water. Distribution studies have shown that the first water washes can be expected to remove phosphoric acid and monobutyl phosphoric acid; the alkaline washes would remove dibutyl phosphoric acid; and the final water wash would indicate the distribution of TBP between CCl_4 and distilled water. For counting the solutions a suitable volume was measured into a large test tube and hydrolyzed by the addition of HI (55% solution), evaporating excess solution, and refluxing for 1 hr. The resulting solution was diluted to 10 ml with water, and an aliquot was placed on a polystyrene film, dried with an infrared lamp, and counted. The alkaline solutions were first acidified with HCl, then counted by direct evaporation of suitably sized aliquots.

(5) Fieser, L. F., and Fieser, M., *Organic Chemistry*, p. 182, D. C. Heath, Boston, 1944.

Water washes (9, 10, 11, and 12, Table 4.7) represent the order of magnitude of the distribution of TBP between CCl_4 and water. The amount of activity in these water solutions was too low to obtain a high degree of precision. These figures indicate that the amount of activity in the water washes 1, 2, 3, and 4 that is contributed by TBP is small. The activity in these washes (0.54%) can be contributed by H_3PO_4, monobutyl phosphoric acid, and dibutyl phosphoric acid. The 0.5 *M* NH_4OH that carried 2.22% of the total activity represents the dibutyl phosphoric acid plus the TBP that is soluble in the alkaline solution. The distribution of TBP between CCl_4 and alkaline solutions is not available at present. Summarizing, it seems evident that, while the material balance in this test is low (86.4%), the amount of ester interchange under the conditions of this experiment did not exceed a few percent.

TABLE 4.7

Distribution of P^{32} in Batch Extractions

Conditions: 5 *g* of tri-*n*-butyl phosphate (P^{32}) and 5 *g* of di-*n*-butyl phosphoric acid heated 5 hr in a boiling water bath, diluted with CCl_4 to 50 ml, extracted with equal volumes of aqueous phase as indicated.

Solution		Activity (%)	
Starting		100*	
Water wash	1	0.27	
	2	0.091	
	3	0.095	
	4	0.081	
Total			0.54
0.5 *M* NH_4OH wash	5	1.53	
	6	0.28	
	7	0.23	
	8	0.18	
Total			2.22
Water Wash	9	0.003	
	10	0.001	
	11	0.001	
	12	0.004	
Total			0.009
Residual, CCl_4		83.6	
Material Balance			86.4

*56.3 μc.

2. Extraction of Uranium with Trialkyl Phosphates. A series of equilibration tests was made with 0.75 *M* trialkyl phosphate in carbon tetrachloride as the organic phase and 3 *M* HNO_3 and 0.2 *M* uranyl nitrate hexahydrate in the aqueous phase. Equal volumes, 25 ml of each phase, were tumbled end over end at 25°C for 1 hr. At the end of this time the centrifuged and separated phases were sampled for analysis. No volume changes were detectable in any phase. Uranium and HNO_3 were determined volumetrically by L. T. Corbin's analytical group; they are reported in Table 4.8.

Reproducibility in the determination of uranium and nitric acid is demonstrated by the data for the feed solution and the reproducibility of the combined equilibration and analytical determination by the four different tests with tri-*n*-butyl phosphate. Since the differences in the apparent uranium extracted by tri-*n*-butyl phosphate vary nearly as much as the apparent uranium extraction by the other alkyl phosphates, it appears evident that the structure of the alkyl group has no large influence on the amount of uranium extracted from 3 *M* HNO_3.

Analytical Development. The quantitative estimation of phosphorus in organic compounds depends upon the conversion of the phosphorus to orthophosphate. Simmons and Robertson[6] have demonstrated that alkyl esters of phosphoric acid can be rapidly hydrolyzed by 55% HI and the phosphorus determined by precipitation with molybdate. This method, as described, suffers from the fact that a large excess of HI was employed which had to be removed before precipitation. The method has been modified by us and has been found very useful in the determination of total phosphorus and radioactive phosphorus in solutions.

About 100 mg of ester was weighed by difference into a test tube (2.5 by 15 cm) and 1 ml of 55% HI was added. The solution was heated gently for 1 hr so that condensate washed down the sides of the test tube. Distilled water (5 ml) was used to wash down the walls, a drop of hydrazine hydrate was added to discharge the color of iodine, and magnesium ammonium phosphate was precipitated as described by MacKenzie and Dean.[7] Phosphorus found in tri-*n*-butyl phosphate, 11.48%; calculated, 11.63%.

(6) Simmons, W. R. and Robertson, J. H., "Determination of Total Phosphorus in Organic Phosphate," *Anal. Chem.* 22, 294 (1950).

(7) MacKenzie, A. J., and Dean, L. A., "Measurement of P^{31} and P^{32} in Plant Material," *Anal. Chem.* 20, 559 (1948).

TABLE 4.8

Distribution of U and HNO_3 Between Alkyl Phosphates in CCl_4 and Water
(Equilibrated 1 hr at 25°C)

ALKYL GROUP	AQUEOUS PHASE		ORGANIC PHASE	
	U (mg/ml)	HNO_3 (moles/liter)	U (mg/ml)	HNO_3 (moles/liter)
Ethyl	9.46, 8.57	2.95, 2.95	40.24, 40.70	0.13, 0.15
n-Propyl	6.34, 6.29	2.90, 2.90	42.76, 42.52	0.16, 0.15
Isopropyl	4.52, 5.60	3.00, 3.00	45.41, 44.15	0.22, 0.21
n-Butyl	6.64, 6.46	2.80, 2.77	41.86, 42.85	0.15, 0.14
	7.58, 7.56	2.80, 2.87	44.03, 44.03	0.20, 0.16
	5.48, 5.48	2.90, 2.90	43.80, 43.77	0.25, 0.21
	4.84, 4.90	3.00, 3.00	44.15, 44.12	0.17, 0.17
Isobutyl	6.90, 6.32	3.00, 3.00	42.63, 42.63	0.20, 0.18
sec-Butyl	4.43, 4.31	3.00, 3.00	45.33, 44.60	0.19, 0.18
n-Amyl	6.57, 6.49	3.00, 2.90	43.01, 42.80	0.15, 0.13
	Aqueous Feed			
	49.32	3.10		
	50.34	3.05		
	49.40	3.10		
	49.62	3.13		

The above method has been modified for the estimation of P^{32}. The sample, either pure or in solution, was measured into the test tube, and the excess solvent was evaporated either before or after the addition of HI for hydrolysis. Carrier (10 mg) in the form of NaH_2PO_4 was added to the hydrolysate just before precipitation of the magnesium ammonium phosphate. The combined filter and counting plate is being modified and will be described in detail later.

CHARACTERIZATION OF INORGANIC SPECIES IN SOLVENT EXTRACTION

Zirconium in Aqueous HCl-$HClO_4$ (J. P. McBride and R. W. Stoughton). The partition of a cation between thenoyl trifluoroacetone (TTA)—benzene and aqeuous phases containing complexing anions has been used by several investigators to determine the chemical formulas of the complexes formed and the concentration constants associated with their formation.[8,9] This report covers an investigation of the complexing of Zr by Cl^- in $HClO_4$-HCl mixtures, 1 to 3 *M* in H^+, as determined by the TTA-extraction method, using Zr^{95} tracer to follow the partition.

Discussion of Method. It has been demonstrated that the zirconium species extracted into TTA-benzene from $HClO_4$ and from HCl solution is a neutral molecule formed by the reaction of Zr^{4+} with four diketone molecules.[8,10] It has also been demonstrated that at acidities 1 *M* or greater and at zirconium concencentrations less than 10^{-4} *M* the chief species in these solutions are Zr^{4+} or complexes of Zr^{4+} with Cl^-.[10,11] It may be assumed then, as a first approximation, that the complexing of Zr by Cl^- can be represented by the general expression

$$Zr^{4+} + nCl^- \underset{}{\overset{k_n}{\rightleftharpoons}} ZrCl_n^{(4-n)+} \qquad (1)$$

The partition, aqueous over benzene, of Zr between aqueous mixtures of ClO_4^- and Cl^- and a TTA-benzene solution may then be formulated as

$$\text{Distribution ratio} = \frac{[Zr^{4+}] + [ZrCl^{3+}] + [ZrCl_2^{2+}] \ldots}{[ZrT_4]_b} \qquad (2)$$

(8) Connick, R. E., and McVey, W. H., *The Aqueous Chemistry of Zirconium*, UCRL-101 (Mar. 1, 1948).

(9) Day, R. A., Jr., and Stoughton, R. W., *Chemistry of Thorium in Aqueous Solutions. I. Some Organic and Inorganic Complexes*, ORNL-468 (Jan. 5, 1950).

(10) McBride, J. P., and Stoughton, R. W., "Extraction of Zirconium and Hafnium into TTA-benzene," *Chemistry Division Quarterly Progress Report for Period Ending June 30, 1950*, ORNL-795, p. 98 (Oct. 3, 1950).

(11) Connick, R. E., and Reas, W. H., *The Hydrolytic Behavior of Zirconium in Perchloric Acid Solution*, UCRL-261 (September, 1948).

where the subscript b denotes the benzene phase and T represents TTA. Substituting in Eq. (2) the values for the concentrations of the various Zr complexes as expressed in Eq. (1),

$$\text{Distribution ratio} = \frac{[Zr^{4+}] + \sum_{n=1}^{m} k_n [Zr^{4+}][Cl^-]^n}{[ZrT_4]_b} \tag{3}$$

where k_n is the concentration constant associated with the formation of $ZrCl_n^{(4-n)+}$ from Zr^{4+}. When $[Zr^{4+}]$ is factored out, the following expression is obtained:

$$\text{Distribution ratio} = \frac{[Zr^{4+}]}{[ZrT_4]_b}\left[1 + \sum_{n=1}^{m} k_n [Cl^-]^n\right] = \text{D.R.}^0 \left[1 + \sum_{n=1}^{m} k_n [Cl^-]^n\right] \tag{4}$$

where D.R.^0 equals the distribution ratio obtained in the absence of Cl^-, or, in other words, with pure ClO_4^- solution at the same acidity and the same TTA concentration. If a monochloro species is first formed, a plot of D.R. vs. $[Cl^-]$ should yield a curve whose limiting slope as $[Cl^-]$ approaches zero is equal to $(\text{D.R.}^0)(k_1)$. Higher chloride complexes may be identified by plotting the value of $\left[\frac{\text{D.R.}}{\text{D.R.}^0} - 1 - \sum_{n=1}^{m-1} k_n [Cl^-]^n\right]$ vs. $[Cl^-]^m$ where the correct value of m is the one yielding a straight line. Another method would be to plot the value of $\log\left[\frac{\text{D.R.}}{\text{D.R.}^0} - 1 - k_1[Cl^-]\right]$ vs. $\log [Cl^-]$. In this case the slope of the line would be the average number of chlorides associated with each Zr in the higher complexes. In the solutions investigated below only the mono- and trichloro species appear to be of importance, although a dichloro complex is not definitely excluded.

Experimental. Four series of partition experiments were performed using the following aqueous mixtures:

$$\mu(HClO_4 + HCl) = 1,\ [H^+] = 1$$
$$\mu(HClO_4 + HCl) = 2,\ [H^+] = 2$$
$$\mu(HClO_4 + HCl) = 3,\ [H^+] = 3$$
$$\mu(HClO_4 + NaClO_4 + HCl) = 3,\ [H^+] = 1$$

In all cases 3 ml of a TTA-benzene solution 10^{-5} *M* in Zr with Zr^{95} tracer was equilibrated (70 to 120 hr) at 25°C with 3 ml of the appropriate aqueous phase. At the end of the equilibration, aliquots of each phase were mounted

and counted on the third shelf of a standard β counter. In cases in which salt was added (series 4), aliquots of the aqueous phase were extracted with a benzene phase containing a large excess of TTA, and the resulting benzene phase was mounted for counting.

Zr^{95} tracer was freshly purified for use in the runs by precipitating the niobium daughter with MnO_2 from an 8 *M* HNO_3 solution of the mixture (by adding $KMnO_4$ at about 95°C), centrifuging, and, after diluting the supernatant, extracting the tracer into a TTA-benzene solution of the appropriate concentration for use in the runs. Inactive Zr from a stock solution of $ZrOCl_2$ in 0.1 *M* oxalic acid was added before the precipitation of MnO_2 and extracted into the TTA-benzene along with the tracer.

Table 4.9 gives the conditions and the results obtained for each series of runs.

Discussion. All distribution ratios obtained above show an initial linear dependence on chloride concentration characteristic of the formation of a monochloro complex of zirconium. The limiting slopes, S, as the chloride concentration approaches zero and the distribution ratios at $[Cl^-] = 0$ were evaluated by the method of least squares from the partition data up to 0.75 *M* for each set of conditions. The concentration constants associated with the formation of the monochloro complex may then be evaluated from the expression

$$S = (\text{D.R.}^0)(k_1) \qquad (5)$$

Table 4.10 gives the values found for S, D.R.^{0}, and k_1 for each set of conditions investigated. The values for k_1 have been rounded off to two significant figures.

The quantities in parentheses for $\mu = 1$, $[H^+] = 1$ were obtained by averaging the S, D.R.^{0}, and k_1 found by the least-squares evaluation of the data up to 0.75 *M* with the values obtained using the data only up to 0.5 *M* (i.e., at 0.75 *M*; $S = 0.662$, D.R.$^0 = 0.393$, $k_1 = 1.7$; at 0.5 *M*, $S = 0.576$, D.R.$^0 = 0.404$, $k_1 = 1.4$). The distribution ratio obtained at 0.75 *M* under these conditions appeared relatively high when compared with the relative increase found at this concentration for the other conditions investigated.

TABLE 4.9

Zirconium Partition Between Aqueous and Benzene Phases

CHLORIDE CONCENTRATION	D.R., Zr IN AQUEOUS/Zr IN BENZENE	MATERIAL BALANCE (%)
$\mu(HClO_4 + HCl) = 1, [H^+] = 1$; equilibrium TTA concentration = 0.00667 *M*; initial Zr concentration in benzene = 1×10^{-5} *M*		
0.0	0.401	97.5
0.067	0.447	98.9
0.25	0.549	99.2
0.50	0.692	98.6
0.75	0.913	97.7
1.00	1.09	98.1
$\mu(HClO_4 + HCl) = 2, [H^+] = 2$; equilibrium TTA concentration = 0.01344 *M*; initial Zr concentration in benzene = 0.8×10^{-5} *M*		
0.0	0.405	97.8
0.133	0.487	101.4
0.333	0.612	98.3
0.667	0.772	99.6
1.00	1.04	97.8
1.33	1.31	97.2
1.67	1.41	97.8
2.00	1.86	98.2
$\mu(HClO_4 + HCl) = 3, [H^+] = 3$; equilibrium TTA concentration = 0.02048 *M*; initial Zr concentration in benzene = 1×10^{-5} *M*		
0.0	0.322	97.4
0.10	0.395	98.5
0.20	0.402	97.6
0.30	0.481	99.0
0.50	0.532	97.2
0.75	0.606	96.7
1.00	0.760	99.4
1.25	0.803	99.1
1.50	1.00	98.9
1.75	1.25	100.0
2.00	1.42	100.5
2.25	1.54	98.8
2.50	1.77	98.8
2.75	2.11	99.3
3.00	2.35	98.8
$\mu(HClO_4 + NaClO_4 + HCl) = 3, [H^+] = 1$; equilibrium TTA concentration = 0.00667 *M*; initial Zr concentration in benzene = 1.1×10^{-5} *M*		
0.0	0.613	95.6
0.67	0.758	95.3
0.25	0.806	98.5
0.50	1.07	96.9
0.75	1.24	96.9
1.00	1.49	98.9

TABLE 4.10

Formation Constants for the Monochloro Zirconium Complex

μ	$[H^+]$	S	D.R.^{0}	k_1
1	1	(0.619)	(0.399)	(1.6)
2	2	0.550	0.413	1.3
3	3	0.368	0.343	1.1
3	1	0.839	0.649	1.3

The formation constant is seen to decrease with increasing ionic strength. This corresponds with the changes observed in the value of the formation constant for the monochloro thorium complex over the same range of ionic strength.[12]

The apparent increase in the constant with decreasing acidity at $\mu = 3$ is rather surprising. If the monochloro complexing is assumed to be adequately expressed by

$$Zr^{4+} + Cl^- \underset{}{\overset{k_1}{\rightleftharpoons}} ZrCl^{3+} \qquad (6)$$

then an increase in Zr hydrolysis would be expected to be evidenced by an apparent decrease in the constant as evaluated by the method described above, all other factors remaining the same. Also, in the absence of other effects, the expected decrease in the activity coefficients in going from a 3 *M* $HClO_4$ solution to a solution 1 *M* in $HClO_4$ and 2 *M* in $NaClO_4$ should result in an apparent decrease in the constant. An apparent increase, however, would result if Zr hydrolysis were favored by the addition of chloride with the formation of a double complex as expressed by one or both of the equations

$$Zr^{4+} + H_2O + Cl^- \overset{k_1'}{\rightleftharpoons} Zr(OH)(Cl)^{2+} + H^+ \qquad (7)$$

$$Zr^{4+} + H_2O + Cl^- \overset{k_1''}{\rightleftharpoons} ZrOCl^+ + 2H^+ \qquad (8)$$

The formation of a double complex similar to the above has been observed for Th^{4+} and IO_3^-.[13]

(12) Waggener, W. C., unpublished data.

(13) Fry, A. J., Barney, J. E., II, and Stoughton, R. W., *Chemistry of Thorium in Aqueous Solutions. I. The Thorium Iodate System: Solubility and Complexes*, ORNL-63 (Jan. 24, 1948).

If the double complex formation is assumed to be a possibility, the Zr partition may be formulated in a more detailed manner as follows:

$$D.R. = \frac{[Zr^{4+}]+[Zr(OH)^{3+}]+[ZrT^{3+}]+[ZrCl^{3+}]+[Zr(OH)Cl^{2+}]+[ZrOCl^{+}]}{[ZrT_4]_b} \quad (9)$$

where ZrT^{8+} has been added to the aqueous species for the sake of completeness and because the TTA concentrations in the experiments being compared differ by a factor of 3. Then

$$D.R. = \frac{[Zr^{4+}]}{[ZrT_4]_b}\left[1 + \frac{k_h}{[H^+]} + \frac{k_t[HT]}{[H^+]} + k_1[Cl^-] + \frac{k_1'}{[H^+]}[Cl^-] + \frac{k_1''}{[H^+]^2}[Cl^-]^2\right] \quad (10)$$

$$D.R. = D.R.^0\left\{1 + \frac{(k_1 + k_1'/[H^+] + k_1''/[H^+]^2)[Cl^-]}{1 + k_h/[H^+] + k_t[HT]/[H^+]}\right\} = D.R.^0(1+k_1^*[Cl^-]) \quad (11)$$

where

$$D.R.^0 = \frac{Zr^{4+}}{ZrT_4}(1 + k_h/[H^+] + k_t[HT]/[H^+])$$

k_1^* = the apparent formation constant for the monochloro complex

k_h and k_t = the equilibrium constants of the reactions

$$Zr^{4+} + H_2O \underset{}{\overset{k_h}{\rightleftharpoons}} ZrOH^{3+} + H^+$$

$$Zr^{4+} + HT \underset{}{\overset{k_t}{\rightleftharpoons}} ZrT^{3+} + H^+$$

Using the above formulation, it is easily seen that the apparent formation constant for the monochloro complex should:

1. Decrease with increasing hydrolysis (i.e., with formation of $ZrOH^{3+}$)
2. Decrease with increasing TTA concentration if TTA complexing is important
3. Increase with decreasing acidity if double complexing is significant

Acid-dependence data for extraction suggest that $k_h/[H^+]$ is negligible at 3 *M* H^+ and is less than 0.4 at 1 *M*. TTA-dependence data indicate $k_t[HT]/[H^+]$ to be less than 0.1 in 3 *M* HCl and less than 0.3 in 1 *M* HCl.[14]

The distribution ratios at higher chloride concentrations give evidence of further complexing. The nature of the higher complexes may be somewhat delineated from the data obtained for $\mu = 3$, $[H^+] = 3$. Figure 4.1 is a plot of the D.R. vs. $[Cl^-]$ using these data. The solid line is a theoretical curve corresponding to

$$D.R. = 0.343(1 + 1.07[Cl^-] + 0.1[Cl^-]^3) \qquad (12)$$

where 1.07 is the actual result of the least-squares evaluation of the monochloro constant. The goodness of fit is indicated by an average deviation of 3.6%. An equally good fit may be obtained using a parameter associated with the formation of a dichloro complex. In this case

$$D.R. = 0.343(1 + 1.07[Cl^-] + 0.05[Cl^-]^2 + 0.08[Cl^-]^3 \qquad (13)$$

is obtained.

(14) McBride and Stoughton, *op. cit.*

NOT CLASSIFIED
DWG. 9712

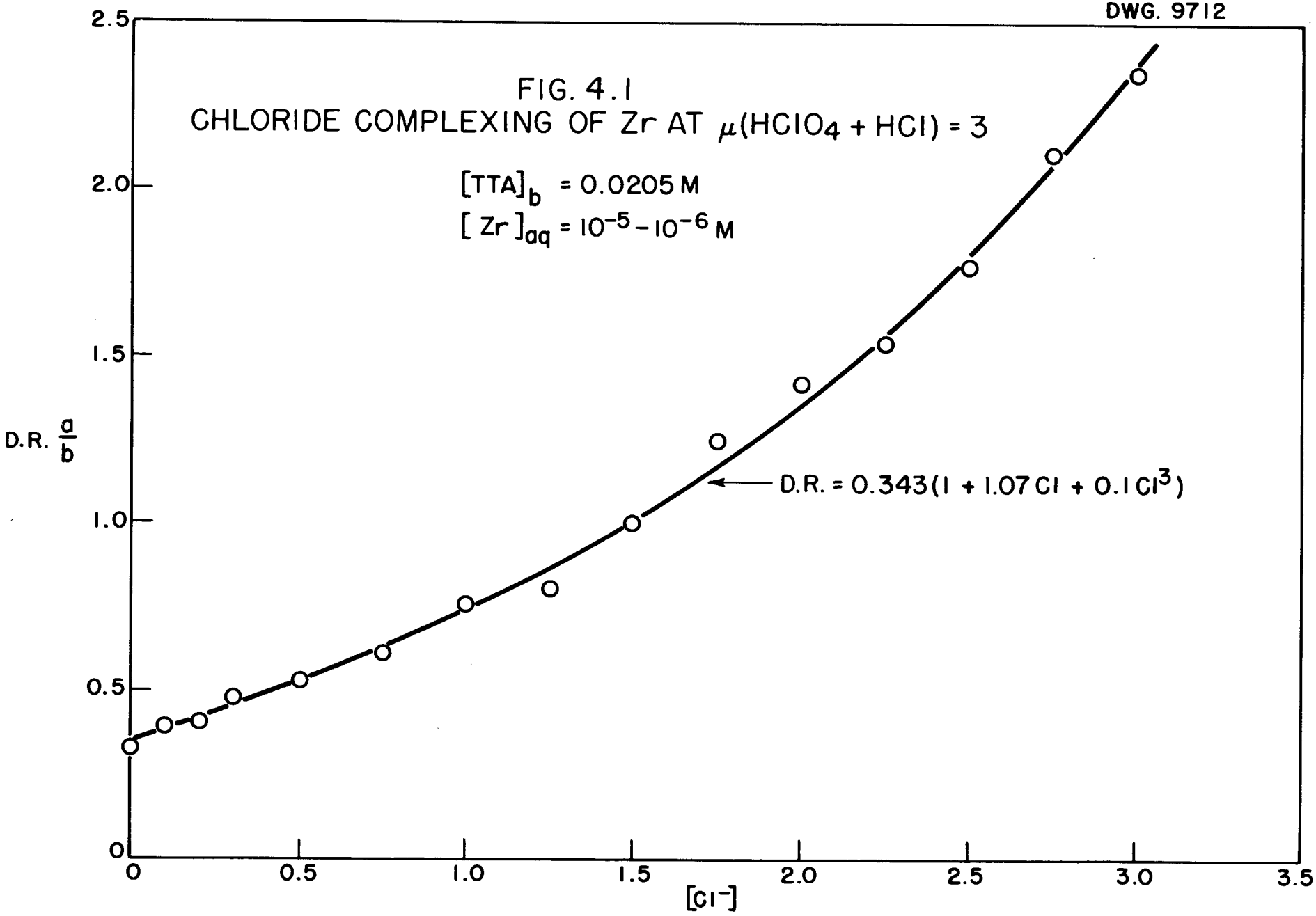

It may be concluded that under the conditions of the experiment the constant associated with the formation of the dichloro complex, if it exists, is probably no greater than that of the trichloro and that both are probably less than 0.1.

Nitric Acid in Tributyl Phosphate (O. E. Myers and R. W. Stoughton). The study of the distribution of nitric acid between water and tributyl phosphate (TBP) has been continued. The previous analysis of the data[15] has been extended by introducing activities in place of concentrations.

Since the activity of a solute must be the same in both phases at equilibrium, it is possible to define a quantity g which is proportional to the activity coefficient of nitric acid in the organic phase,

$$g = f_{\pm}^{2} c^{2}/y = x^{2}/y$$

where

$f_{\pm}$ = mean molar activity coefficient of nitric acid in the aqueous phase

c = molar concentration of aqueous HNO_3 at equilibrium

y = molar concentration of HNO_3 in TBP

$x = f_{\pm} c$

(The use of this equation with existing data for aqueous nitric acid depends on negligible effects of small amounts of dissolved TBP or diluent.)

For equilibrations with undiluted TBP, described in the previous quarterly report,[16] a log y vs. log x diagram was prepared, and values of log g obtained from this curve were plotted against y. These graphs are reproduced as Figs. 4.2 and 4.3. When coupled with previously reported evidence for a 1:1 mole ratio complex $(HNO_3 \cdot TBP)_n$, Fig. 4.3 provides a good indication that in the region 0.02 to 4 f HNO_3 in TBP (where the curve is a straight line of rather large positive slope) we are dealing with a nearly undissociated monomeric complex, $HNO_3 \cdot TBP$.

(15) Myers, O. E., and Stoughton, R. W., "Inorganic Species Extracted in Solvent Extraction," *Chemistry Division Quarterly Progress Report for Period Ending June 30, 1950*, ORNL-795, p. 96 (Oct. 3, 1950).

(16) *Ibid.*

[redacted]

DWG. 9733

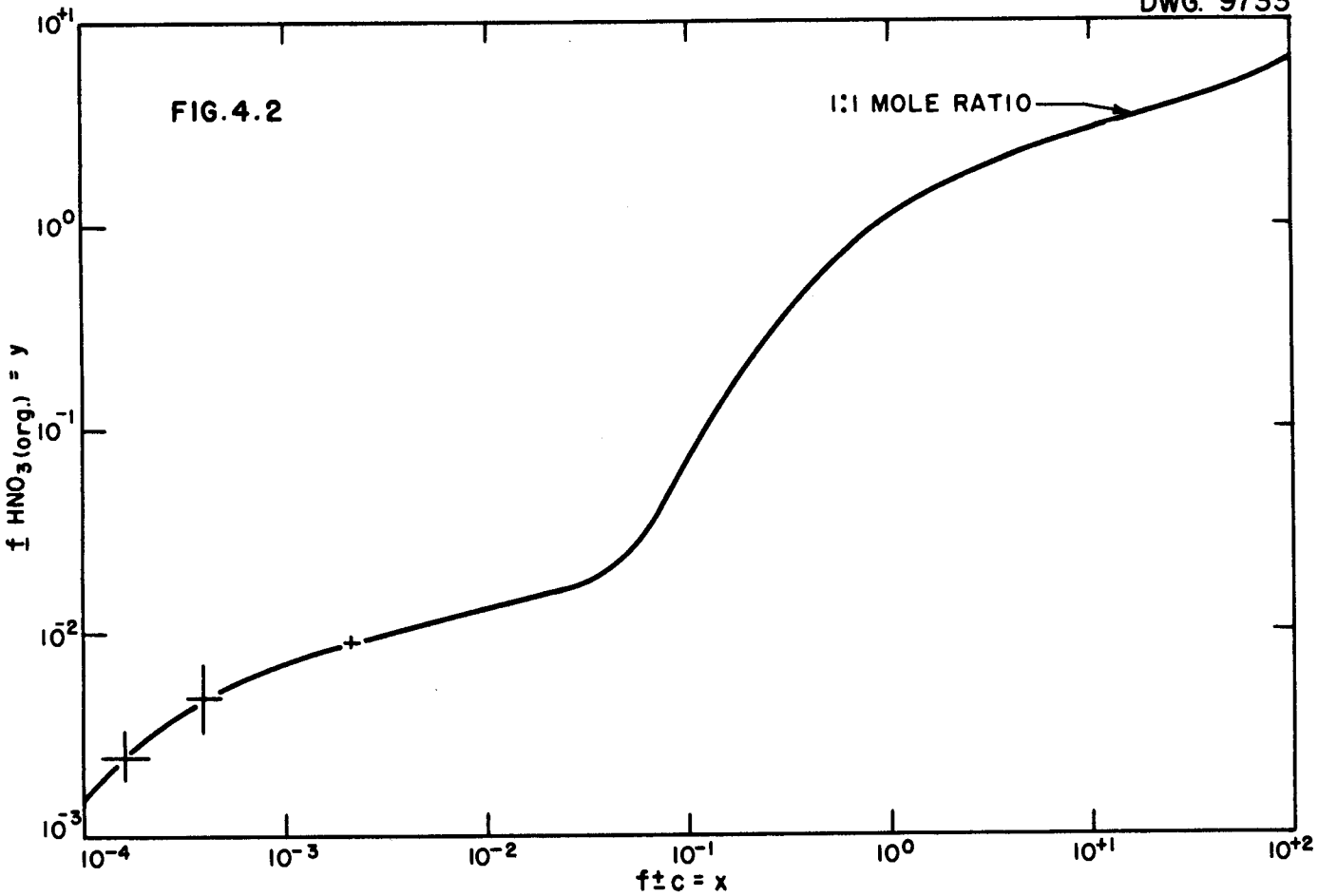

LOGARITHM OF HNO_3 CONCENTRATION IN 100% TBP AT 25°C VS. LOGARITHM OF SQUARE ROOT OF HNO_3 ACTIVITY PRODUCT IN AQUEOUS PHASE AT EQUILIBRIUM

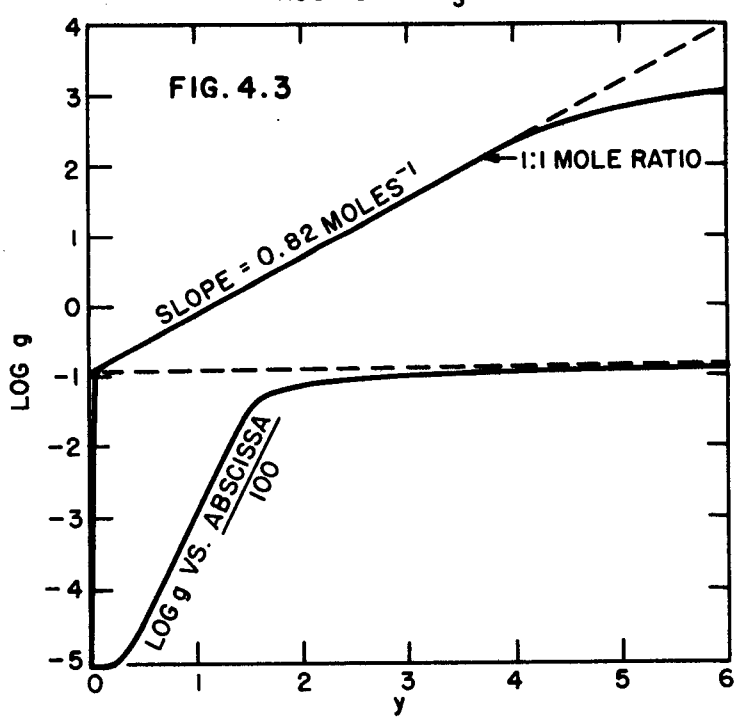

LOGARITHM OF ACTIVITY COEFFICIENT VS. HNO_3 CONCENTRATION IN 100% TBP AT 25°C

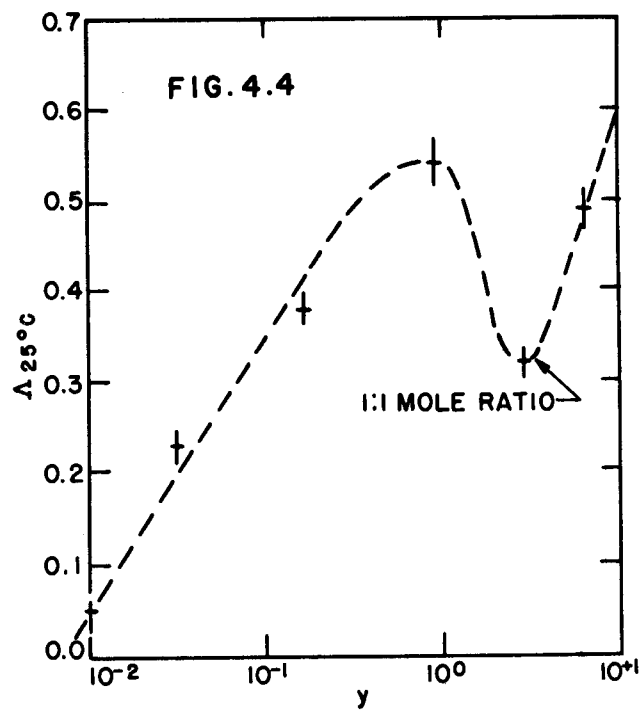

EQUIVALENT CONDUCTANCE AT 25°C VS. LOG HNO_3 CONCENTRATION IN 100% TBP

Electrical conductivity tests, with an estimated accuracy of about 5%, have been made on nitric acid solutions in TBP. For experiments with undiluted TBP the equivalent conductances observed were:

Formality of HNO_3 in TBP	$\Lambda_{25°}$ $\left[\frac{mho\ cm^{-1}}{eq/cm^3}\right]$	$\Lambda_{50°}$ $\left[\frac{mho\ cm^{-1}}{eq/cm^3}\right]$
0.0105	0.051	0.063
0.0320	0.23	0.28
0.164	0.38	0.42
0.920	0.54	0.64
2.92	0.32	0.43
6.40	0.49	0.67

It is of interest that the equivalent conductivity exhibits a dip near the 1:1 mole ratio point and that it is an *increasing* function of concentration except for the dip (Fig. 4.4). This behavior is consistent with the suggested three distinct equilibria in the HNO_3-TBP system, discussed in the previous quarterly report.[17]

A dry box for titrations has been constructed which, it is hoped, will permit the sufficiently precise determination of the equilibrium water content of the organic phase. These data should suffice to complete the problem at hand.

A number of crystalline salts were tested for TBP solubility, and the results are given for their possible general interest:

Soluble	Insoluble
$FeCl_3$	$Co(NH_4SO_4)_2$
$Co(NO_3)_2$	$NiSO_4$
$Ni(NO_3)_2$	$NiCl_2$
$CoCl_2$	$AlCl_3$
$CrCl_3$	$NaNO_3$
	$Al(NO_3)_3$

(17) Myers and Stoughton, *op. cit.*

ELECTROCHEMISTRY

ELECTRODEPOSITION OF SILVER FROM DILUTE SOLUTIONS

J. C. Griess

Introduction. The electrodeposition behavior of traces of silver was the subject of a report originating at this laboratory.[1] Subsequently, this work has been extended, in collaboration with Dr. L. B. Rogers of Massachusetts Institute of Technology, to include the following: The effect of different acids and of cation impurities on the potential at which traces of silver are deposited, the effect of the treatment or conditioning of the electrode before use, and the deposition behavior of silver at concentrations which give a deposit about one atom thick over the entire surface.

The present work covers the concentration range from trace (10^{-9} to 10^{-8} *M*) to 10^{-4} *M*, a range not well covered in the previous work.

Experimental. The apparatus used to study the deposition behavior consisted of a 100-ml gold cup, made from 5-mil gold foil, which served as cathode. The seams of the cup were hammer-forged to eliminate the necessity of welding. The electrolyte was 75 ml of a 0.1 *M* $HClO_4$ solution containing sufficient carrier-free Ag^{111} to give an appreciable counting rate. Both the anode and the reference electrode, a saturated calomel electrode (S.C.E.), were connected to the cell by means of saturated potassium nitrate bridges; a motor-driven stirrer provided the agitation. The desired cathode potential was held constant within a few millivolts by means of a regulator previously described.[2]

The detailed procedure for obtaining a deposition curve was as follows: The cathode potential was first adjusted to +1.20 volts vs. S.C.E. and a sample of the electrolyte was taken. The potential was then changed in a negative direction by increments of 25 to 50 mv until a potential was reached at which all the silver was deposited. The time of electrolysis at each potential was 30 min (established by preliminary experiments as the time to

(1) Rogers, L. B., Krause, D. P., Griess, J. C., Jr., and Ehrlinger, D. B., *Electrodeposition Behavior of Traces of Silver*, ORNL-118 (Aug. 3, 1948).

(2) Lamphere, R. W., and Rogers, L. B., *An Instrument for Controlled-potential Electrolysis*, ORNL-117 (Aug. 3, 1948).

reach equilibrium), and at the end of this time an aliquot of the electrolyte was taken for analysis. After all the silver had been deposited, the cathode potential was again adjusted to +1.20 volts, at which potential all the silver was stripped from the electrode. Then a calculated amount of inactive silver was added, and the procedure was repeated at the new concentration. In Fig. 4.5 are shown several deposition curves for concentrations ranging from trace to 10^{-4} *M*.

The solution was analyzed by evaporating a 50-λ aliquot on a small watch glass, counting it by means of a standard G-M tube, and comparing the counting rate with that of an equal aliquot of the original solution.

In order to study the deposition more closely in the intermediate concentration range, a new solution which had a silver concentration of 5.4×10^{-6} *M* was prepared, and a deposition experiment with points taken at intervals of 25 to 40 mv was run. After the run was complete, the silver was stripped from the electrode. The following day the silver was plated onto the gold at +0.15 volts. After equilibrium had been reached, the potential was changed in a positive direction, a sample was analyzed at each potential setting, and a stripping curve was plotted. Both curves are shown in Fig. 4.6.

Discussion. The curve labeled "trace" in Fig. 4.5 represents four different silver concentrations: $\leqslant 10^{-8}$ *M*, 5×10^{-8} *M*, 1×10^{-7} *M*, and 3×10^{-7} *M*. All these concentrations gave similar waves no more than 20 mv apart, and this was considered to be within the experimental error. At higher concentrations very marked differences occurred.

The waves beginning at approximately +0.3 volt are the waves characteristic of macro behavior; those at about +0.9 volt are characteristic of "pure trace" behavior. The intermediate waves, while not fully understood, are real and perhaps represent the deposition of silver on different crystal faces or on different types of "active centers." This explanation is comparable to that given for certain gas adsorption curves reported in the literature.(3)

The experiments with silver concentrations of 1.8×10^{-6} *M* and 3.6×10^{-6} *M* were repeated, and the duplicate waves followed very closely the waves shown in Fig. 4.5 However, it should be noticed that the waves for different concentrations of silver do not always appear at the same potential. At present

(3) Ross, S., and Boyd, G. E., *New Observations on Two-dimensional Condensation Phenomena*, MDDC-864 (no date; decl. Apr. 11, 1947).

NOT CLASSIFIED
DWG. 9697

FIG. 4.5
THE ELECTRODEPOSITION OF SILVER ON GOLD FROM SOLUTIONS CONTAINING VARIOUS SILVER ION CONCENTRATIONS

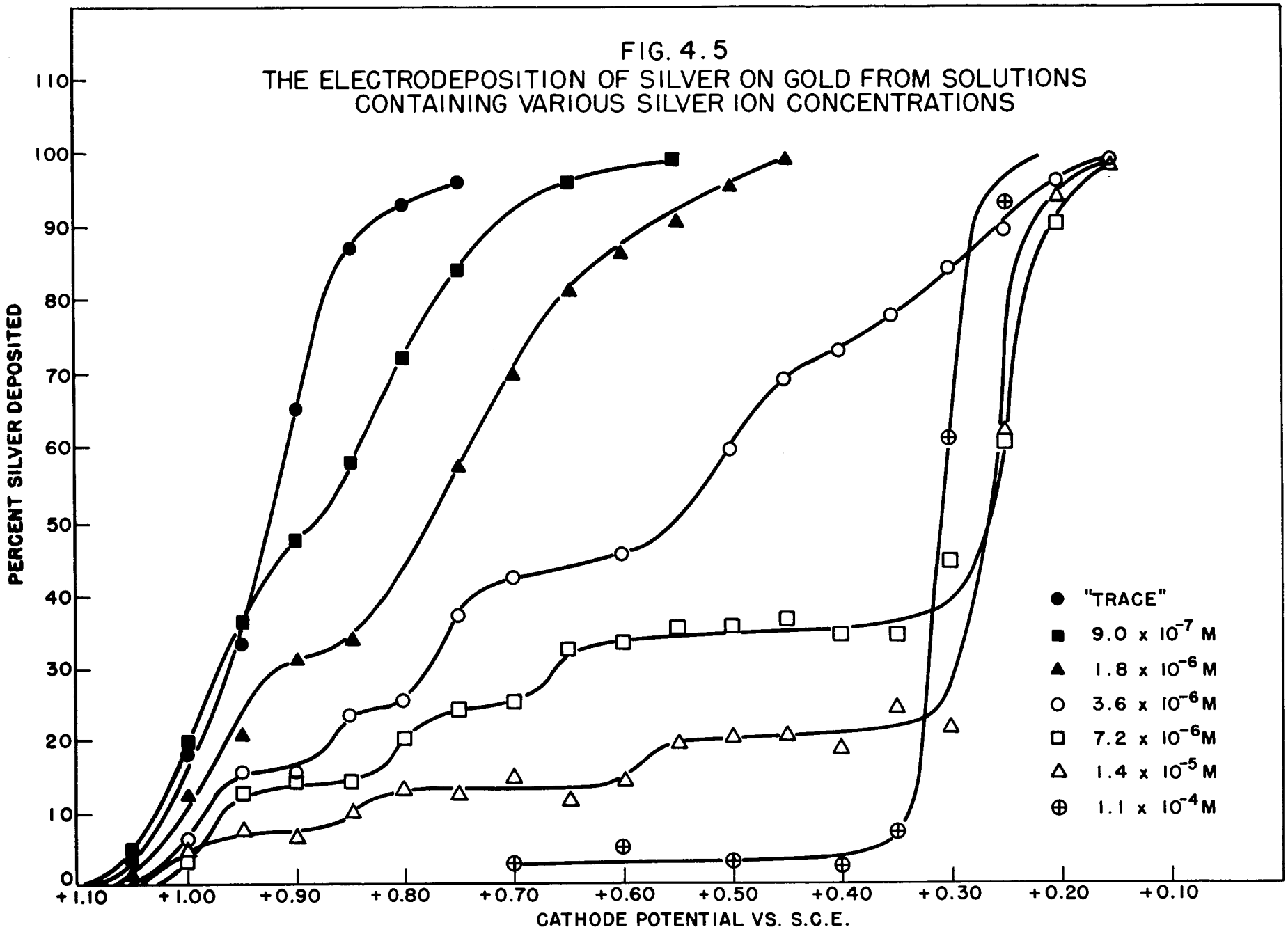

NOT CLASSIFIED
DWG. 9698

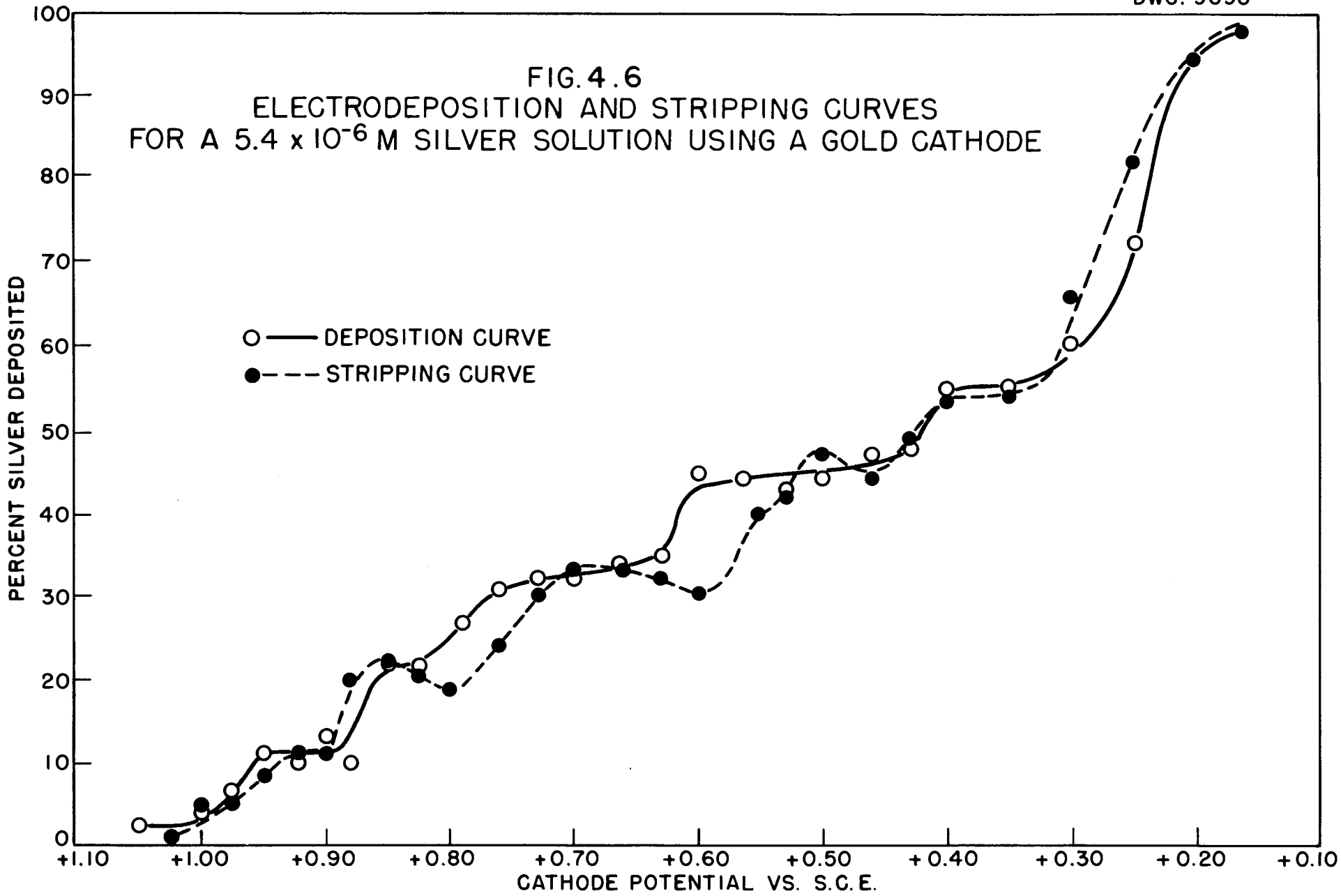

FIG. 4.6
ELECTRODEPOSITION AND STRIPPING CURVES
FOR A 5.4×10^{-6} M SILVER SOLUTION USING A GOLD CATHODE

this phenomenon remains unexplained.

The curves in Fig. 4.6 show how closely the stripping curve follows the deposition curve. On each curve there are five waves in addition to the wave characteristic of macro behavior. The agreement between the stripping and deposition curves is remarkable in view of the fact that on other metals there is usually a 100- to 200-mv difference.

Another point of interest on all the curves for solutions more concentrated than 3.6×10^{-6} *M* is the agreement between the calculated and the experimental macro wave. If it is assumed that the macro wave does not begin until the entire gold surface is covered with a monolayer of silver atoms, it should be possible to calculate the point on the vertical axis where the macro wave begins by a knowledge of the concentration and volume of solution, the cross-sectional area of a deposited silver atom, and the area of the electrode. This last statement presupposes, however, that the true surface area and the plane surface area are equal and that no multilayers are formed until the entire surface has been covered with a monolayer. Since the plane area of the gold cathode was 85 cm^2, the surface should have just been covered when 40% of the silver in the 7.2×10^{-6} *M* solution was deposited. The experimental value was 35%. Similarly, the surface should have been covered when 54% of the silver in a 5.4×10^{-6} *M* solution was reduced; the macro wave began when 56% of the silver was deposited. The agreement is very good, and, in fact, considering the nature of the assumptions, perhaps fortuitous.

ION EXCHANGE

LITHIUM ISOTOPE SEPARATION

J. H. Gross R. E. Wacker
C. W. Keenan

Introduction. The investigation of this separation was undertaken because of the need for high-purity Li^7 as a coolant for high-power reactors. The possibility of producing separated Li^6 also is now of interest. Work on this problem has continued as previously planned.[1,2]

Experimental. *Hot-column Experiment with Nalcite HCR.* An experiment was run in a Nalcite HCR column at 70°C (column IV). All other operating variables were held as close as possible to the values used in the previously reported[3] Nalcite HCR experiment at 30°C (column II). The same separation scheme was used, *i.e.*, development of a band of Li^+ with 0.1 *M* HCl. The assay results are given in Table 4.11; in Fig. 4.7 they are compared with those obtained at 30°C.

TABLE 4.11

Lithium Isotope Separation on Ion-exchange Resin Column at 70°C

Conditions:

Bed: 20 cm^2 by 146 cm Nalcite HCR, 70- to 200-μ spheres
Temperature: 70°C
Eluant: 0.1 *M* HCl
Flow rate: 0.16 to 0.17 cm/min

SAMPLE	% OF TOTAL DEVELOPED Li^+	ASSAY (atom % Li^7)
1 (Leading edge)	0.16	93.912 ± 0.015
2	0.60	93.629 ± 0.023
3	3.22 - 3.31	93.270 ± 0.056
4	6.19 - 6.34	93.244 ± 0.012
5	10.55 - 10.75	93.012 ± 0.045
6	15.37 - 15.48	92.892 ± 0.018
7 (Trailing edge)	91.43 - 91.60	91.643 ± 0.015
Feed		92.472 ± 0.041

(1) Gross, J. H., Neely, J. F., Jr., and Boyd, G. E., "Lithium Isotope Separation," *Chemistry Division Quarterly Progress Report for Period Ending March 31, 1950*, ORNL-685, p. 113 (June 16, 1950).

(2) Gross, J. H., Boyd, G. E., Wacker, R. E., Neely, J. F., Jr., and Bohimann, E. G., "Lithium Isotope Separation," *Chemistry Division Quarterly Progress Report for for Period Ending June 30, 1950*, ORNL-795, p. 106 (Oct. 3, 1950).

(3) *Ibid.*

[redacted]

DWG. 9699

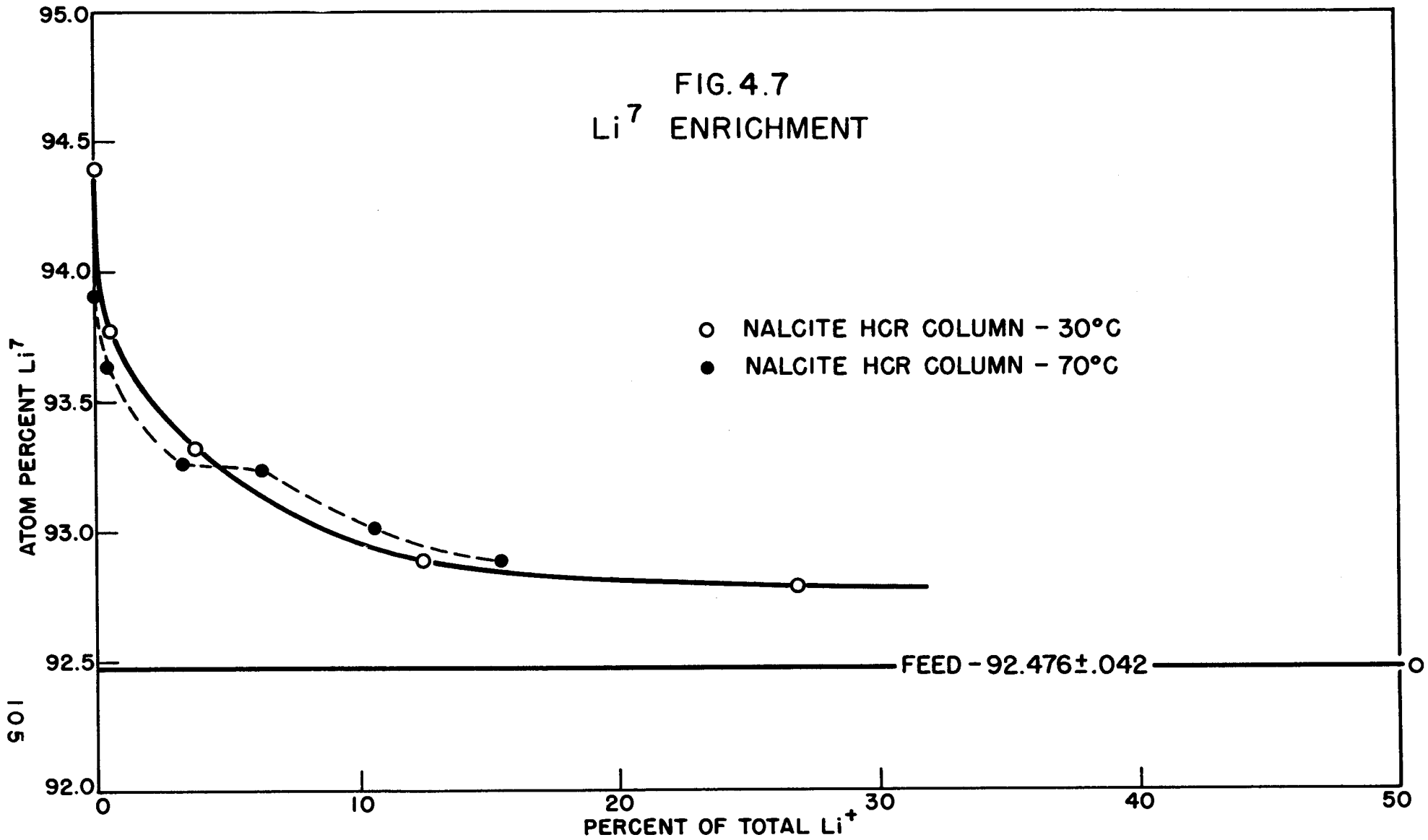

Further assay results are being obtained at various points in the eluted band.

Experiments with IRC-50. Data obtained by Blanco[4] showed that the sodium capacity of IRC-50, a carboxylic exchanger made by Rohm and Haas, varies from near zero at *p*H 4 to about 9.5 meq per gram of oven-dried resin at *p*H 9. This extreme variation in capacity, which is due to the weak acid nature of the resin, and the accompanying very large volume change could not be tolerated in a sensitive column separation. Therefore, before the IRC-50 column could be used, a *p*H range in which its capacity was essentially constant had to be found. The capacity of the resin for $Li^+ + NH_4^+$ was determined between *p*H 8.7 and 10.2 by equilibrating it with $LiCl$-NH_4Cl-NH_4OH solutions and measuring the concentrations of the ions on the resin. Table 4.12 gives the results, which show that at a *p*H of about 10 the capacity is constant.

TABLE 4.12

Capacity for $Li^+ + NH_4^+$ of IRC-50 Ion-exchange Resin

*p*H	CAPACITY (meq/g)	SOLUTION CONCENTRATIONS (molarity)		
		Li^+	NH_4^+	NH_4OH
8.70	9.7	0.074	0.126	0.038
9.12	9.8	0.087	0.111	0.088
10.12	9.9	0.076	0.124	0.918
10.20	9.9	0.088	0.109	0.970

The "capacity" described here is actually a measure of the metal ion—H^+ equilibrium distribution; at very low hydrogen-ion concentration (*p*H 10) the

(4) Blanco, R. E., *Laboratory Development of an Ion Exchange RaLa Process*, ORNL-620 (June 2, 1950).

measured $Li^+ + NH_4^+$ capacity is virtually equal to the true capacity, that is, the number of equivalents of exchange groups per unit of resin.

The equilibrium constant for the reaction

$$Li^+ + NH_4R \rightleftharpoons LiR + NH_4^+$$

was also determined. It has the value 0.60 for the concentrations of Li^+ and NH_4^+ shown in Table 4.12.

Using a *p*H of 10, an experiment was conducted with IRC-50 at 30°C (column V). The bed, 7.4 cm^2 by 38.5 cm, consisted of the ammonium form of a batch of IRC-50, the hydrogen form of which had been hydraulically classified in the particle-size range of 60 to 150 μ. (Conversion from the hydrogen form to the ammonium or lithium form causes the exchanger-bed volume to increase by a factor of 2.) The hydrogen form had been washed exhaustively with acetone to remove colored organic impurities. A band of lithium resin was developed in the bed at a flow rate of 0.15 cm/min. The eluant was 0.05 *M* in NH_4Cl, and was made 1 *M* in NH_4OH to hold the *p*H above 10, thus ensuring constant bed capacity. An effluent conductivity record was made, but it was worthless because of repeated formation of bubbles in the conductivity cell below the bed. No bubble formation was observed in the exchanger bed.

At the time of writing, a single isotopic analysis has been completed in this experiment. The leading 1.0% of the total Li^+ developed contained 92.852 ± 0.046 atom % Li^7. Further samples have been submitted for analysis.

Discussion. The isotopic-analysis data for Nalcite HCR at 70°C (column IV) do not show significant differences from the data at 30°C (column II). After isotopic analyses of 25 to 30% of the Li^+ eluted at 70°C are obtained, it will be possible to compare integral enrichment over the first 30% of the band at 70°C with the corresponding figure for operation at 30°C. At 30°C, the integral concentration in the first 30% of the band is estimated at 93.0 atom % Li^7. The preliminary results (see Fig. 4.7) strongly indicate that there will be no particular advantage in operating at the higher temperature.

The enrichment obtained in the first 1% of the band from column V (IRC-50 at 30°C) when compared with the corresponding enrichment in column II (Nalcite

HCR at 30°C) suggests that the IRC-50 column offers about the same separation factor per unit length as does the Nalcite HCR column, under the operating conditions of the two cases. The shortage of isotopic analytical data prevents immediate confirmation of this estimate by comparison with other sections of the bands, but at present it is presumed that the IRC-50:Li^+:NH_4^+ system will not be significantly better than the Nalcite-HCR:Li^+:H^+ system in effecting the desired separation. A decision as to the advisability of making a full-scale column experiment with IRC-50 must await further isotopic analyses of the column V effluent.

5. CHEMICAL PHYSICS

NEUTRON-DIFFRACTION STUDIES

H. A. Levy and S. W. Peterson

DEVELOPMENT OF DOUBLE-CRYSTAL SPECTROMETER

During this period the new neutron spectrometer has been brought into full working use on a 24-hr-per-day schedule. Many improvements in operation have been made, one of the most useful being the development of automatic recording of diffraction patterns using a rate meter specially designed by Fairstein (described on p.151) linked to a Brown recorder. Tape recording by a traffic counter of neutron counts from a scaler is still being employed along with the automatic recording but will probably eventually be discontinued.

Study of the neutron-reflecting properties of a number of salt and metal single crystals led to the selection of a new monochromator crystal. A single crystal of copper, prepared by F. A. Sherrill of the Physics Division, has been found to give a fivefold increase in monochromatic beam intensity over the sodium chloride crystal formerly used, with appparently no loss in resolution and with a wavelength substantially the same as that given by the sodium chloride crystal.

The large gain in intensity achieved by the use of a copper crystal made it feasible to attempt to improve the resolution of the spectrometer with some sacrifice of this increased intensity. The results of a large number of experiments testing the resolution of the instrument under various conditions led to the use of Soller slits 1/8 in. wide in front of the detector to collimate the diffracted beam from the sample. Adoption of this device has narrowed the diffraction peaks located at small angles from 2½° to less than 1° at half height. Use of another pair of Soller slits in the beam impinging on the monochromator is planned in an attempt to decrease the wavelength spread of the beam and further improve resolution.

Other developments which are underway include a multiple-crystal monochromator and an automatic beam-intensity regulator; they will be described in more detail in a future report.

NEUTRON-DIFFRACTION INVESTIGATIONS

A large number of samples have been prepared for neutron-diffraction study and diffraction patterns have been obtained from them under various conditions. Some of this has been done in collaboration with other workers.

Dr. W. O. Milligan of Rice Institute, a summer participant in the research program at the Laboratory, brought with him a number of samples, chiefly colloidal in nature, which were examined. These included silica gel prepared under various conditions, chromic oxide gel, vitreous silica, and scandium orthovanadate. Vitreous silica in the form of a clear plate gave an especially interesting type of amorphous pattern which was thoroughly examined over a wide range of values of sin θ/λ. Fourier analysis of these data is underway.

Dr. Bredig of the Physics Division has examined uranium carbide with the neutron spectrometer. Even at temperatures as high as 1200°C no change in the crystalline phase of UC_2 from that at room temperature was observed.

The following compounds have been prepared in a highly deuterated form and examined as powders with the neutron spectrometer:

KHF_2	NH_4HF_2	LiOH	$CO(NH_2)_2$
NH_4F	NH_4Br	KH_2PO_4	

In addition, neutron-diffraction patterns have been obtained on the following materials, all in powder form:

Cr metal	Cr_2O_3	PbO (red form)	Sc_2O_3
Ni metal	SiO_2 (cryst.)	Li_2TiO_3	

STRUCTURE OF KHF_2

The neutron-diffraction study of KHF_2 has been satisfactorily completed. New samples of deuterated KHF_2 have been prepared and examined, and the older data have been carefully re-examined. The results of the various runs have been shown to give good agreement with a symmetrical bifluoride ion mode, the hydrogen atom being uniquely situated midway between the fluorines. The results will be discussed in detail in a forthcoming report.

CALORIMETRY OF RADIOACTIVITY

G. H. Jenks and F. H. Sweeton

In the previous quarterly report[1] the study of the efficiency with which the cavity type of ionization chamber measures heat dissipation in graphite in a reactor was described as complete. Since then, however, further measurements have been made to determine the relative amounts of ionization occurring in various gases contained in the chamber when the chamber is irradiated by gamma rays only. The ionization was measured in dry air, carbon dioxide, argon, and helium, all of which were obtained from tank supplies. The gamma source employed was the Co^{60} source designed by Ghormley and Hochanadel[2] for work in radiation chemistry.

The results of the measurements may be applied in the interpretation of the results of the pile measurements in several ways: (1) They make possible a determination of the extent to which neutrons affected the chamber measurements in the pile, (2) the average energy per ion pair for each of the gases can be calculated from an assumed value for one gas, and (3) they permit a second calibration of the chamber against a calorimetric measurement by Hochanadel and Ghormley (see section on Radiation Chemistry p. 119) of the heat generated in water by the cobalt source. A report, ORNL-923, fully describing this work as well as that in the pile, has been completed and is being issued.

The problem[3] of calorimetrically measuring the energy involved in the decay of C^{14} has been reundertaken, and work is continuing.

(1) Jenks, G. H., and Hairston, J. J., "Calorimetry of Radioactivity," *Chemistry Division Quarterly Progress Report for Period Ending June 30, 1950*, ORNL-795, p. 127 (Oct. 3, 1950).

(2) Hochanadel, C. J., and Ghormley, J. A., forthcoming report.

(3) Jenks, G. H., and Sweeton, F. H., "Calorimetry of Radioactivity," *Chemistry Division Quarterly Progress Report for Period Ending March 31, 1950*, ORNL-685, p. 129 (June 16, 1950).

MICROWAVE SPECTROSCOPY

ZERO-POINT VIBRATIONAL ENERGY CONSIDERATIONS IN POLYATOMIC MOLECULES

John Kilpatrick*

A theoretical examination of the effect of zero-point vibrations upon the moments of inertia of polyatomic molecules, in particular the symmetric tops, has been undertaken. Such information would provide more accurate values of the molecular structural parameters obtained from microwave spectroscopy. At present, molecular structures are obtained from moments of inertia of a molecule with various isotopic substitutions. The failure to correct for zero-point vibrational energy is one of the factors preventing complete utilization of available precision of microwave methods. Once a molecular structure is accurately determined, the substitution of isotopes into the molecule will allow their masses to be determined with comparable accuracy. The method employed involves the use of certain data provided by infrared spectroscopy, and the necessary data are available in the literature for most molecules currently of interest. The present status of the development shows promise of giving at least an estimate of the effect. Further work on the problem is continuing at Rice Institute.

PARAMAGNETIC RESONANCE PHENOMENA

J. H. Goldstein** and R. Livingston

A paramagnetic substance placed in a magnetic field will show resonance absorption of radio-frequency energy when the intensity of the magnetic field and frequency of the radiation are so adjusted as to satisfy the Larmor precession condition. The phenomenon is essentially identical with the nuclear induction experiment. The resonance frequencies for most nuclei fall in the radio-frequency region centering near 20 Mc for convenient magnetic-field intensities. In the paramagnetic case for comparable fields the resonance frequencies lie in the microwave region.

Many classes of materials exhibit this phenomenon, for example, paramagnetic salts such as chrome alum and copper sulfate, organic free radicals, and crystals containing F-centers. The work undertaken on this program during the

* Summer visitor to the Chemistry Division from Rice Institute, Houston, Texas.
** Summer visitor to the Chemistry Division from Emory University, Atlanta, Georgia.

past summer was exploratory in nature and was designed to ascertain the general applicability of the technique.

Several experimental approaches were tried. In one experiment a microwave balanced-bridge technique developed at Duke University[1] was used. The apparatus consisted of a Magic-T bridge, and reflections were observed from powdered or solid samples placed in rectangular wave-guide nonresonant cells. The method was abandoned because of the need for relatively large samples and because the ultimate sensitivity was not so high as desired.

In another experiment the simple straight-through absorption method was used in which the sample was placed inside the rectangular wave-guide transmission line. Here, too, as expected, the sample size and sensitivity were limiting factors.

The system[2] in use at present employs a cylindrical resonant cavity operated in the TE_{0ln} mode. Powdered samples are loaded into a fine capillary and suspended from the top plunger of the cavity; solid samples are suspended directly from the top plunger. Because of the inherent sensitivity, only small samples are required, in many cases only a few milligrams.

All experiments were tried in the K-band region (24,000 Mc). The frequency was maintained constant, and the magnetic field was swept by a motor-driven mechanism attached to the magnet power supply. Signals were recorded on a Brown strip-chart recorder with 3 mv full-scale sensitivity. In this way resonance absorption curves were automatically and continuously traced.

A large number of observations of others have been repeated on a variety of paramagnetic salts, including copper sulfate, chrome alum, and manganous sulfate. The one reported observation[3] of resonance in an F-centered crystal (LiF) has been confirmed without difficulty.

The material currently being studied is the stable free radical tri-*p*-biphenylmethyl, of which no previous studies by this method have been reported. Using a sample of 5 to 10 mg of questionable purity, a very sharp resonance

(1) "Microwave Research," *Duke University Quarterly Progress Report for November 1, 1948 to February 1, 1949*, NP-711.

(2) Beringer, R., and Castle, J. G., Jr., "Magnetic Resonance Absorption in Nitric Oxide," *Phys. Rev.* 78, 581 (1950).

(3) Hutchison, C. A., Jr., "Paramagnetic Resonance Absorption in Crystals Colored by Irradiation," *Phys. Rev.* 75, 1769 (1949).

was observed. The studies will be continued with a purer preparation. O. K. Neville of the organic chemistry group is collaborating on this work.

METHYL IODIDE STUDIES

R. Livingston

The equipment for determing the nuclear spin of I^{131} is now complete. After a successful test run with I^{129}, two runs were carried out with I^{131}, using about 0.5 curie in each experiment. W. Gordy and O. R. Gilliam of Duke University collaborated on the measurements.

The starting material needed for the experiments was I^{131} contained in a sodium iodide solution with a total volume not exceeding about 10 ml and with a minimum of extraneous salt content. As a result of consultation with A. F. Rupp and others of the Operations Division, it was decided to make as simple a modification of the present I^{131} production method as would produce the needed material. Since exact specifications could not yet be given, it was felt that this approach was better than attempting to develop a new method at this time. In the usual production method, the final step consists in distilling the iodine and water into a receiver containing 5 ml of 0.5 *M* NaOH and 1 ml of 0.1 *M* Na_2SO_3. For the present experiments the Operations Division carried out a special run in which 1.1 ml of 6% H_2SO_3 was placed in the receiver, 100 ml of distillate was collected, and 3.4 ml of 0.5 *M* NaOH was added to neutralize the excess acid. During the distillation the ionization-chamber current monitoring the receiver rose to a peak of 25 arbitrary units and then dropped to 16, indicating the loss of considerable iodine and the absence of reserve reducing agent in the solution. Following the distillation the volume was reduced by evaporation to about 40 ml. A quick assay of the product showed the solution to contain about 129 millicuries of I^{131} per milliliter. Four milliliters of this product was used immediately for the first run, and 5.6 ml was set aside for the second.

In the first run the preparation of the methyl iodide was satisfactory, although the yield, 64% based on radioactivity measurements, was less than expected. However, the spectrometer did not work well, and no frequency measurements could be made, although several very weak lines were observed in the expected region.

In the second run, carried out two days after the first, the spectrometer performed extremely well, but the chemical synthesis went poorly. When the second sample of I^{131} was evaporated to dryness, a large portion volatilized. Apparently, during the two days the solution stood, enough hydrogen peroxide was formed by irradiation of the water to oxidize the iodide to iodine. This agrees with the earlier observation that apparently no reserve reducing agent was present in the solution. About 53% of the iodine that did not volatilize was converted to methyl iodide, but the overall yield was too low to permit conclusive microwave observations. The remote-control equipment performed satisfactorily in both runs.

Further microwave measurements were made on CH_3I^{127} and CH_3I^{129}, another sample of I^{129} being prepared for this purpose. The hyperfine separations of 22 lines (J = 2 to J = 3 transition) of CH_3I^{127} and 23 lines of CH_3I^{129}, as well as the isotopic shifts in several lines, were measured with higher precision than previously[4,5] through the use of a stabilized oscillator built by O. R. Gilliam at Duke University. These measurements had two general purposes, the mapping of this region of the CH_3I spectrum for the masses 127 and 129 for use in future studies on other iodine isotopes (which will contain I^{127} and I^{129} as impurities), and the determination of more accurate values for the moments of inertia of CH_3I and for the nuclear quadrupole coupling constants.

The calculations from the data are incomplete, but the following preliminary values have been obtained by the use of the first-order theory: for the nuclear quadrupole coupling of I^{127}, -1926 Mc, which is 0.4% lower than the accepted value, -1934 Mc,[6] measured on other transitions and serves as an internal standard for the present measurements; for I^{129}, -1357 Mc, which is 4.5% lower than the previous value of -1422 Mc. The latter value was obtained from much less extensive data and was rather uncertain, while the present value is probably accurate to better than 1%. The ratio of nuclear quadrupole moments (I^{129} to I^{127}) with the new value for I^{129} becomes 0.705.

(4) Livingston, R., Gilliam, O. R., and Gordy, W., "The Nuclear Spin and Quadrupole Moment of I^{129}," *Phys. Rev.* 76, 149 (1949).

(5) Gordy, W., Simmons, J. W., and Smith, A. G., "Microwave Determination of the Molecular Structures and Nuclear Couplings of the Methyl Halides," *Phys. Rev.* 74, 243 (1948).

(6) *Ibid.*

The calculation of the isotopic shift in the hypothetical unsplit rotational transitions has not yet been made. It will be useful in calculating a more accurate structure for the CH_3I molecule.

EXPERIMENTS IN CHEMICAL KINETICS WITH MOLECULAR BEAMS

E. H. Taylor

Work has been interrupted by the departure of P. J. P. Chastagner. The revised apparatus, incorporating a window in the vacuum tank for observation of the position of the detectors, has been tested in a single experiment. The whole system performed satisfactorily, and it appears to be ready for use.

6. RADIATION CHEMISTRY

DECOMPOSITION OF AQUEOUS SOLUTIONS OF FISSIONABLE MATERIALS

J. W. Boyle
F. J. Fitch
C. J. Hochanadel
J. F. Manneschmidt
H. F. McDuffie
D. M. Richardson
M. D. Silverman
A. W. Smith
F. H. Sweeton

About twenty pile irradiations of aqueous UO_2SO_4 in stainless steel have been performed during this quarter. The results so far obtained are pressure-time curves during the irradiations and qualitative observations of the solution and the metal after the irradiation. Large-scale precipitation of the uranium is detected during a run by a fall in the gas pressure.

These results are being supplemented by analyses of the irradiated solutions and of the gases produced. These measurements should be completed on the runs to date within a few weeks.

Experiments have been started to determine the conditions of neutron flux, temperature, UO_2SO_4 concentration, and acidity under which UO_4 will precipitate.

The results of the recent irradiations are summarized in the HRE Quarterly Progress Report.[1] They indicate that suitably pretreated type 347 stainless steel will withstand aqueous UO_2SO_4 (40 g of U^{235} per liter) for as long as 14 days in a neutron flux of about 5×10^{11} neutrons/(cm^2)(sec).

(1) *HRE Quarterly Progress Report for Period Ending August 31, 1950*, ORNL-826 (Oct. 24, 1950).

A CALORIMETRIC DETERMINATION OF THE YIELD FOR THE OXIDIZATION OF FERROUS SULFATE BY COBALT GAMMA RAYS

J. A. Ghormley and C. J. Hochanadel

Introduction. The oxidation of ferrous ion in air-saturated sulfuric acid solution has proved to be a convenient method for integrating the X- or γ-ray dose absorbed by an aqueous medium. The calibration of such an actinometer in terms of energy absorption has been carried out in the past by comparing the ionization produced in an air-filled chamber with the chemical change produced in the solution irradiated in a similar cell and exposed to the same radiation field. Unfortunately, yields obtained in this manner by various workers do not agree, as shown in the following tabulation:

	μmoles/liter, 1000 r	Yield (G)
Fricke and Morse[2]	17.3	18.2
Shishacow[3]	15.3	16.0
Miller *et al.*[4]	19.7	20.6

Using the cobalt γ source, it proved feasible to measure calorimetrically the energy absorbed by a sample of water and to compare this with the chemical change produced in a ferrous sulfate solution irradiated under identical conditions. In these measurements, the assumptions made in converting from ionization in air to energy absorption in aqueous solution are eliminated. A yield of 15.7 ferrous ions oxidized per 100 ev was obtained.

Experimental. The rate of absorption of γ-ray energy by the water sample was measured in the adiabatic calorimeter shown in Fig. 6.1. This calorimeter was inserted in the brass source positioner and fixed in place in the cavity of the shield housing the cobalt source. (A description of the source is to be published.) The source was lowered into the positioner, where it surrounded

(2) Fricke, H., and Morse, S., "The Chemical Action of Röntgen Rays on Dilute Ferrosulfate Solutions as a Measure of Dose," *Am. J. Roentgenology and Radium Therapy* 18, 430 (1927); "The Action of X-Rays on Ferrous Sulphate Solutions," *Phil. Mag.* 7, 129 (1929).

(3) Shishacow, N. A., "The Action of X-Rays on Ferrous Sulfate Solutions," *Phil. Mag.* 14, 198 (1932).

(4) Miller, N., "Quantitative Studies of Radiation-induced Reactions in Aqueous Solution. I. Oxidation of Ferrous Sulfate by X and γ Radiation," *J. Chem. Phys.* 18, 79 (1950).

NOT CLASSIFIED
DWG. 9958

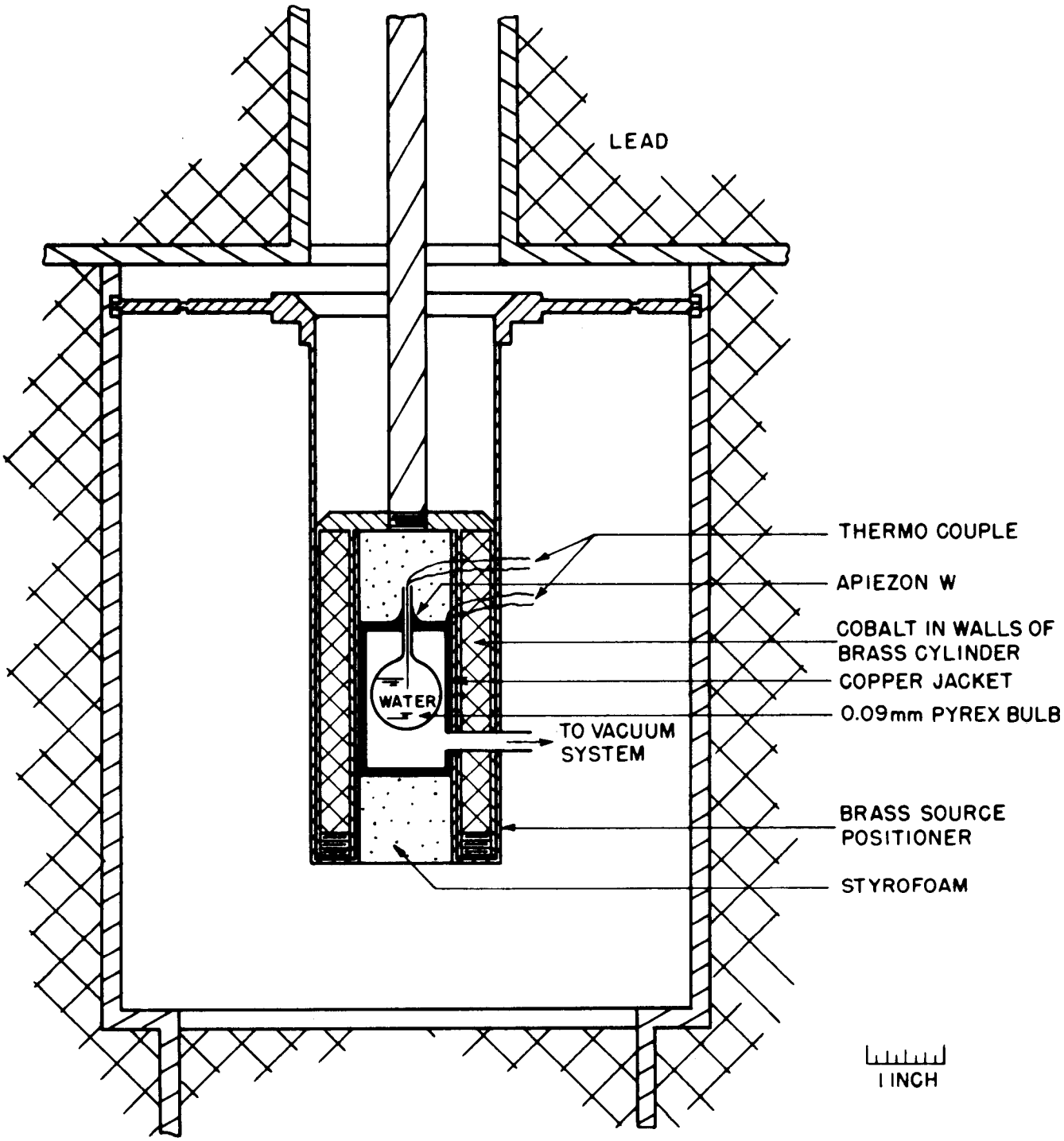

FIG. 6.1
CALORIMETER FOR MEASUREMENT
OF GAMMA RAY ENERGY ABSORBED IN WATER

the calorimeter. The rates of temperature rise of the water and of the copper jacket were followed using a double White potentiometer. The temperature of the copper jacket was adjusted to that of the water sample by means of a heater placed in the cavity of the lead shield.

The yield was measured by three methods, two employing analysis for ferrous ion and one for ferric. Ferrous ion was measured either by titrating with 10^{-3} *M* ceric sulfate prepared by diluting 0.1 *M* ceric sulfate standardized against arsenious oxide, or by the colorimetric method using orthophenanthroline. Ferric ion was determined colorimetrically by the thiocyanate method using iron wire as standard. Results obtained by all methods agreed within 2%.

Results and Discussion. The results obtained were as follows:

Rate of temperature rise	0.01040 deg/min
Weight of water	5.99 g
Weight of glass bulb	0.30 g
Total heat capacity	6.02 cal/deg
Rate of energy absorption in system	0.0626 cal/min
Rate of energy absorption in water	0.0595 cal/min
Rate of energy absorption in 10^{-3} *M* $FeSO_4$—0.4 *M* H_2SO_4 solution	0.01015 cal/(cc)(min) 2.65×10^{17} ev/(cc)(min)
Rate of Fe^{++} oxidation	69.0 μmoles/(liter)(min)
Yield, *G*, ions Fe^{++} oxidized per 100 ev	15.7 ± 0.3

The effects of a number of impurities on the yields for this reaction are shown in the following table:

$FeSO_4$ (*M*)	H_2SO_4 (*M*)	GAS PRESENT	ADDED MATERIAL	YIELD [μmoles/(liter)(min)]
1.334×10^{-3}	0.4	Air	Pure water	68.5
1.334×10^{-3}	0.4	Air	10^{-3} *M* KBr	64.9
1.050×10^{-3}	0.4	O_2	Pure water	69.4
1.050×10^{-3}	0.4	O_2	1.25×10^{-5} *M* CH_3OH	69.4
10^{-3}	0.4	Air	Ordinary distilled water	67.8
10^{-3}	0.4	Air	Tap water	67.7

Our value for the rate of energy absorption in water can be compared with a value obtained by Jenks (see Chemical Physics section of this report, p. 110) using a graphite-wall ionization chamber. From measurements of ion current produced by the Co^{60} source, he calculated 0.0107 cal/(g H_2O)(min). Correcting our value of 0.00993 cal/(g H_2O)(min) for the observed difference of 5.9% between rate of Fe^{++} oxidation for a sample in our calorimeter and another sample in the same bulb surrounded by 4 mm of water, and also applying a 2% correction for self-absorption in our sample, we obtain 0.0108 cal/(g H_2O)(min).

The value of 15.7 that we obtained for the yield is in agreement with that of Shishacow but considerably lower than that reported by Fricke (18.2) or the most recent value obtained by Miller of 20.6. It is felt that the discrepancy arises in the measurement of energy absorption by the ionization chamber method. The data on impurities make it seem unlikely that differences in purity of solutions are responsible for the divergent values.

Dose Rate from the Cobalt Source. Using the value from Lea's book[5] of 93.12 ergs/g for the energy absorbed in water for 1 r of radiation near this wavelength, we obtain the value of 4850 r/min in the center of the cylinder containing the cobalt.

(5) Lea, D. E., *Actions of Radiations on Living Cells*, p. 8, Macmillan, New York, 1947.

YIELDS FOR DECOMPOSITION OF WATER BY Co^{60} GAMMA RADIATION

C. J. Hochanadel

Forward Reaction. The yield of the forward reaction is taken to be the yield of the products H_2 and H_2O_2 formed immediately following the primary act of dissociation of the water molecule. This yield can be estimated in a number of different ways:

1. By measuring the H_2O_2 and H_2 formed by a very short exposure of pure water to radiation. Either analysis for micro quantities of product must be made or values obtained at high doses must be extrapolated in order to compensate for the back reaction.

2. By adding a solute such as Br^- which prevents the back reaction occurring by catalytically combining the free radicals H and OH which did not enter into direct formation of product molecules. The H_2O_2 and H_2 formed in the forward reaction are then measured.

3. By adding an oxidation-reduction system which reacts with part of the species produced by irradiation. One example is nitrite-nitrate, which is oxidized by OH and H_2O_2 and reduced by H but not by H_2. The net result is an oxidation equivalent to the H_2O_2 formed in the forward reaction plus the formation of an equivalent amount of H_2. Another example is the ferrous-ferric system with oxygen, which is oxidized by the OH, H_2O_2, and H (through HO_2), leaving the H_2 formed in the forward reaction.

In the second two methods, the validity of the calculated yields depends upon the validity of the mechanisms used in the interpretation.

Tables 6.1 and 6.2 show yields measured by methods 2 and 3:

The initial yield of H_2O_2 in Br^- solutions is essentially independent of both Br^- and H^+ concentrations over the range studied and is taken to be $G = 0.43$. At higher doses the yield drops, especially at higher *p*H and Br^- concentration, presumably because of H_2O_2 decomposition. This value is somewhat lower than that reported by Fricke[6] of 0.50.

The yield obtained from ferrous sulfate oxidation is still lower and at present cannot be explained. The ferrous oxidation is not so simple as the suggested mechanism[7] would indicate.

(6) Fricke, H., and Hart, E. J., "The Decomposition of Water by X-Rays in the Presence of the Iodide or Bromide Ion," *J. Chem. Phys.* 3, 596 (1935).

(7) Krenz, F. H., and Dewhurst, H. A., "The Mechanism of Oxidation of Ferrous Sulfate by γ Rays in Aerated Water," *J. Chem. Phys.* 17, 1337 (1949).

TABLE 6.1

Yield of H_2 During Oxidation of Acid Ferrous Sulfate Solution

Initial Fe^{++} = 5440 μmoles/liter
Initial H^+ = 0.4 M H_2SO_4
Initial O_2 = 1250 μmoles/liter

Fe^{++} OXIDIZED (μmoles/liter)	H_2 FOUND (μmoles/liter)	G_{H_2} = G_{Fe}* (molecules H_2/100 ev)
3050	70.3	0.36
3820	84.0	0.34
4525	102.5	0.36

*Based on $G_{Fe^{++}}$ = 15.7 Fe^{++}/100 ev.

TABLE 6.2

Yield of H_2O_2 in Radiation Decomposition of Water in Presence of Bromide

SOLUTION				EXPOSURE TIME	H_2O_2	$G_{H_2O_2}$**
KBr (M)	HBr (M)	H_2SO_4 (M)	GAS	(min)	[μmoles/(liter)(min)]	(molecules H_2O_2/100 ev)
10^{-3}		10^{-4}	Helium*	5.0	1.36	0.30
				13.3	1.6	0.36
				30.0	1.23	0.28
				30.0	1.24	0.28
				60.0	0.83	0.19
10^{-3}		10^{-3}	Helium	5.0	1.88	0.42
				15.0	1.89	0.42
				30.0	1.90	0.43
0	10^{-3}	0	Helium	10.0	1.89	0.43
				20.0	1.86	0.42
				30.0	1.84	0.41
10^{-3}		10^{-3}	O_2 (~1250 μmoles/liter)	5.0	4.38	0.98
				15.0	4.00	0.90
				30.0	3.87	0.87
				6.0	3.34	0.75
10^{-4}		10^{-3}	Helium	10.0 (avg. of 4)	1.85	0.42 ± 0.01
				20.0	1.88	0.42
				20.0	1.89	0.42
				60.0	1.82	0.41
10^{-2}		10^{-3}	Helium	10.0	2.0	0.45
				10.0	2.0	0.45
				15.7	1.86	0.42
				16.0	1.85	0.42
				20.0	1.84	0.41
				30.0	1.80	0.40
				31.9	1.76	0.40
				51.0	1.66	0.37

* Purified by passing through copper at 450°C and a charcoal trap at 196°C.

**Based on yield for Fe^{++} oxidation of 15.7 Fe^{++}/100 ev.

Measurement of Radical Yield for Water Under Co^{60} Gamma Irradiation. Not all the primary ionization leads to the relatively stable products H_2 and H_2O_2; part leads to radicals H and OH which escape the zone of their formation without recombining to H_2O, H_2O_2, or H_2. The measurement of the yield of these radicals is of comparable interest to that of the stable products. An estimate of this radical yield can be obtained from measurements of H_2O_2 produced in aqueous solutions of mixed H_2 and O_2. If the following reaction scheme is postulated for the initial stage before products have accumulated,

$$H_2O \longrightarrow \tfrac{1}{2}H_2O_2 + \tfrac{1}{2}H_2;\ \text{yield of } H_2 \text{ or } H_2O_2 = G_F \qquad (F)$$

$$H_2O \longrightarrow H + OH;\ \text{yield of H or OH} = G_R \qquad (R)$$

$$H + O_2 \longrightarrow HO_2 \qquad (1)$$

$$OH + H_2 \longrightarrow H_2O + H \qquad (2)$$

$$H + O_2 \longrightarrow HO_2 \qquad (3)$$

$$HO_2 + HO_2 \longrightarrow 2H_2O_2 \qquad (4)$$

then

$$G_{H_2O_2} = G_F + G_R$$

since each H and each OH escaping from the track yield ultimately $\tfrac{1}{2}H_2O_2$.

$G_{H_2O_2}$ was measured with cobalt γ rays for a solution containing approximately equal concentrations of H_2 and O_2; it was found to be 2.9 molecules of H_2O_2 per 100 ev and to be constant up to 25 μmoles of H_2O_2 per liter (about 5 min in the source). Using the value of 0.43 (see above) for G_F, G_R is found to be 2.47 pairs of radicals per 100 ev. The yield of water decomposed is then 2.47 + 2(0.43) = 3.33 molecules of H_2O per 100 ev.

The yield of 2.9 molecules of H_2O_2 per 100 ev is equal to that obtained by Hart[8] for the oxidation of formic acid in dilute aqueous solution. In this case each pair of radicals oxidizes 1 formic acid molecule, as does each H_2O_2 molecule, so that both experiments lead to the same G_R.

(8) Hart, E. J., *Argonne National Laboratory Summary Report for October, November, December, 1949, Chemistry Division, Section C-II*, ANL-4427 (July 28, 1950).

STORAGE AND RELEASE OF ENERGY IN IONIC SOLIDS SUBJECTED TO IONIZING RADIATION

J. A. Ghormley (with H. A. Levy)

An attempt has been made to determine the role of impurities in the thermoluminescence of potassium bromide. Potassium bromide samples from three different sources were compared by melting each in a platinum dish, pouring into a platinum boat to cool, irradiating 10 min at -196°C with Co^{60} γ's of intensity 2000 r/min, and measuring the light emitted on warming. Glow curves for visible light from two of the samples were found to be similar to each other (lower curve in Fig. 6.2), but different from that of the third sample, "Baker's Analyzed" KBr. It was assumed that impurities in this sample altered its luminescence characteristics, and some salt from the same source was subsequently purified by passing a 0.2 *M* solution through a Dowex-50 cation-exchange column previously treated with 6 *N* HCl. Solution, collected after the hydrogen ions of the ion-exchange column were replaced by potassium, was boiled down to a volume at which salt crystallized out on cooling, and the thermoluminescence of the fused salt was measured as before.

A solution of one of the other samples was subsequently passed through the same ion-exchange column, and the thermoluminescence was measured. Glow curves for the two purified samples were nearly identical, and in the three predominant peaks were very similar to the glow curve of the original Baker's Analyzed KBr. The solution passed through the ion-exchange column may be assumed to be purified with respect to multivalent cations, the impurity ions most likely to influence the luminescence of the salt. The results suggest that the predominant features of the glow curve for the visible region of the spectrum for the fused Baker's Analyzed KBr are perhaps characteristic of the naturally occurring lattice imperfections in pure KBr.

Phosphorescence emission spectra (thermostimulated) of all the KBr samples showed a sharp emission band in the ultraviolet with a peak at 3200 A and a broad band in the visible with a peak at about 5000 A. In some of the samples another band was observed at 2900 A. This probably corresponds with the 2940 A band reported by Kats[9] to be the only band between 2000 and 3200 A. Some typical emission spectrum curves are shown in Fig. 6.3. Glow curves

(9) Kats, M. L., "Luminescence and Distribution of Local Energy Levels in Photochemically Colored Alkali Halide Crystals," *Zhur. Eksptl. Teoret. Fiz.* 18, 501 (1948).

NOT CLASSIFIED
DWG. 9888

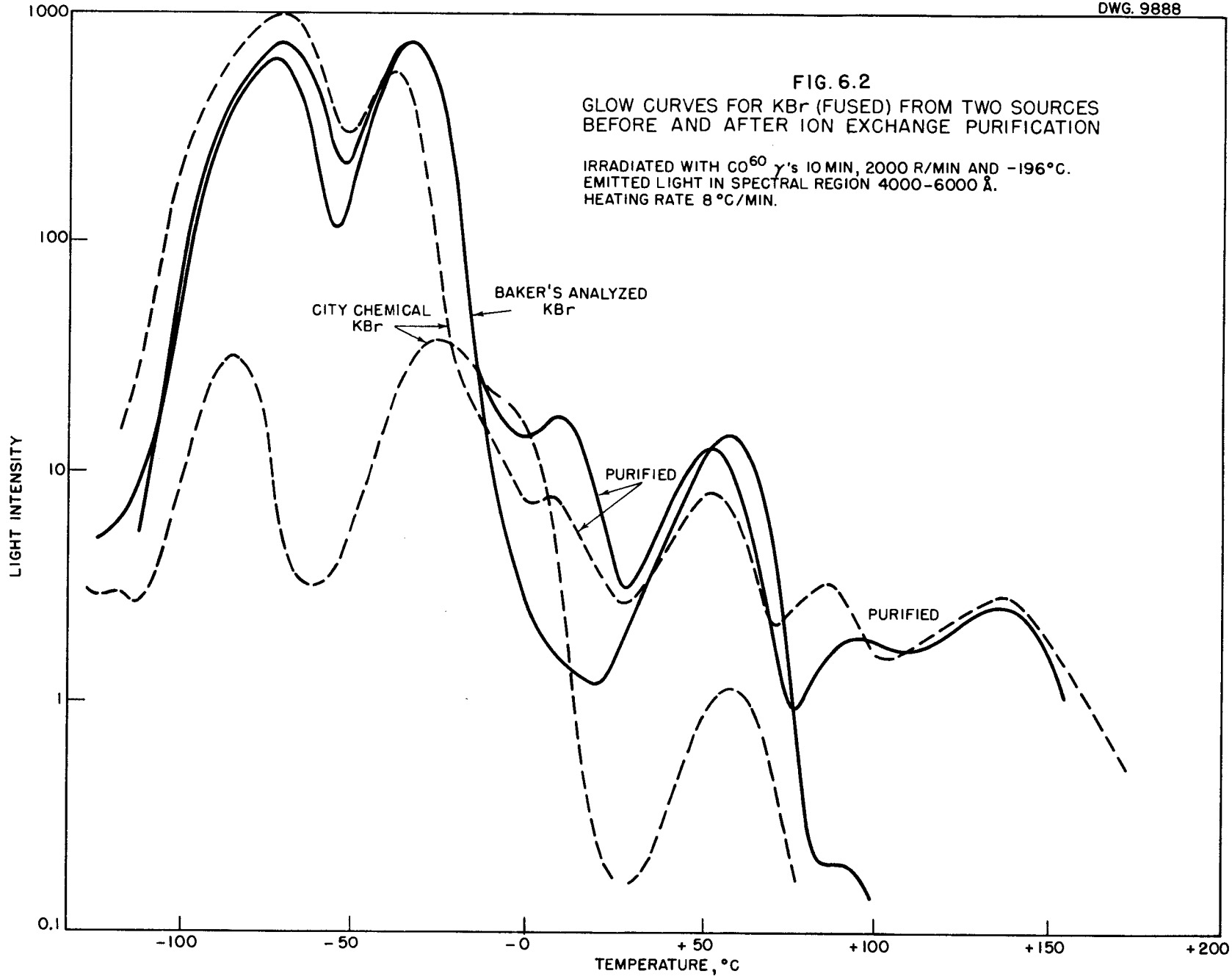

FIG. 6.2
GLOW CURVES FOR KBr (FUSED) FROM TWO SOURCES BEFORE AND AFTER ION EXCHANGE PURIFICATION

IRRADIATED WITH CO^{60} γ's 10 MIN, 2000 R/MIN AND -196°C.
EMITTED LIGHT IN SPECTRAL REGION 4000-6000 Å.
HEATING RATE 8 °C/MIN.

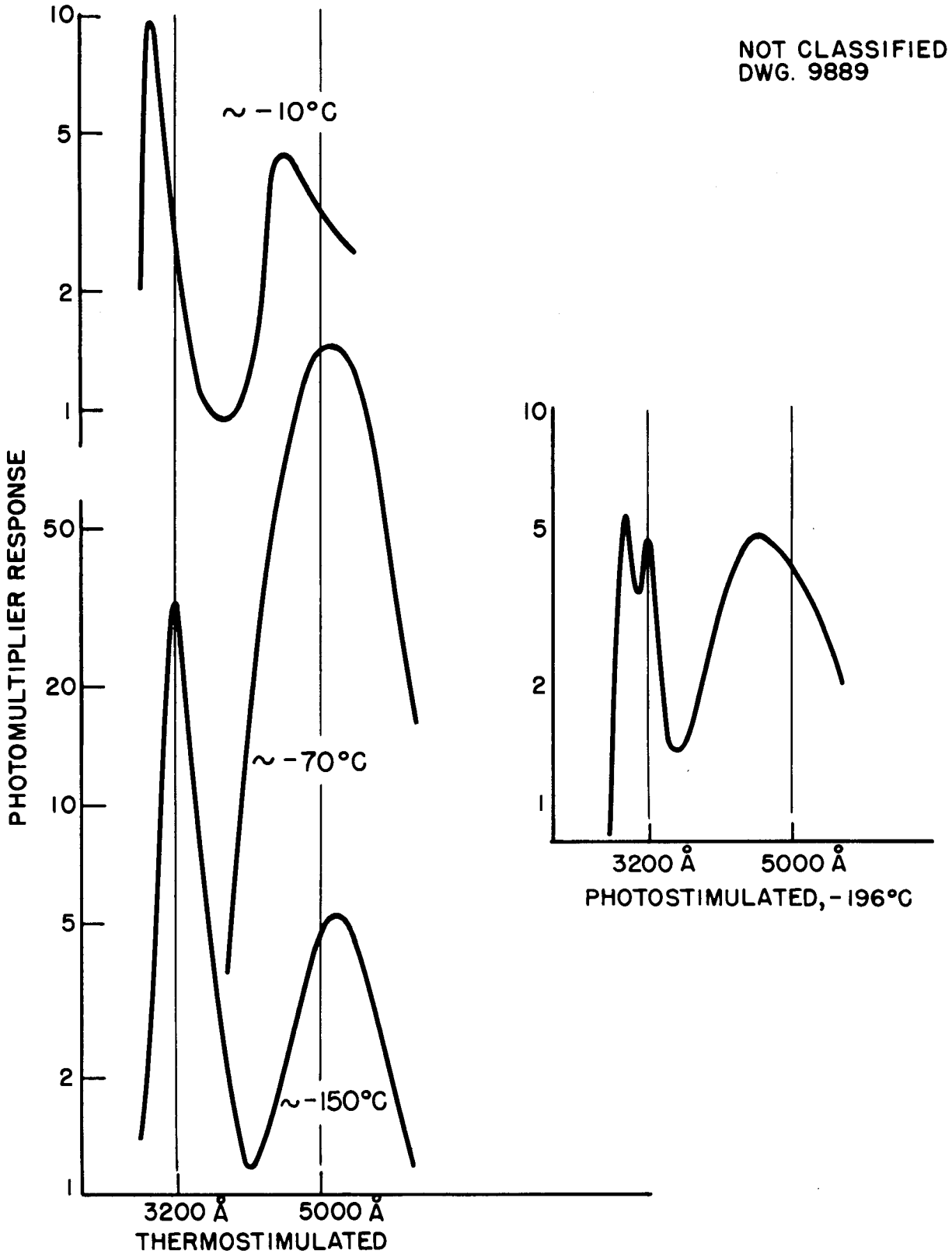

FIG. 6.3
TYPICAL PHOSPHORESCENCE SPECTRA OF FUSED PURIFIED KBr AFTER 10 MIN IRRADIATION AT 2000 R/MIN AND -196°C

measured simultaneously for visible (4000 to 6000 A) and ultraviolet (3200 A) are given in Fig. 6.4. As observed by Kats, peaks in glow curves for KBr for visible and ultraviolet do not appear at the same temperatures. In this respect KBr behaves differently from LiF, which has corresponding peaks for the visible and ultraviolet emission bands.[10]

A sample of fused KBr was irradiated at -196°C with γ rays, then, without warming, exposed to red and infrared light from a tungsten lamp with Corning No. 2404 filter (100% absorption below 6100 A, 88% transmission above 6700 A). The F-center peak is 6000 A with about 1/3 maximum absorption at 6300 A. Three emission bands excited by this light were observed, with peaks at 2900, 3200, and ~5000 A, as shown in Fig. 6.3. On warming a γ-irradiated sample after exposure to red and infrared light, the resulting glow curve for visible light was found to have the two predominant peaks at temperatures of -70 and -30°C reduced by a factor of about 100 in light intensity.

When a small amount of copper ion was added (about 0.01% $CuSO_4$) to the KBr before melting, the glow curve for visible light had the same three predominant peaks (-70, -30, and +55°C), each increased by a factor of 100 in light intensity. The emission spectrum had the usual peak at 5000 A and a new peak at about 4000 A, but no peaks at shorter wavelengths.

Each peak in the glow curve may be interpreted as being associated with thermal release of electrons or holes from traps having a definite configuration. The data suggest that the presence of the copper does not appreciably change the relative concentration of the predominant traps, and that it hence has either no effect on the traps or an equal effect on more than one. As indicated by the change in the emission spectrum, the added copper does influence the emission process which follows release of electrons or holes from their traps.

(10) See *Chemistry Division Quarterly Progress Report for Period Ending June 30, 1950*, ORNL-795, p. 140 (Oct. 3, 1950).

NOT CLASSIFIED
DWG. 9890

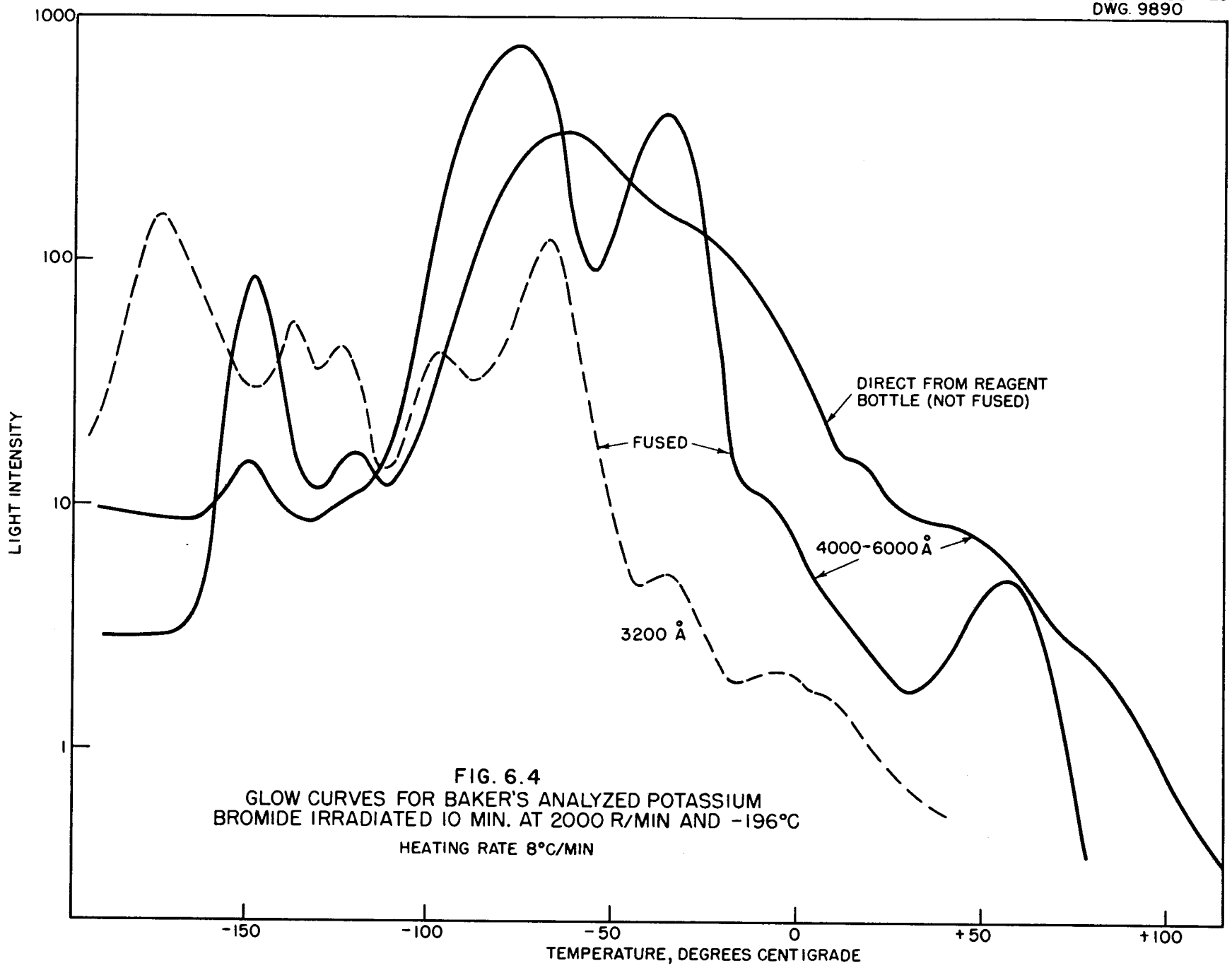

FIG. 6.4
GLOW CURVES FOR BAKER'S ANALYZED POTASSIUM BROMIDE IRRADIATED 10 MIN. AT 2000 R/MIN AND -196°C
HEATING RATE 8°C/MIN

EFFECTS OF IONIZING RADIATION UPON HETEROGENEOUS CATALYSTS

J. A. Wethington (with E. H. Taylor)

Difficulties have been experienced with the measurement of isotopic exchange in the H_2-D_2-HD system. It was planned to use the exchange reaction

$$H_2 + D_2 \rightleftharpoons 2HD$$

to assess the activity of catalysts before and after irradiation. As a result, attention has been again directed toward the hydrogenation of ethylene, and this reaction is being used to look for possible effects of radiation upon catalytic activity.

7. INSTRUMENTATION

A GAMMA SCINTILLATION SURVEY METER

R. A. Dandl and C. J. Borkowski

The circuit of Fig. 7.1 shows a scintillation survey meter designed for maximum gamma sensitivity. The three features of interest are the amplifier trigger, the high-voltage supply, and the d-c connection of the photomultiplier for measurement of intense sources.

The amplifier features good stability over the life of the tubes and batteries, constant pulse shape, and good overload characteristics. Stabilization is accomplished by means of d-c plate-to-grid feedback of each stage. This type of feedback makes the amplifier relatively insensitive to tube and battery voltage changes. The diode-coupled trigger pair is sensitive and stable and has a relatively constant wave shape. The overload characteristics are a result of the three-stage configuration. The positive pulse out of the second differentiation network on the grid of the second stage is grid-current limited, which works very satisfactorily when the grid is fed by a sufficiently small coupling condenser. There are two back-kick clippers functioning also as diode restorers, which, in conjunction with the trigger configuration, satisfactorily prevent multiple pulsing. The amplifier rise time is of the order of 1.5 μsec and a 1.5-mv pulse is required for triggering.

Since a negative high-voltage supply is used, it is a simple matter to provide a switching arrangement which connects the anode to the vacuum-tube voltmeter, allowing d-c measurement of intense sources. The high-voltage supply is very stable and is a modified version of the supply described on p. 155.

It should be mentioned that the amplifier trigger arrangement with 1.5 mv sensitivity has given some very flat plateaus from Geiger counters and beta proportional counters, in which the maximum-size pulse was of the order of several volts.

Performance characteristics, such as overall stability, battery life, and sensitivity, will be discussed in a subsequent report.

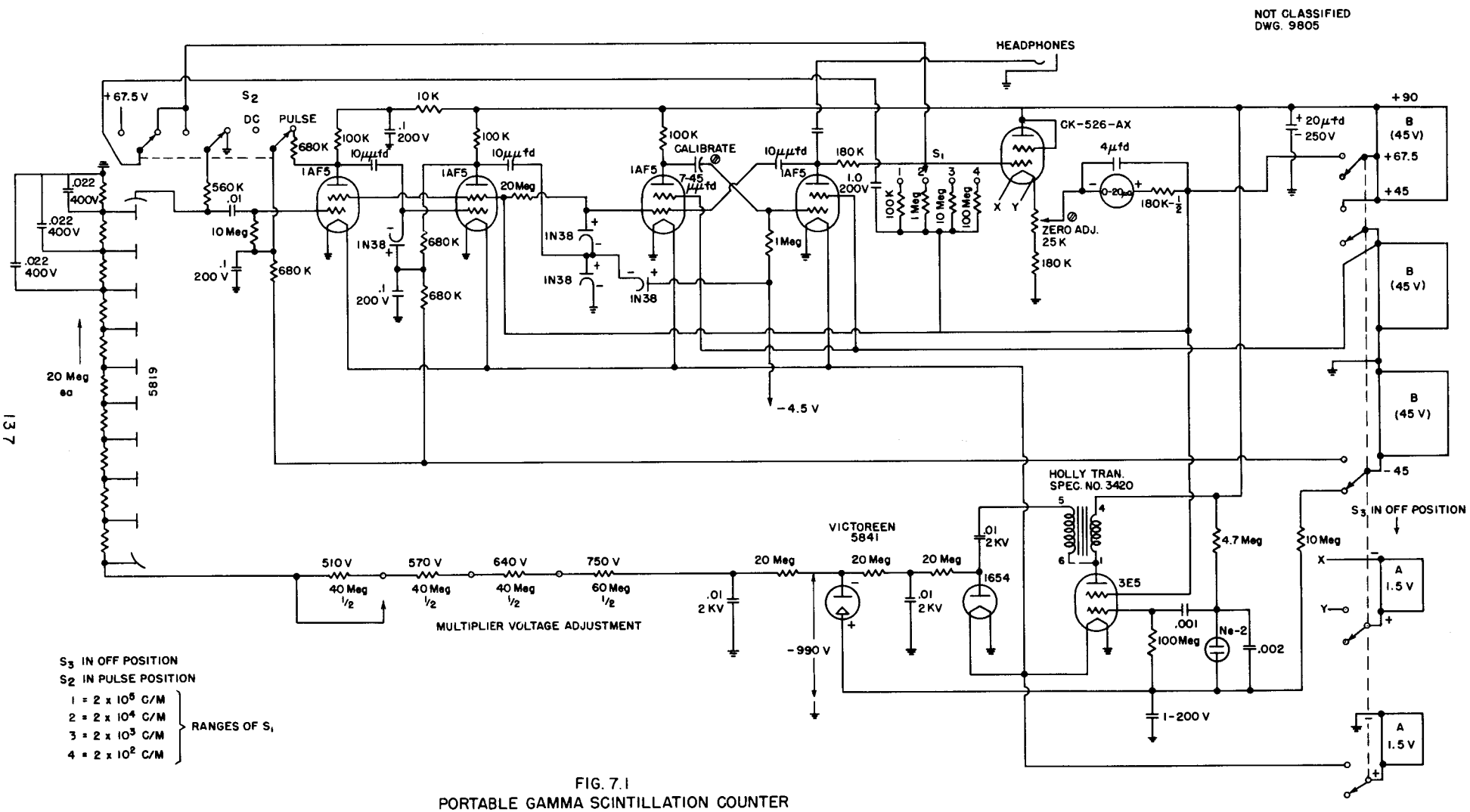

FIG. 7.1
PORTABLE GAMMA SCINTILLATION COUNTER

PULSE ANALYSIS USING PHOTOGRAPHIC DENSITY MEASUREMENTS

R. S. Stone and C. J. Borkowski

Work is underway on methods of pulse-height recording with a view to the development of improved methods. As a first step, existing techniques are being examined. Experiments with a moving-film photographic method in which each pulse is recorded separately were reported in ORNL-795; experiments with a stationary film and densitometer are reported here. The latter method has already been used with short exposures for short half-life activities,[1] but it was apparent that its general use (including long exposures) would introduce different problems, such as fogging, and would have to be evaluated by experiment.

The same setup was used in this as in the moving-film work. The pulses from a proportional counter were fed through an A-1 preamplifier into an A-1 amplifier and thence to a DuMont 248 oscilloscope. This was used with a 5-μsec sweep and ample horizontal gain in order to stretch out the pulse and give as flat a top as possible. A differentiating-circuit (220-$\mu\mu$f mica-capacitor 500,000-ohm tapered potentiometer) was inserted at the input to the oscilloscope synchronizing circuit (at the grid of V106B) in order to help eliminate multiple pulsing. An intensity setting of 50 in the 4-kv position was found to offer about the best compromise between intensities so high as to give the whole tube face a film-fogging glow, and intensities so low as to require exposures long enough to permit general room-light leakage and filament glow to begin to fog the film. A 5JP11A tube was used for its highly photoactinic phosphor, and Eastman Linagraph Ortho film was used for its high speed and low red sensitivity, which helps eliminate recording of the reddish light from the oscilloscope tube filament. The film was developed in Microdol in order to get the better resolution and long tone scale that are characteristic of a soft-working developer. The Fairchild Oscillo-Record Camera was used without the moving-film feature and with the lens stop varied from f1.5 to f2.8, depending upon the number of pulses to be recorded.

It was desired, first, to check the deflection linearity of the system. In this step, the input to the preamplifier went through the A-1 and oscilloscope amplifiers to the tube face, where it was photographed, and the developed film was motor-driven through the densitometer at a constant rate, in the

(1) Kahn, J. H., and Goodrich, M., personal communication.

direction corresponding to the oscilloscope Y axis. The output from the densitometer was fed to a Brown strip-chart recorder; voltage levels in the input were thus represented by displacements along the time axis of the recorder chart. The Constant-Q pulse generator was used as an accurately variable voltage pulse source, and exposures were made with its output connected to the preamplifier in the system described above. Base lines were obtained by a method used by Kahn and Goodrich of the Physics Division, in which the deflection plate connections are shorted to ground, the selector switch is shifted from "amplifier" to "terminals," and a short exposure is made. Typical examples of data obtained in this way are shown in Fig. 7.2. It may be seen that response of the system to voltage changes is quite linear, and with one calibration point energy can be read as a linear function of distance along the time axis of the chart with very little error.

The next question concerns the relation between density and exposure. Theoretically, within the limits of correct exposure, there should be a linear relation between density and logarithm of exposure. How closely this ideal is approached is determined in the following manner: The exposures given at the various voltages in the previous deflection measurement are varied with the speed of the camera shutter in order to give the different lines densities due to exposures of 1/10, 1/5, 1/2, 1 sec, etc. Exposure can be related to the number of pulses "contained" in each line, *i.e.*, 1/5 sec should give about twelve pulses from the 60-cps generator. The quantity recorded by the Brown recorder is really density, D, but since logarithmic chart paper is used, the quantity actually read is opacity, O ($D = \log O$). When this is replotted on log paper, displacement is again proportional to density, and on log-log paper a graph of opacity vs. number of pulses should give a linear relation. In Fig. 7.3 are three typical graphs, from which it is seen that the linearity here is not nearly so good as in the deflection-vs.-voltage relation. However, several points may lie considerably nearer the lines than shown. For example, in curve b_1 the 1/25-sec exposure has been taken to represent two pulses (statistically the more probable number), although 1/25 sec could also yield three pulses. Taking the number as three puts the point very close to the general trend of the other points. The curves drawn give the relations $n = 2.4 \times O^{1.00}$ for curve b_1, $n = 2.3 \times O^{1.34}$ for b_2, and $n = 4.53 \times O^{1.41}$ for b_3.

We thus have relations for translating the opacity (density) of the film at a given displacement from the base line into the number of pulses recorded

NOT CLASSIFIED
DWG. 9783

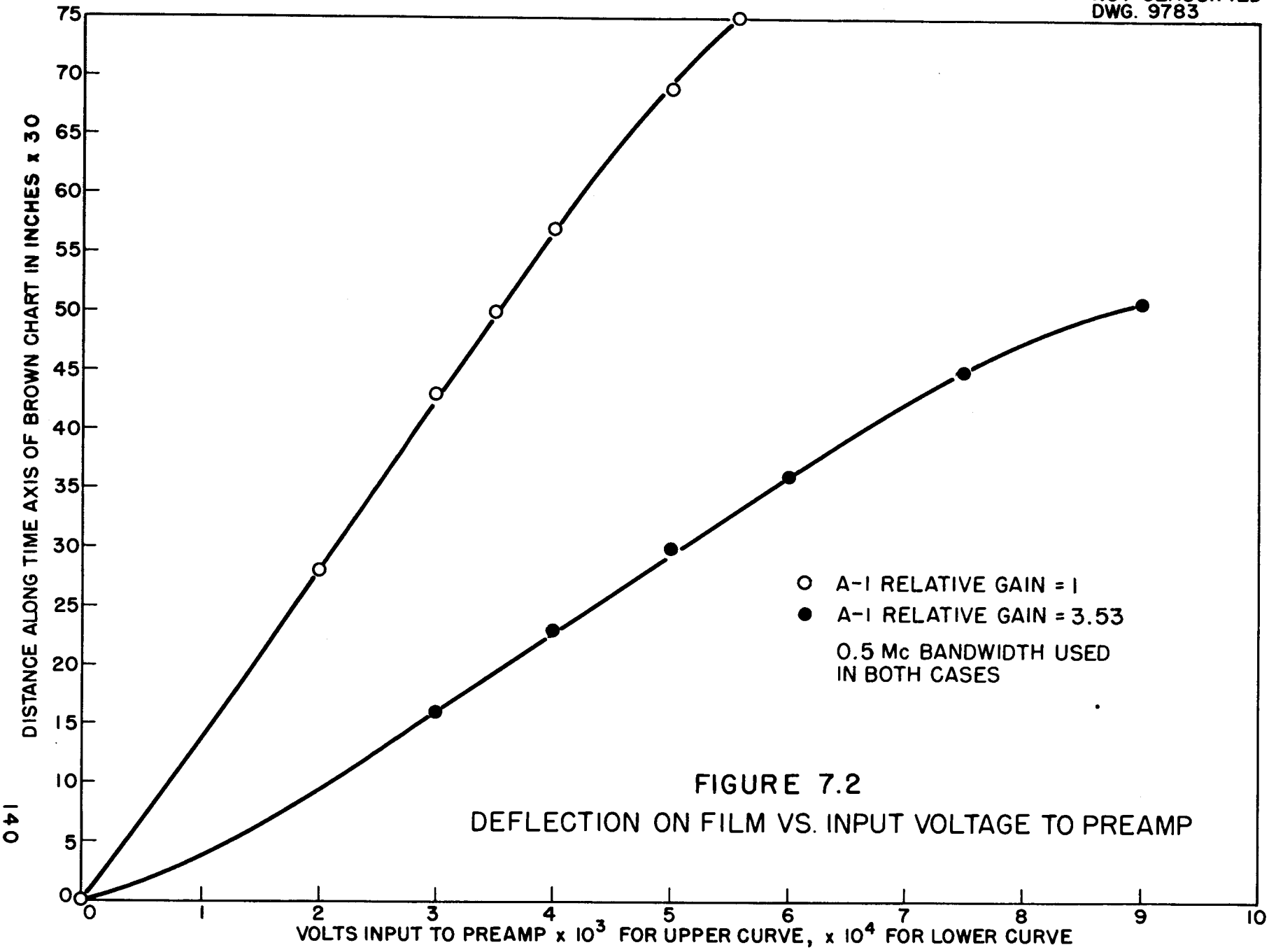

FIGURE 7.2
DEFLECTION ON FILM VS. INPUT VOLTAGE TO PREAMP

NOT CLASSIFIED
DWG. 9784

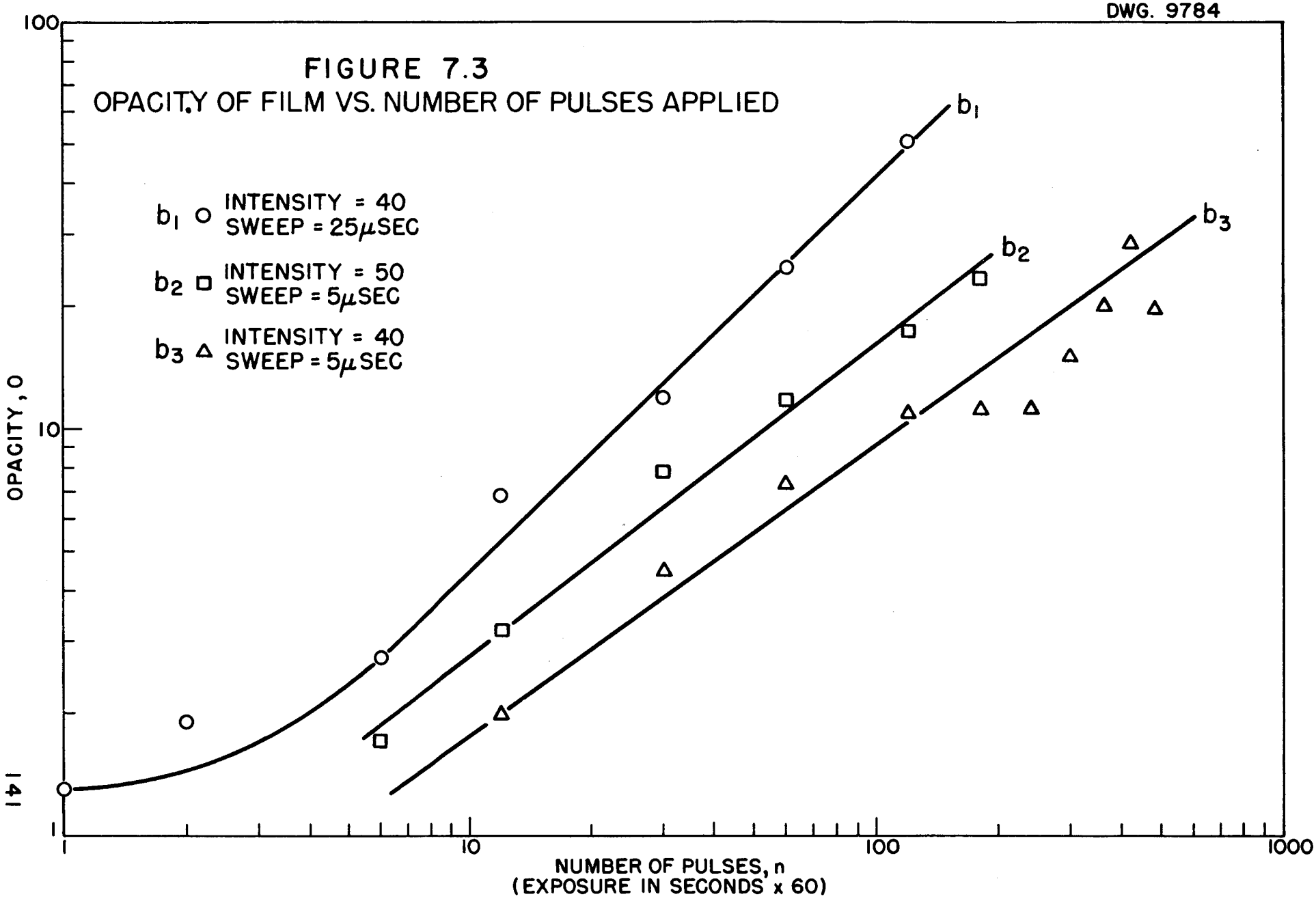

at a certain energy. Unfortunately, there are considerations which make this calibration less than 100% reliable. For one thing, these calibrating exposures are made in a matter of seconds, with no detectable fogging of the film, whereas sample counts often extend over 24 hr, in which time a certain amount of general fogging of the film is practically unavoidable, from stray light in the tube phosphor if from no other source. This makes a given density on the actual run represent a smaller number of pulses than the calibration indicates. A background film may be run and its density subtracted from that of the sample film, but the true correction is not so simple as this since some of the fogged silver grains if not taken by fog would have been sensitized by the true exposure, and unless rather elaborate sensitometric conditions are made, a certain unreliability from this source must be accepted. The overall effect if background is merely subtracted from the count is that a given density in a measurement represents more pulses than in the calibration.

Inaccuracies may also be caused by the so-called "intermittancy effect." This is a property of photographic emulsions which results in less darkening from an exposure broken up into a number of installments than from the same exposure given continuously. However, a large number of rapidly given flashes approaches the effect of one exposure and the 60-cps calibration pulses come closer to fulfilling this condition than the randomly distributed and less frequent sample pulses. Hence this effect will also tend to make a given darkening of the sample film represent more pulses than the calibration indicates.

A third source of inaccuracy is the density-vs-log-exposure curve itself, since, as seen above, it is only approximately linear. Moreover, the resolving power of the densitometer is somewhat limited, although this is partly due to lag in the Brown recorder and could be improved by slowing down the film drive.

Fortunately, these inaccuracies are practically all in absolute peak heights, not in relative peak heights or energy, and hence should not cause too much difficulty in determining the existence of a peak or calculating its energy. Nonetheless, the peak could conceivably be displaced by a nonuniform (energy-wise) background at a level close to that of the sample, where subtraction of somewhat inaccurate quantities of comparable magnitudes is involved. The general conclusion is the same as that reached before, *i.e.*, the method is basically less accurate than separate pulse recording and measuring,

but ease in reading makes it still worthy of consideration. The method was therefore tried on an actual sample, as follows:

The setup was first energy-calibrated by running a 6500-c/m Sn^{113} sample (24.2-Kev In $K\alpha$ ray) for 2 min. The resulting densitometer record was plotted as curve c_1 on Fig. 7.4. It is seen that 32.5/30 in. on the Brown chart represents 24.2 Kev, giving 23.3 Kev per inch as the energy conversion factor. A density-vs.-exposure calibration was then made as described before (curve b_3 of Fig. 7.3), and $n = 4.53 \times O^{1.41}$ was taken for this film.

The actual sample was a very weak La^{138} source (about 30 c/m), and a line was expected at 32.3 Kev (Ba $K\alpha$ ray). An exposure of 24 hr at $f1.5$ was made with the intensity set at 40. A background exposure was made under the same conditions. The results were plotted as curves c_2 and c_3 of Fig. 7.4, and it may be seen that there is a peak at about 32.5 Kev. Figure 7.5, a graph of sample count minus background, shows the form of the energy spectrum more clearly, and indicates that the peak is at 33.0 Kev. This is quite close to the theoretical value.

It is thus seen that under the right circumstances the density method of pulse analysis is capable of giving results comparable to separate pulse recording, and with much less time and labor in reading. However, when closely adjacent peaks must be resolved, when accurate ratios of peak heights are important, or when a high nonuniform background makes correct peak location critically dependent upon subtracted values, the moving-film method should probably be employed.

NOT CLASSIFIED
DWG. 9785

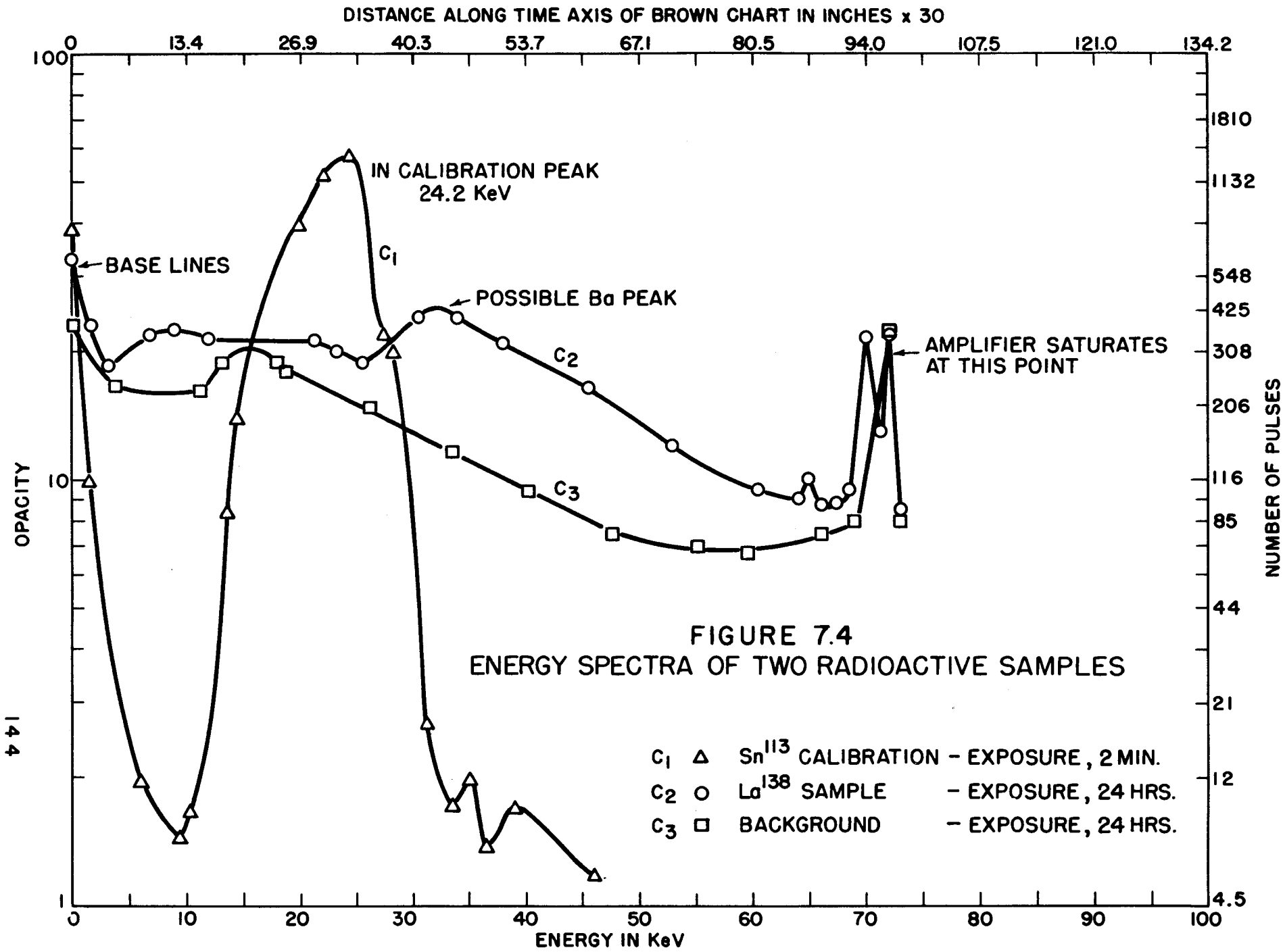

FIGURE 7.4
ENERGY SPECTRA OF TWO RADIOACTIVE SAMPLES

NOT CLASSIFIED
DWG. 9786

FIGURE 7.5

ENERGY SPECTRUM OF La^{138} SOURCE WITH BACKGROUND SUBTRACTED

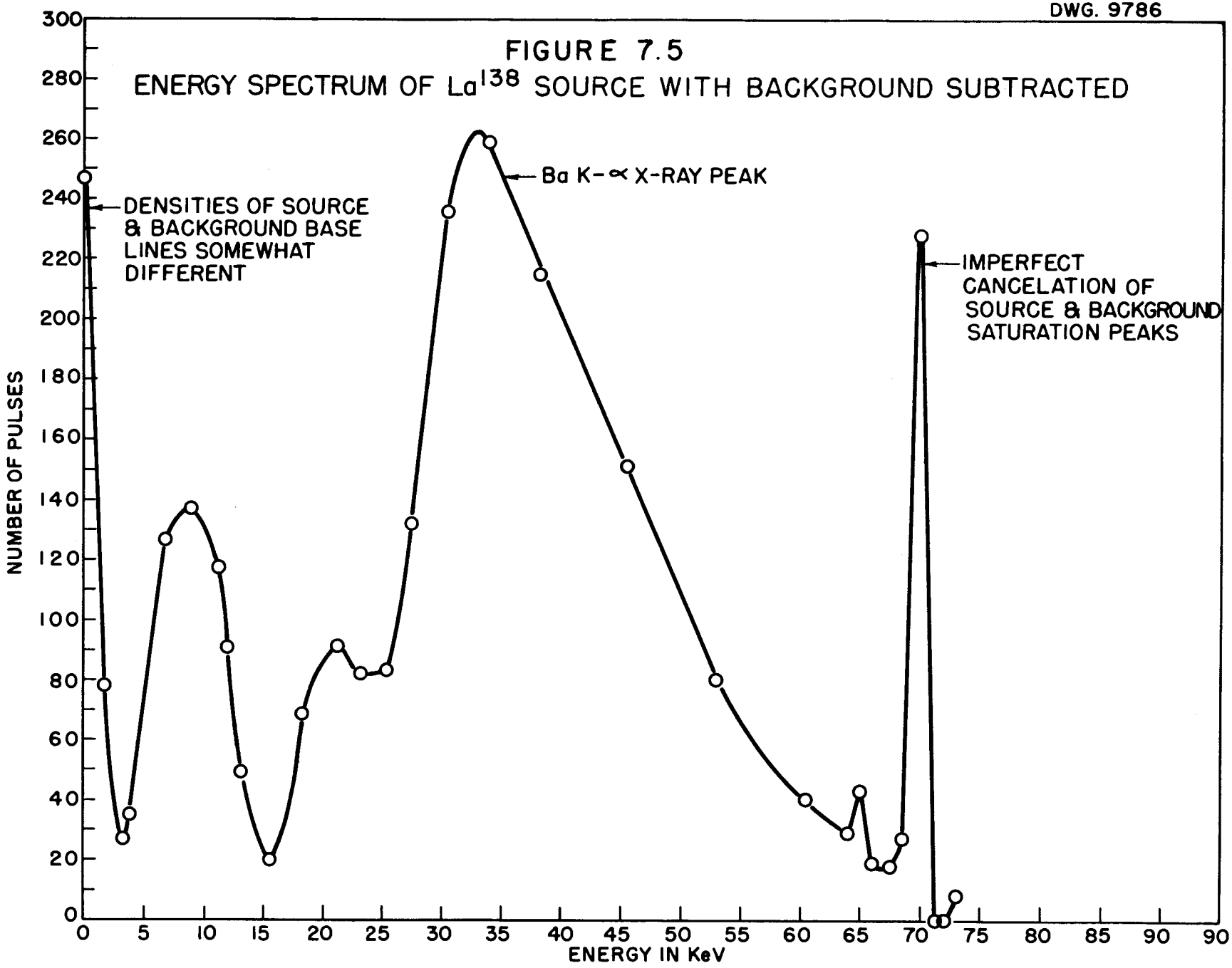

INSTRUMENTATION FOR NEUTRON DIFFRACTION

J. K. East H. A. Levy
S. W. Peterson

The operation of a neutron-diffraction spectrometer requires that the intensity of a neutron beam be continuously recorded over a large range of scattering angle. Because suitable scanning speeds are slow (of the order of 5° per hour), a complete pattern requires 12 to 24 hr continuous running and necessitates a system stable over this interval. Simultaneous monitoring of the incident neutron beam is desirable, and monitoring of the background is sometimes necessary. For the spectrometer discussed on p. 110 the counting rate of the diffracted beam is of the order of 50 to 500 neutrons per minute for about 1° of angle subtended by the detector, and peaks in the diffraction pattern have a width at half-height of 1 to 2°.

In two spectrometers designed and operated by E. O. Wollan and C. G. Shull of the Physics Division, accumulated counts over a predetermined time interval (4 or 6 min) are printed by a modified traffic counter. A sequence control mechanism periodically stops the spectrometer and causes the traffic counter to record background by closing a cadmium shutter or the incident beam intensity by switching to a second BF_3 counter. Plotting the data is laborious, and the time lost during background and incident-beam counts is considerable. In addition, the recording of accumulated counts over a fixed time interval probably does make optimum use of the data.

We have investigated the use of count-rate meters and strip-chart recorders in this application. Major considerations are the following: (1) the rate meter must have a stable zero over the time required to complete a pattern; (2) the time constant must be adjustable to the minimum statistical fluctuation consistent with the resolution desired in the diffraction pattern; and (3) rather low counting rates must be accommodated. Rate meters incorporating these features, similar to the meter designed for the α-particle range analyzer,[1] have been in use for several months with satisfactory performance. A new rate meter with greater stability and low-impedance output has been designed by E. Fairstein (see p. 151) and promises even more satisfactory performance.

(1) Fairstein, E., "Modifications of the Sweep Type Differential Alpha Energy Analyzer," *Chemistry Division Quarterly Report for the Months June, July, and August, 1948*, ORNL-176, p. 85 (Nov. 9, 1948).

In the system now in use (Fig. 7.6) the diffracted neutron beam is detected by a BF_3 proportional counter 20 in. long and 2 in. in diameter, filled with enriched BF_3 (28 cm Hg) and argon (2 cm Hg). The pulses are fed to a cathode-follower preamplifier, then to an A-1 linear amplifier, and finally to a linear count-rate meter connected to one pen of a multipoint Brown potentiometer. D-c power, 1900 volts, is supplied by a standard scaler (Nuclear Instrument Company). The incident beam is monitored by a small BF_3 proportional counter with brass windows, front and back, through which the beam passes. About 1% of the neutrons are counted, the pulses being fed to a preamplifier, then to the amplifier of a standard scaler, and to a second linear rate meter, the output of which is fed to a second pen of the Brown potentiometer. The two pens print alternately at 6-sec intervals. The diffraction pattern (Fig. 7.7) and the beam intensity are thus recorded on the same strip-chart.

Since background has been reduced to a negligible level by improved shielding of the large counter, no provision for recording background has been made. Traffic-counter recording of data has been maintained to calibrate and check the behavior of the rate meter but will probably eventually be abandoned.

A further improvement in instrumentation now being prepared is the following: a multispeed drive for the spectrometer which will allow greater latitude in choice of time constant and hence greater precision of data. This is being achieved by a three-speed synchronous motor (900, 1800, and 3600 rpm) manufactured by Electric Indicator Company, Stamford, Connecticut, in conjunction with gear-change mechanism (8:1 to 1:1). This system will allow scanning speeds of ½, 1, 2, 4, 8, and 16° per hour in contrast to the present fixed speed of 5° per hour. Consideration is being given to equipping the Brown potentiometer with a similar motor in order to maintain a fixed relation between scanning speed and chart speed.

A device to maintain the incident-beam intensity constant within limits has been designed and partially constructed. It consists of a pair of aluminum wedges so mounted as to insert a variable thickness of absorber in the incident neutron beam. The wedges are driven by a Brown potentiometer motor actuated by the deviation of the output of the monitoring count-rate meter from a fixed potential.

NOT CLASSIFIED
DWG. 9807

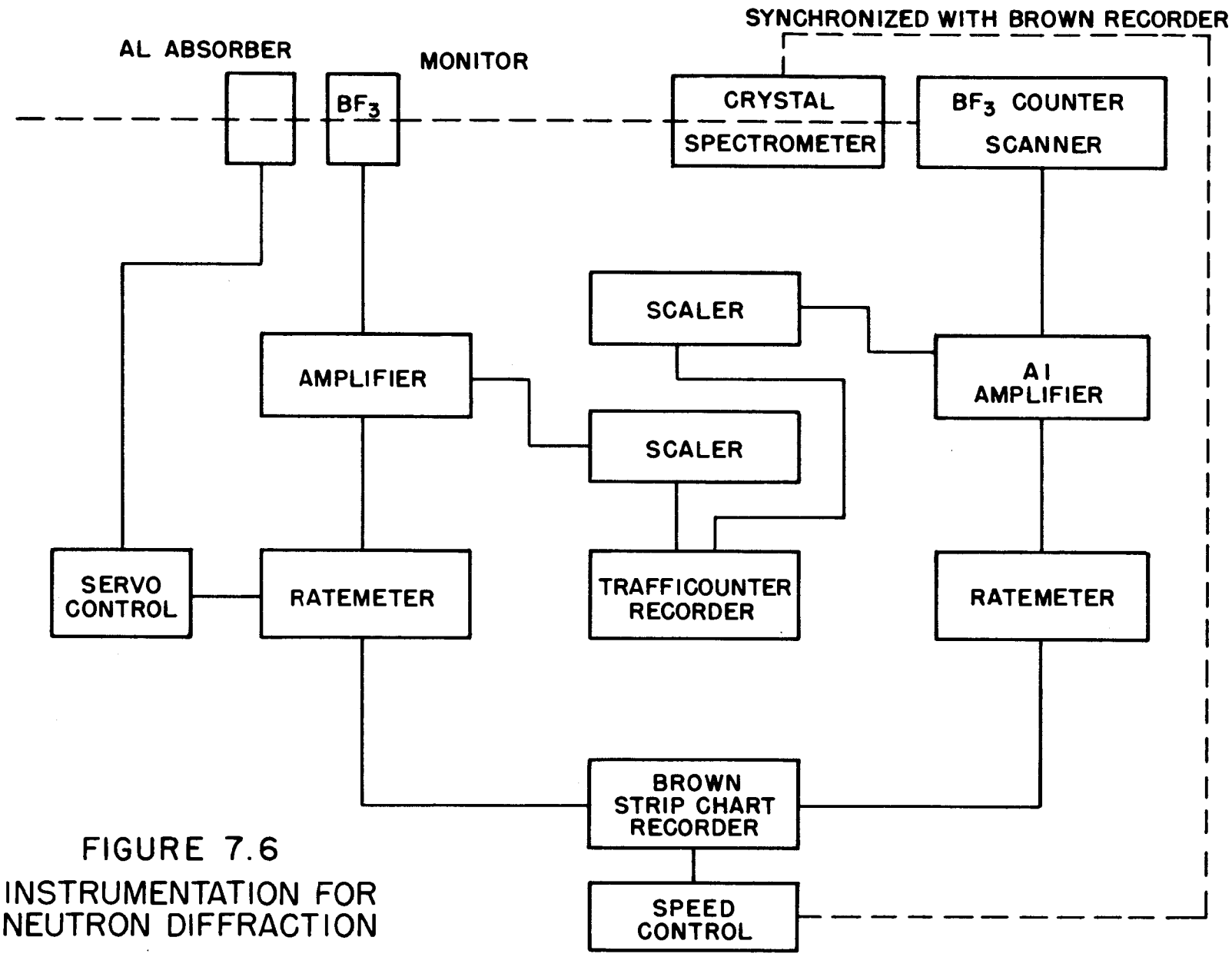

FIGURE 7.6
INSTRUMENTATION FOR NEUTRON DIFFRACTION

NOT CLASSIFIED
DWG. 9920

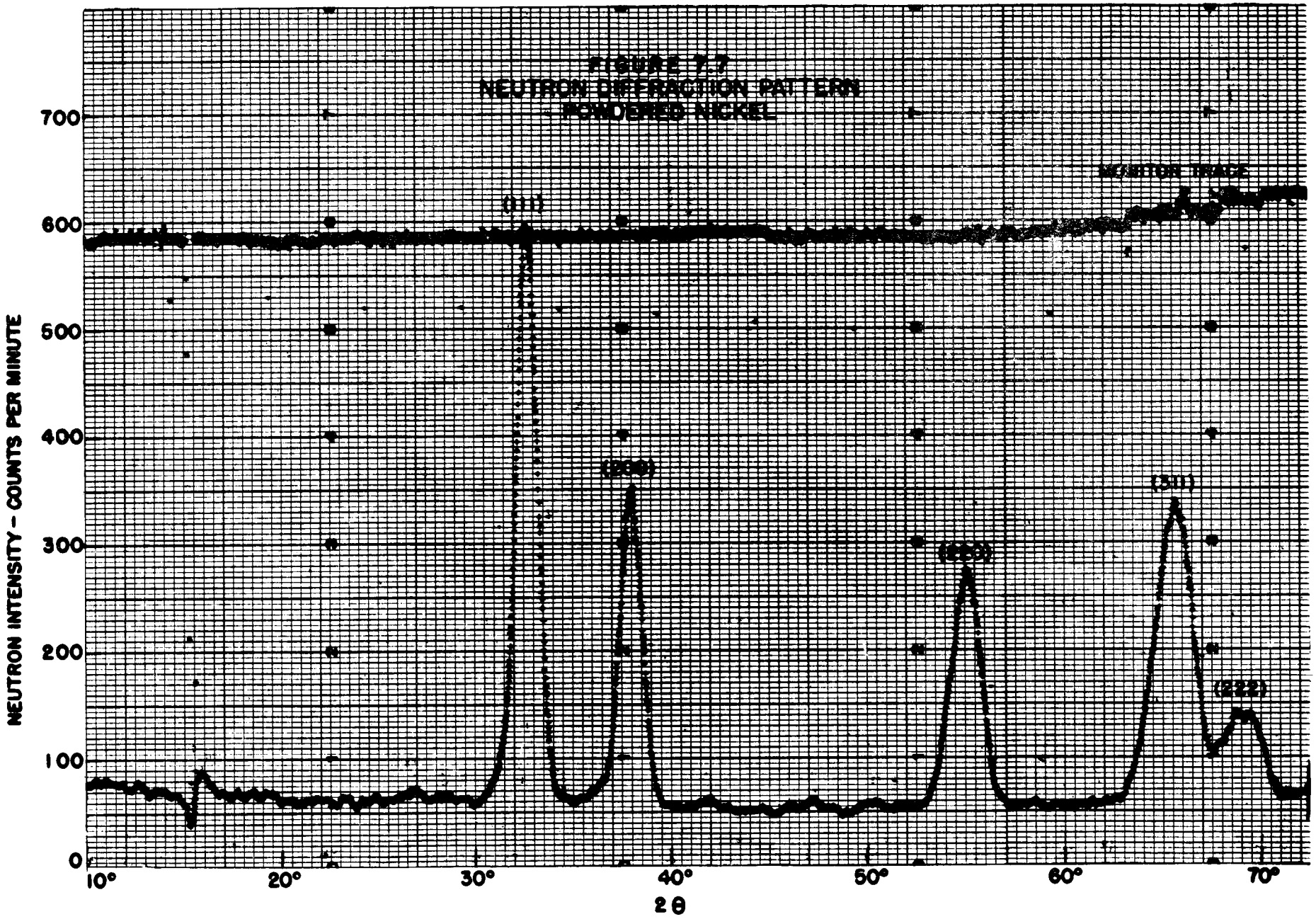

FIGURE 7.7
NEUTRON DIFFRACTION PATTERN
POWDERED NICKEL

Limit controls to stop the spectrometer and Brown recorder if the servo described above loses control (*e.g.*, in case of pile shutdown) are being planned.

Experiments are underway on higher pressure fillings of BF_3 counters in order to obtain higher counting efficiency.

A RELIABLE COUNT-RATE METER

Edward Fairstein

A linear count-rate-meter circuit has been designed for those applications requiring exceptional reliability of operation and very low drift rate. The immediate incentive for its development was the need for a means of recording neutron-diffraction patterns. The first model of the instrument has been in continuous operation for more than a month at the time of this writing, with excellent overall stability.

Specifications. The following specifications were set up:

Range. 100 to 200,000 c/m by steps in a 1-2-5 series.

Integrating Time. To give standard deviations of 1.4, 2, 3.8, 4.5, 6.3, and 20% of the full scale reading. Unused integrating condensers are precharged to avoid a jump in meter reading when switching.

Input pulse requirements. Any width from 0.1 to 100 μsec, of either polarity, and of any amplitude between the limits of 0.5 and 100 volts.

Calibration. An internal scalar circuit locked to the supply-line frequency is provided to give a pulse rate equal to the line frequency.

Meter. A 0- to 1-mamp panel meter is provided. There is also a connector to provide a signal for a 10-mv Brown recorder. A 0- to 1-mamp Esterline-Angus recorder can also be supplied from the circuit, although no specific provision has been made for it. The meters operate at ground potential.

Accuracy. ±1% after being zeroed and calibrated.

Drift rate. The long-term zero drift is about 1% of the full scale reading per week. After an aging period of a week the calibration drift is considerably less than this. The short-term drifts are not detectable.

Resolution loss. About 1%, or less, per 100,000 c/m.

Circuit Description. A detailed description of the circuit (Fig.7.8) follows:

T_1 is a diode restorer in the input which is not to be used when operating from an A-1 amplifier.

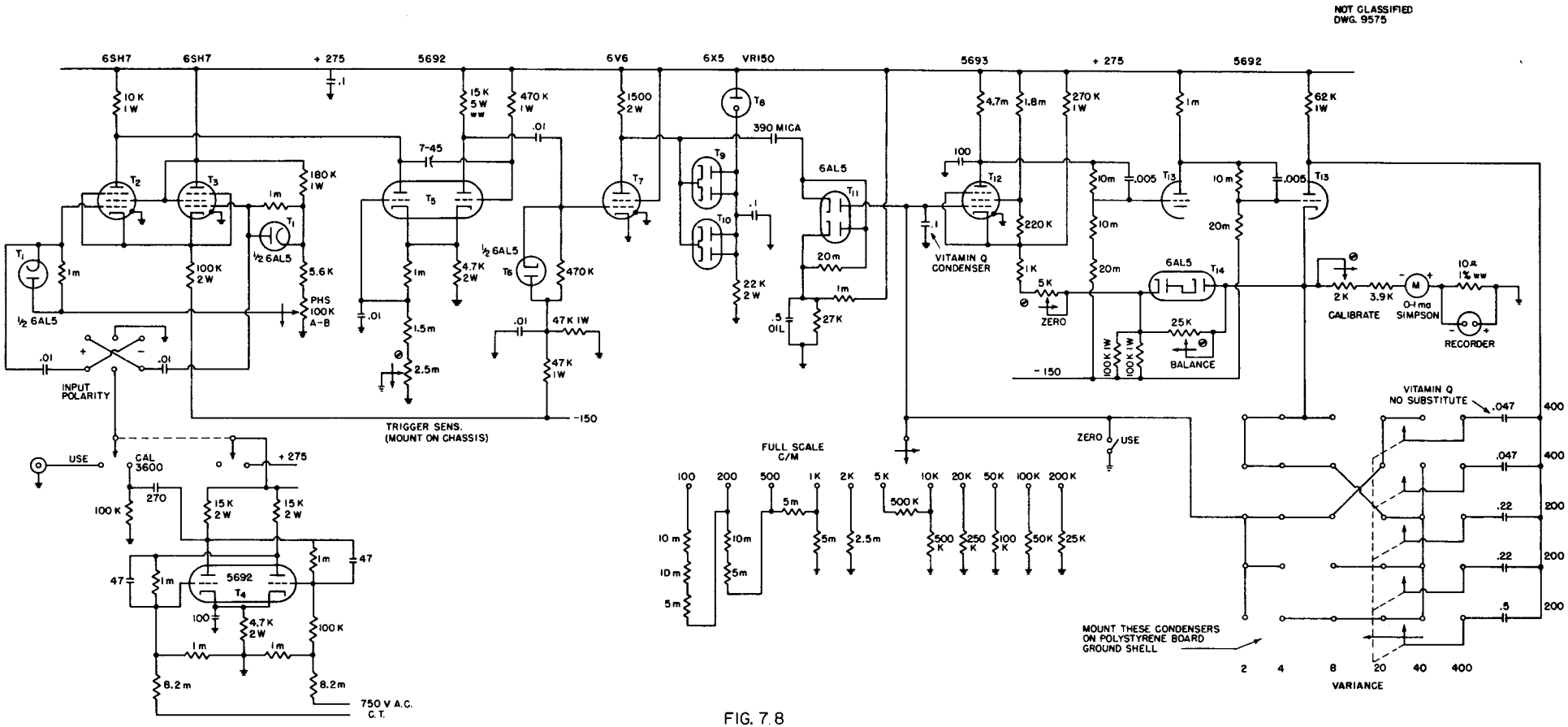

FIG. 7.8
LINEAR COUNT RATE METER

T_2 and T_3 are the pulse-height selector tubes. These are connected as a cathode-coupled amplifier to prevent grid current from flowing with high amplitude pulses. T_3 is normally conducting. The pulse-height selector control varies the bias on the off tube, T_2. Positive input pulses are routed to the off tube and negative pulses to the on tube by the input polarity switch.

T_4 is connected as a scalar to provide the calibrating signal for the rate meter.

T_5 is a univibrator pulse shaper. Its output pulse width is adjusted to 3 or 4 μsec. The circuit is such that the output width is nearly independent of the applied pulse width, even for pulses much longer than 3 μsec.

T_7 is an amplifier with a low impedance output. It is normally biased to complete cutoff. The positive pulse from T_5 drives it far into the grid-current region. T_6 is a diode restorer to prevent bias shifts with changes in counting rate. T_9 and T_{10} are diode clamps to limit the output voltage of T_7 to within 1% of the value determined by T_8. Without the clamps, the output voltage pulse is about 250 volts and is dependent upon the condition of T_7. With the clamps the output voltage is 150 volts and is constant to 1% throughout the useful life of T_7.

T_{11} is the rate-meter diode, used in a conventional circuit.[1] The coupling condenser is such that it becomes charged to over 99% of its final charge in 3 μsec. This makes the calibration independent of small changes in driving pulse width.

The vacuum-tube voltmeter consists of T_{12}, T_{13}, and T_{14}. T_{14} provides compensation for the effects of heater voltage changes. When the balance control is properly adjusted, the voltmeter zero does not change by a perceptible amount for line voltage changes between the limits of 100 and 130 volts. T_{12} and T_{13} are connected as a feedback amplifier. The stabilization factor ($A\beta$) is about 140. The grid current of T_{12} has a normal range of 5×10^{-11} to 5×10^{-12} amp, depending upon the particular tube. This current is not sufficient to cause a noticeable zero offset under conditions of maximum rate-meter sensitivity. The full scale input voltage is about 5 volts.

(1) Elmore, W. C., and Sands, M., *Electronics*, p. 250, McGraw-Hill, New York, 1949.

To conserve space and cost, low-valued integrating condensers are used. These are connected in the feedback loop in such a way that their effective capacity is multiplied by 15. This method has one disadvantage: Because of the voltage drop across the condenser, the insulation resistance between terminals must be at least 10^{11} ohms to cause no more than a 1% zero offset on the most sensitive scale. Luckily, a guard-ring arrangement can be used to eliminate the effects of surface leakage. Vitamin Q condensers (manufactured by Sprague Electric Co.) with the shell grounded have proved to be satisfactory, both from this standpoint and from that of a sufficiently low dielectric hysteresis factor. A polystyrene mounting board is necessary.

Unused portions of the integrating network are connected to the low impedance output of the vacuum-tube-voltmeter circuit. This keeps them charged to the proper level to avoid switching transients. It is important that the switch used here be of the open-circuiting type to avoid connecting the voltmeter output and input during the switching process.

The higher valued resistors in the rate-meter circuit should be mounted on a board with better insulation properties than the usual type. Polyethylene-insulated wire should be used for connecting these resistors. The zero-use switch should have a bakelite, rather than paper, shell.

A HIGH-STABILITY LOW-DRAIN PORTABLE HIGH-VOLTAGE SUPPLY

R. A. Dandl and C. J. Borkowski

The high-voltage supply shown in Fig. 7.9 is basically of the relaxation-oscillator interrupter-tube type, without the usual disadvantages. The usual battery-operated high-voltage supply of this type is very sensitive to load changes and battery-voltage changes. The circuit in Fig. 7.9 is so arranged that battery-voltage changes have little effect on the relaxation-oscillator frequency. Changes in interrupter-tube current, as well as load changes, are also compensated for.

The mechanism of regulation is as follows: A change in the battery voltage causes a change in current in the interrupter tube, which results in a change in the high-voltage output. This high-voltage change, acting through the corona regulator, causes a compensating change in the control grid bias of the interrupter tube. Since the relaxation-oscillator voltage is approximately twice the striking voltage of the neon bulb, the oscillator frequency is relatively insensitive to battery-voltage changes, ensuring continuous operation near peak efficiency.

The regulation mechanism for load changes is nearly identical to that for battery-voltage changes. The change in frequency and current through the relaxation oscillator is slight, resulting in almost constant current through the corona regulator tube, which is obviously desirable. It follows that the current through the corona regulator tube is the same as the average relaxation-oscillator current; this current can be adjusted by use of an empirical method based on the following equations:

$$i = C(V_s - V_c)f$$

$$f = \frac{1}{RC \log \left[\frac{V_s - V_c}{E_{bb}} + 1 \right]} \qquad (1)$$

NOT CLASSIFIED
DWG. 9806

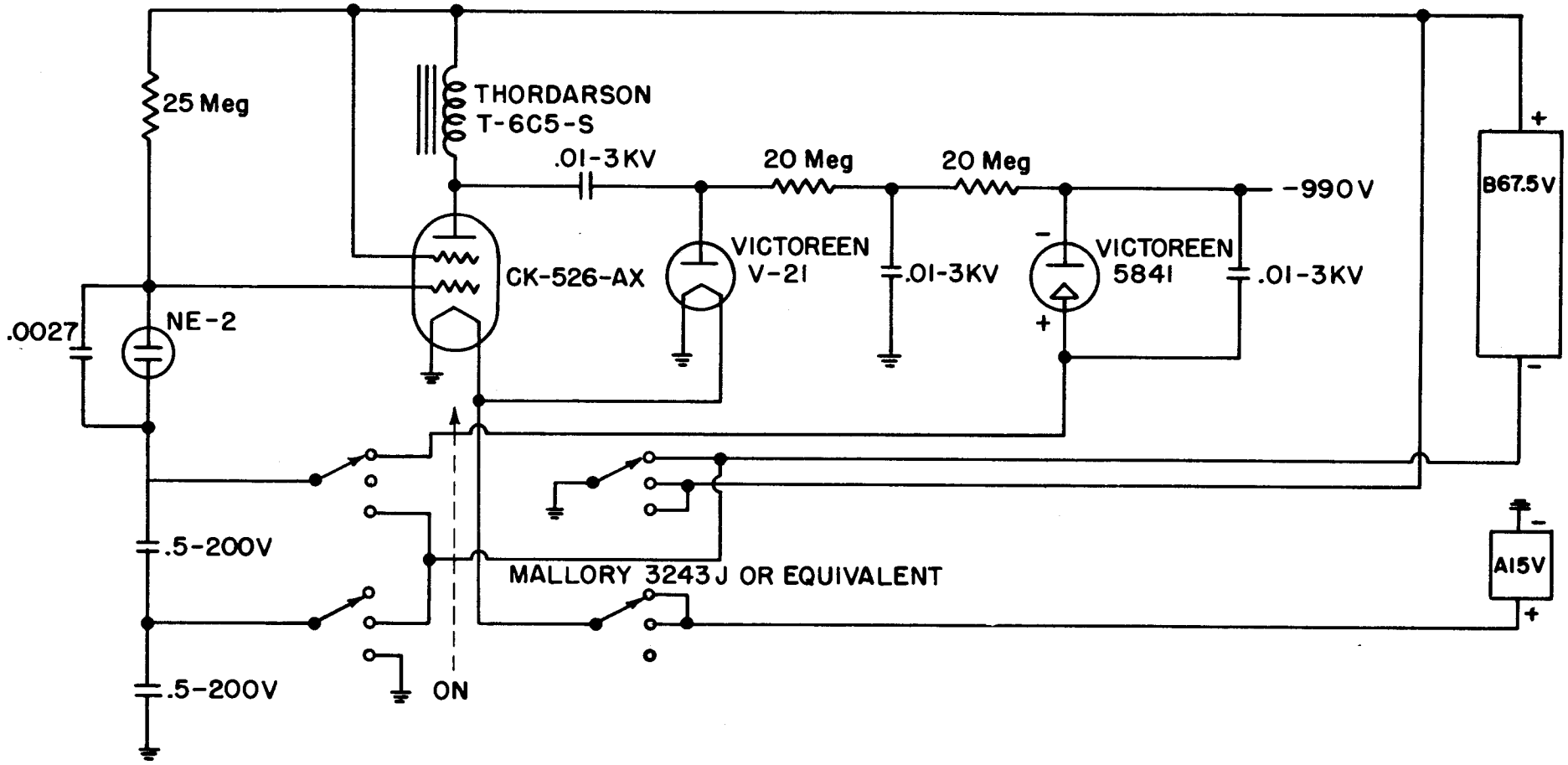

FIGURE 7.9
REGULATED BATTERY OPERATED HIGH VOLTAGE SUPPLY

$$i = \frac{V_s - V_c}{R \log \left[\frac{V_s - V_c}{E_{bb}} + 1 \right]} \tag{2}$$

where

i = current through corona regulator

f = frequency of relaxation oscillator

RC = tank circuit of relaxation oscillator as shown in Fig. 7.9.

V_s = neon-bulb striking voltage

V_c = neon-bulb cutoff voltage

E_{bb} = B battery voltage

From Eq. (2) it is readily seen that the corona-regulator-tube current is primarily a function of R, and that the frequency can be changed independently of the current by varying C. The ease of these two adjustments makes the circuit applicable to a variety of tubes and inductors, the procedure being one of setting up the circuit for optimum current drain through the corona regulator and maximum efficiency of B battery current. The corona-regulator current drain is adjusted by varying R, and the frequency for maximum efficiency is adjusted by minimizing the B battery current as a function of C.

The optimum frequency, f_0, is determined by the time, t_0, required for the inductor to become almost completely charged (where $t_0 = K/f_0$, $K \approx 0.25$ for most sharp-cutoff tubes and neon bulbs). If the interrupter tube is left on for a time longer than t_0, too large a fraction of the input power will be dissipated in the resistance of the coil. If the interrupter tube is left on for a time shorter than t_0, too large a fraction of the input power will be dissipated by the screen grid. It should be mentioned that t_0 is an almost linear function of the size of the inductance for inductances with similar saturation characteristics. Also, inductances that saturate at the low levels of peak plate current encountered in devices of this sort are more efficient since they charge up more rapidly, resulting in lower screen losses. Inductors with the lowest resistance consistent with small size are desirable since

they permit obtaining the necessary peak plate currents from lower voltage B batteries. A transformer whose primary has the previously mentioned characteristics would be desirable provided the windings are sufficiently tightly coupled.

Table 7.1 gives the performance specifications for the supply shown in Fig. 7.9.

TABLE 7.1

Performance Specifications for Regulated Battery-operated High-voltage Supply

E_{bb} = 67.5 volts E_f = 1.5 volts E_{hv} = 990 volts

CHANGES MADE TO TEST REGULATION	$i_{corona\ tube}$ (μa)	i_{bb} (ma)	E_{avg}
None	3	0.33	990
E_{bb} and E_f changed by 25%	2.4	0.33	986.5
Added a load of 217 megohms	2.9	0.75	988
Added a load of 217 megohms and changed E_{bb} and E_f by 25%	2.3	1.1	984

The relatively complicated switching arrangement is necessary to furnish sufficient negative voltage to start the relaxation oscillator and bias the interrupter tube in its operating region. The switch is swept through the center position, and the supply builds up full regulated voltage in about 10 sec. Once started, the corona regulator furnishes the negative voltage necessary to operate the neon bulb.